FORMULATION OF DC ENERGY FACTOR AND ENERGY-BASED CONTROL METHOD FOR HIGH EFFICIENCY POWER ELECTRONICS CONVERSION SYSTEMS

SHI ZHANGHAI

Ph.D

The Hong Kong Polytechnic University

2012

The Hong Kong Polytechnic University

Department of Electrical Engineering

Formulation of DC Energy Factor and Energy-based Control Method for High Efficiency Power Electronics Conversion Systems

SHI ZHANGHAI

A thesis submitted in partial fulfilment of the requirements for the degree of Doctor of Philosophy

January 2012

CERTIFICATE OF ORIGINALITY

I hereby declare that this thesis is my own work and that, to the best of my knowledge and belief, it reproduces no material previously published or written, nor material that has been accepted for the award of any other degree or diploma, except where due acknowledgement has been made in the text.

_____(Signed)

SHI ZHANGHAI (Name of student)

Abstract

This thesis is to examine the energy handling in DC-DC converter systems. The management of the energy in terms of energy factor is the core area of the examination. The theory derived is extended to the family of DC-DC power converters from which the efficiency and its implication in power factor as that in the AC counterpart are studied.

The main purpose of this thesis is the extension of the understanding of the energy handling in power converters. The conventional AC power factor is a start point. Its exploration to DC system, mainly the DC-DC power converters are thoroughly done. There are a number of new concepts that have been explored. These include the variation energy factor, non-active energy and non-active power.

Besides the classical switched-mode power converters, the tapped-inductor converters are used as examples of study in their energy handing. Systematic formulations indicated energy handling have been obtained for the converters.

Five main aspects of works carried out in this thesis have been clarified below.

A series of novel concepts such as Energy Storage (E_S), Energy Factor (F_E), Buffer Energy (E_B) and Buffer Energy Factor (F_{EB}) are reviewed and presented to quantitatively describe the energy behaviour in DC-DC converters. Energy storage and energy factor are used to represent the amount and ratio of energy stored in DC-DC converters during operation. Buffer energy and buffer energy factor are used to evaluate the variation of energy storage in DC-DC converter. Explicit definitions of these energy-related concepts have been also presented. Formulations of these concepts have been deducted for inductor, capacitor and transformer in various DC-DC converters.

The definitions of buffer energy and buffer energy factor are further extended on the basis of theory of non-active power. Through the extended definitions buffer energy and buffer energy factor can be applied not only to DC systems but also to AC systems. The correlations and distinctions among buffer energy and reactive

energy, buffer energy factor and power factor have been clarified.

On the basis of energy factors and buffer energy factors, comparison study has been carried out for basic topologies of DC-DC converters. Useful results for design of DC-DC converter have been obtained. The correlations between efficiency and buffer energy factor are also presented. In general, efficiency of DC-DC converter decreases when buffer energy factor increases.

Tapped-inductor converters have been researched carefully by this thesis. A number of special topologies of tapped-inductor converters have been explored. Static performances of tapped-inductor Boost converter have been examined. Comprehensive comparisons between tapped-inductor Boost converter and conventional Boost converter have been carried out. The comparisons include stress of components, efficiency, energy factors and buffer energy factors. Experimental results reveal the superiority of tapped-inductor converter over their conventional counterpart on the occasion of large voltage conversion ratio. Tapped-inductor converter is the promising single-stage high-efficiency choice for future DC distribution systems. Experimental results reveal the main drawbacks of tapped-inductor converter including spike and power loss caused by non-ideal coupling of tapped inductor.

Compared with conventional Boost converter, the design of closed loop controller for tapped-inductor converter is more challenging. This thesis has researched the buffer energy factors during transient time. The design of controller for tapped-inductor Boost converter has been studied. The application of one famous energy-based control method: passivity-based control to tapped-inductor Boost converter has been researched. The overall performances of control are analyzed. The comparison between peak-current mode control and passivity-based control has been carried out through theory and experiment. These researches can provide useful references for the controller design of tapped-inductor DC-DC converters.

Publications arising from the thesis

Journal papers

[1] Z. H. Shi, K. W. E. Cheng, and S. L. Ho, "Formulation of buffer energy and experimental results of energy factor of DC–DC converters," *International Journal of Circuit Theory and Applications*, vol. DOI: 10.1002/cta.815. (Published)

[2] Z. H. Shi, K. W. E. Cheng, and S. L. Ho, "Boundary condition analysis for higher order converters using energy factor concept," *Circuits, Systems & Signal Processing*. (Accepted)

[3] Z. H. Shi, K. W. E. Cheng, and S. L. Ho, "Static Performance and Parasitic Analysis of Tapped-Inductor Converters", *IET Power Electronics*, (Under review).

Conference papers

[1] S. Zhanghai, K. W. E. Cheng, S. L. Ho, and L. Jiongkang, "Energy factor and its associated boundary condition analysis for higher order converters," presented at Universities Power Engineering Conference (AUPEC), Australia, 2008.

[2] Zhanghai Shi, K. W. E. Cheng, S. L. Ho, and X. Wei, "More general definition of energy factor and its application in isolated converters," presented at 3rd International Conference on Power Electronics Systems and Applications (PESA), 2009.

Acknowledgements

First and foremost, I would like to express my deepest gratitude to my chief supervisor, Prof. K. W. Eric Cheng, for his time, knowledge, talent, patience, encouragement and support. This thesis would not have been possible unless his patient guidance and continuous help.

I greatly appreciate helps and support from my co-supervisor Prof. Siu Lau Ho, who has made available his support in a number of ways.

I would like to thank Dr. B.P. Divakar for his discussion and instruction on the reactive power theory, and thank Dr. Nelson Chan for his kind helps.

I would also like to thank Dr. W. L. Chan, for excellent instruction in digital signal processing and generously present me the DSP control board. I must also thank Dr. W. N. Fu, Dr. Kelvin Chan, and Dr. C. K. Lee for their valuable suggestions, comments and support on experiments.

I have to thank all my friends and colleagues in the Power Electronics Research Centre, especially Mr. K. F. Kwok, Mr. Jiong Kang Lin, and Miss. Y. K. Cheng, for all their helps, supports and valuable hints.

I would like to thank my parents and my brother. Their selfless love provides me the energy to move on continuously.

Finally, thanks for financial support from the Research Grants Council of Hong Kong under the General Research Fund with project No. PolyU 5136/06E.

Table of contents

List of figures

List of tables

List of abbreviations

DC	Direct Current
AC	Alternating Current
RMS	Root Mean Square
PoL	Point of Load
CCM	Continuous Conduction Mode
DCM	Discontinuous Conduction Mode
FE	Energy Factor
FEB	Buffer Energy Factor
EMI	Electro-Magnetic Interference
EMC	Electro-Magnetic Compatibility
MMF	Magnetic Motive Force
PID	Proportional-Integral-Differential
PBC	Passivity-Based Control
PCH	Port-Controlled Hamiltonian
RHP	Right Half Plane
PWM	Pulse Width Modulation
DSP	Digital Signal Processor

List of symbols

E_S	Energy storage
E_B	Buffer energy
F_E	Energy Factor
F_{EB}	Buffer energy factor
L	Inductor
L	Inductance
C	Capacitor
C	Capacitance
R	Resistor
R	Resistance
f_s	Switching frequency
T_s	Switching period
D	Duty ratio
K	Circuit parameters, which is equal to $2L/RT_s$
M	Voltage conversion ratio of DC-DC converters
η	Efficiency
ϕ	Magnetic flux
Ψ	Magnetic flux linkage

Chapter 1 Introduction

This chapter firstly introduces the background and motivation of the thesis. Then the literatures in the field of the research topic of the thesis are reviewed. Lastly the structure of the thesis is presented.

1.1 Background and motivation

1.1.1 Efficiency requirements

Efficiency is one of the main concerns for all power electronics systems. Nowadays everyone has to face the challenge of increasingly severe energy crisis. There are mainly two ways to solve this problem. One is to develop new energy sources, especially renewable and green energy sources, such as wind power, solar energy, tide energy and biomass energy. Another way is to increase the efficiency of energy utilization. In terms of power converters, because of their wide applications, the small increase in efficiency of each converter can cause significant reduction of total energy loss in the world. Many organizations have specified the requirements on efficiency for DC power supply through various standards and guidelines. In recent years, the standards for efficiency of power supply have been tightened by many organizations. For example, Energy Star Tier II standard has specified the efficiency for external power supply with power level above 49W should be higher than 87%[1]. 80Plus specifies in its silver-level standard on 230V input power supply such that the efficiency under 20%, 50% and 100% load should be higher than 85%, 89% and 85%, respectively[2]. In China, the standard of High Frequency Switch-mode Rectifier for Telecommunications specifies that the efficiency of rectifier (48V DC output) with power level above 1500W should be higher than 90% [3]. Improvement of efficiency is one of the main objectives for industrial power converters. At present, some product of communication power supply with 3kW power level can reach the efficiency over 95%.

1.1.2 Methods to improve efficiency

Both research institute and industry endeavor to improve the efficiency of power converters. The main measures include soft switching technology, improvement of topology and optimization of magnetic design. To improve

efficiency is equivalent to reduce power loss. Generally, power loss of switching devices in converters is divided into two kinds: switching loss and conduction loss.

The evolution of soft switching technology is a milestone in the development of power converters [4-12]. It significantly reduces the switching loss of converters and raises the frequency of converters to a higher level. In recent years soft switching technologies have obtained great development. It now includes many modes of converters such as phase-shift resonant, quasi resonant, series resonant, parallel resonant, series parallel resonant and multi-resonant. Special attention should be paid on the LLC resonant topology. It has become the mainstream topology in the product of communication power supply (48V output) [13-17].

The reduction of conduction loss depends on the innovation of switching devices. Trench technology [18-20] reduces the saturation voltage drop of IGBT. Super junction CoolMOS technology can reduce on-state resistance (Rds(on)) of MOSFET substantially [21-27]. Recently the materials SiC and GaN have been used in the evolution of new ages of power switching devices. These new materials also help to decrease conduction loss, as well as switching loss of switching devices.

1.1.3 A special kind of Loss: ripple loss

There is an important phenomenon has not been paid enough attention. That is the power loss caused by ripple of voltage and current. This kind of power loss depends on the energy-storage components. For example, current ripple of inductor will induce extra RMS copper loss to components in the circuit. Moreover it is the source of magnetic hysteresis loss of inductor (Core loss). The loss caused by current ripple of inductor is severe under discontinuous conduction mode (DCM). In terms of transformer, although it often does not significantly store energy as the inductor, its magnetizing current exists in the form of ripple variation which also causes extra copper loss and core loss to the circuit. The voltage ripple of capacitor is in fact caused by the ripple current during charge and discharge. The ripple current of capacitor is one of the main sources of power losses on the equivalent series resistor (ESR). It is meaningful to research the ripple of DC-DC converters under different topologies and different parameters of components.

From the perspective of energy, ripple of current or voltage is in fact the variation of stored energy of energy-storage components (inductor, capacitor and

transformer). During the operation of power converters, the ripple is to provide temporary energy storage in order to activate the power conversion. This is the intrinsic property of switching power converters. It is also the root of ripple of current or voltage. The average energy storage has important effect on the size or power density of converters. The bigger the energy storage, the larger the size of power supplies. On the other hand, the variation of energy storage brings ripple of current or voltage which causes power loss and reduces efficiency of converters. Moreover, it is one of the main sources of EMI of power converters. These two aspects of energy both have great significance on the quality of power converters. This thesis proposed two concepts: Energy Storage and Buffer Energy to describe the two aspects of energy in DC-DC converters.

1.1.4 Energy storage and energy factor of DC-DC converter

Energy stored in reactive components of power converters is the basic and necessary method for power conversion. The energy is temporarily stored and delivered to the output stage or other terminals periodically subjected to the switching frequency. This inherit property has not been explored thoroughly to DC-DC converters. Especially the characteristic of storage energy with aspects to the power throughput under different converter operation parameters has not been discovered fully. In this thesis, the concept of energy factor has been introduced and illustrated in detail. Comparative research of energy factors of different topologies under different circuit parameters has been carried out.

1.1.5 Non-active power, Buffer energy and Buffer energy factor for DC-DC converter

Are there “reactive power” and “power factor” for DC power system? It is well known that reactive power and power factor play important roles in the analysis of AC power system. In AC power grid, improper handling of reactive power will cause the voltage of some nodes deviated from normal value seriously. Power factor reflects the efficiency of energy transmission.

During the operation of DC-DC converter, a portion of energy absorbed from front-end power supply is stored in the converter during the on-state of switching devices and such energy is delivered to the load during off-state. This portion of energy can be viewed as “non-active energy”. The time derivative of non-active

energy is the “non-active power”. The “non-active power” is counterpart of the conventional concept of reactive power which is originally developed only for sinusoidal AC system. Non-active power of DC-DC converter can cause extra loss to the converter, e.g. core loss of inductor and ripple loss on other components mentioned above.

Recently, DC distribution system and micro grid attract much more interests. More and more renewable energy sources and DC power loads are connected to power grid. For a long time, DC power transmission has been considered as less reactive power handling and higher stability. However, in DC distribution system, equipment of DC power source and load contain lots of switching devices and energy-storage components including inductors and capacitors. DC ripple voltage and current will produce “non-active power”. Like reactive power in AC system, non-active power will also cause power loss to DC distribution system, pollute the power network and degrade the performance of front-end power supply.

Classical concepts of reactive power and power factor cannot be applied directly to the evaluation of the non-active power of DC-DC converters. It is necessary to develop an alternative method to measure the effectiveness of the power handled by DC-DC converters. New concepts are needed to investigate the non-active power and energy process in DC-DC converters.

Following the reactive power and power factor defined for AC system, this thesis proposed a series of novel concepts to describe the energy variation in DC systems. The concepts include: non-active power, buffer energy and buffer energy factor. The significances of these novel concepts have been illustrated in this thesis.

1.1.6 Tapped-inductor DC-DC converters

In recent years, DC distributed system gains significant interests in research. The benefit of the DC distribution over the AC distribution has been presented by many researchers [28-35]. Compared with AC distribution, DC distribution has been shown to be more efficient and provided good power quality in a distribution system. DC distribution allows the flexibility of merging many energy sources [32]. Small-scale DC distribution systems applied in industry includes data centre, vehicles (ship, airplane), charging station and so on.

In DC distribution system, the interconnections between energy sources and DC

buses, as well as DC buses and loads are implemented by DC-DC converters. To reduce power loss, high-efficiency single-stage DC-DC topologies are preferred. For the applications which need very high/low voltage gain without isolation requirement, the tapped-inductor DC-DC converter provides an attractive choice. For example, energy sources such as photovoltaic and fuel cell have low output DC voltage. The energy storage components such as battery cell and super capacitor can also provide low-voltage output effectively. Step-up converter with high voltage gain is required to connect these systems to the high voltage DC bus. Conventional single-stage Boost converter has very low efficiency under extreme high voltage conversion ratio. At these occasions, tapped-inductor Boost converter provides a high-efficiency and low-cost choice.

Tapped-inductor DC-DC converters extend the application of its traditional counterparts. For these applications, unlike conventional DC-DC converter, tapped-inductor converter can avoid the duty ratio falling into extreme range to achieve very high/low voltage gain through controlling the tapped turns ratio of windings. The key feature is the efficiency and reliability is improved in the applications of extreme voltage gain.

Although lots of work on tapped-inductor converter has been carried out previously [36-54], the comparison in detail between tapped-inductor converter and conventional converter does not appear in literatures. Moreover, the energy behaviour of tapped-inductor converter has not been clarified. The non-active power of tapped-inductor converters and its impact on DC distribution system have not been examined too.

Chapter 4 of this thesis uses tapped-inductor Boost converter as the example to illustrate the energy storage, energy factors, buffer energy and buffer energy factors of tapped-inductor converters. The basic principles of operation of tapped-inductor DC-DC converters are reviewed. Then detailed comparisons between tapped-inductor Boost and conventional Boost are carried out, which include the comparison of voltage gain, component stress and efficiency. Experimental results present solid verifications to the analysis of performance of tapped-inductor Boost converter. Similar methods can be extended to other tapped-inductor DC-DC converters.

1.1.7 The function of energy in building of control strategy for DC-DC converters

Like switching device and topology, control is also one of the important aspects of power electronics technology. Although PID control is still the mainstream in industry application nowadays, but nonlinear control technologies will be more widely applied to DC-DC converter because of the continuous improvement of digital signal processor (DSP) and Analog to Digital (AD) sampling technology. The continuous reduced cost, increased speed and complicated function handling of DSP and AD chip are the preferred factors to promote digital realization of nonlinear control algorithms of DC power conversion.

In terms of DC-DC power converters, PID controller provides an easy way to carry out the closed-loop operation of power converter [55-58]. There are systematic theory and successful experience for the PID controller design. PID controller can be implemented by low cost analog IC (integrated circuit). But the theories of classical PID compensation are mainly focused on the linear model of plant. In fact DC-DC power converters are highly nonlinear systems. To apply PID controller into DC-DC converter, it is necessary to make an approximate linearization around the static operating point. The well designed PID controller can achieve good performance in a certain range around the predetermined static operation point. Usually this range cannot be very wide. Outside this range the preset PID controller will degrade and cannot assure stability.

Based on the original nonlinear model, nonlinear control algorithms provide alternative ways to implement closed-loop operation of DC-DC converter. Nonlinear controller can provide global asymptotical stability and can still achieve good performance under a large signal disturbance.

Energy plays a key role in the formation of nonlinear control algorithms. According to Lyapunov's second method for stability, if a positive energy function can be found for a dynamic system, and the energy function decreases with time, then this dynamic system is stable. The difficulty to apply the Lyapunov's second method is to find an energy function, especially for nonlinear systems. However if

we can utilize the real energy stored in physical systems to shape the energy function, things may be simplified. Although the energy function in Lyapunov indirect method is often not necessarily related to real energy, physical energy sometimes can provide an intuitional choice for the energy function.

In fact some nonlinear control methods for DC-DC power converters are exactly based on physical energy stored in inductors and capacitors [59-68]. Passivity-based control (PBC) is the most famous one of such kind of control methods. The basic idea of PBC is to utilize the intrinsic dissipation of nature system and control the injected energy to drive the energy stored in a system to the desired level. In the last ten years passivity-based control gains a great development and wide applications. It also extends into the field of control of power conversion [67-77]. But the application of PBC are mainly concentrated in classical DC-DC converters, such as Buck, Boost, Buck-Boost, phase-shift full bridge converter, and so on. Along with the rapid development and application of micro grids and DC distribution systems, Tapped-inductor DC-DC converter will play an important role because of its virtue of wide conversion ratio, high efficiency and simple structure. It is necessary to research the application of PBC to provide an alternative control method for the Tapped-inductor DC-DC converters.

Most of the previous researches on tapped inductor are mainly focused on the static performance. The research of closed-loop operation of Tapped-inductor converter especially applying modern nonlinear control into Tapped-inductor converter has not been explored enough. Compared to classical DC-DC converters, Tapped-inductor DC-DC converter exhibits different characteristics which bring new challenges to the design of controller. During the operation of Tapped-inductor DC-DC converter, the current of inductor has more than one level. The number of levels can be increased by adding taps. Then the freedom of control can be increased. Because of the discontinuity of inductor current, the mathematical model of conventional converter is invalid for the Tapped-inductor converter. However, although the current changes suddenly at the instant of switching of taps, the *mmf* and energy must be continuous. That means the magnetic flux and magnetizing current of the tapped inductor are continuous. This point can be used to build new models for the control of converter with tapped inductor.

The Chapter 5 uses passivity-based control to implement closed-loop operation for Tapped-inductor Boost converter. The models of Tapped-inductor Boost converter are elaborated in detail. The overall performances of control are analyzed. Comparisons among peak-current mode control, sliding mode control and passivity-based control are carried out.

1.2 Literature review

1.2.1 Review on the origin of concept of energy factor

When the keyword "energy factor" is searched on Google, lots of explanations will be presented. The explanation from Wikipedia is: "An energy factor (EF) is a metric used to compare energy conversion efficiencies of appliances or equipment" [78]. The most common application of energy factor exists in the field of water heater. The words for energy factor from U.S. Department of Energy are: "Use the *energy factor* to determine the energy efficiency of a storage, demand (tankless or instantaneous), or heat pump water heater", "The energy factor (EF) indicates a water heater's overall energy efficiency based on the amount of hot water produced per unit of fuel consumed over a typical day", "The higher the energy factor, the more efficient the water heater. However, higher energy factor values don't always mean lower annual operating costs, especially when you compare fuel sources". The organization of Energy Star has ruled on the energy factor in its "Residential Water Heaters Key Product Criteria". For example, it rules that: for the water heater with type of high-efficiency gas storage, the energy factor must be bigger than 0.67. Energy factor is also applied to compare the efficiency of clothes washer. For the clothes washer, Energy Star presents the definitions of energy factor (EF) and modified energy factor (MEF). "EF" is the quotient of the capacity of the clothes container, C, divided by the sum of the machine electrical energy for the mechanical action of a cycle, M, and the water heating energy required for a cycle, E. "MEF" is the quotient of the capacity of the clothes container, C, divided by the total clothes washer energy consumption per cycle, with such energy consumption expressed as the sum of the machine electrical energy consumption, M, the hot water energy consumption, E, and the energy required for removal of the remaining moisture in the wash load, D. Generally speaking, energy factor is often used to represent the ratio of useful quantity of work to input energy.

In the field of electrical engineering, the concept of energy factor has been put forward and introduced as stored energy ratio and indicated the implication in efficiency and control by Cheng [79] and Luo [63].

The first goal of this thesis is to describe and clarify the energy behaviour of DC systems, especially DC-DC converters, by introducing a series of novel concepts. Some scholars have initiated this work. Lawrenson has proposed a goodness factor for switched reluctance motor (SRM) to express the ratio of active power processed by SRM[80]. In reference[80], stored energy and co-energy are defined for switched reluctance motors. References [81-83] elaborate the concept of DC power factor and use such definition in the analyses of SRM. In these papers the power factor of a machine system can be examined through operating parameter and switching angle. Similar concepts for DC-DC converters were firstly put forward in references [63, 79, 84, 85]. References [63, 85] propose the concepts of Stored Energy and Energy Factor. The stored energy means the energy stored by DC-DC converters during operation. Energy factor indicates the ratio of the stored energy to the output energy. In these papers Luo applied the stored energy and energy factor to the modeling and control of DC-DC converters. On the other hand, it is noticed that the stored energy of DC-DC converter oscillates all the time during operation, the concepts of Variation of Energy Storage (VES) and Maximum Storage Energy Factor (MSEF) for DC-DC converters have been introduced in Ref. [79] by Cheng. The VES is defined as the difference between the maximum energy and minimum energy stored in the inductor or capacitor of DC-DC converters during one cycle under steady state. MSEF is defined as the ratio of the VES to the input energy of the whole circuit in one cycle. In papers [79, 84], Cheng investigates the characteristics of variation of energy storage for some basic DC-DC converters and their isolated version, and points out the relation between efficiency and variation of energy storage. All the above concepts around energy proposed by the above scholars provide new measurements on the performance of DC-DC converters. However their concepts and definitions cannot provide enough information of non-active power in DC-DC converters, and can only be applied to DC-DC converters instead of all electrical systems.

1.2.2 Extension of reactive power and power factor

As mentioned before, the concepts of active power, reactive power and power factor are very important for the analysis for AC electrical systems. Active power is the average value of instantaneous power. It is defined on the basis of balance of physical energy. In pure sinusoidal AC system, reactive power is the remaining portion of power flow after being averaged over a complete cycle of AC waveform. Along with the widely use of electronic devices and nonlinear loads, the original definition of reactive power meets challenges in the field of compensation for reactive power. So many scholars have attempted to revise and improve the definition of reactive power to make it fit for the application of compensation[86-94]. These improvements of reactive power are mainly based on time-domain or frequency-domain method.

Early in 1930, Fryze has proposed that the input current can be divided into two orthogonal components. One is in phase with the input voltage and has the same shape of waveform as that of input voltage. It is called the active component as it is responsible for the supply of the active power P. Another component is obtained by subtracting the active component from the main input current and is called reactive component as it when multiplied by rms value of voltage would give the reactive power. References[88, 89, 92] extended the Fryze's theory.

The above theories about reactive power are all developed for the problem of compensation for reactive power and to improve power factor. Nowadays power electronic devices are widely used in power control. The electrical systems include power electronic devices are usually nonlinear systems, which means the currents may include lots of harmonics. It is necessary to develop a concept to depict the energy process in such power systems including power electronics devices especially in dc power converters. Some novel concepts such as energy storage, variation of energy storage and energy factor to depict the power phenomenon in dc converters have been proposed by previous scholars[63, 79, 84, 85]. But the research on these concepts is not deep enough. Systematic analysis and comparisons of different topologies of DC converter is lacking. The original definitions for these novel concepts are not generous and can be only applied on DC-DC converters but not all

electrical systems. This thesis extends the concepts proposed in refs. [63, 79, 84, 85] based on the decomposition of current. The gap between the application of these concepts in ac and dc systems is completed by the theory of energy factor developed in this thesis.

1.2.3 Review of works on Tapped-inductor DC-DC converter

Tapped-inductor DC-DC converter has the potential to be widely applied in DC distribution system as the interface between DC bus and point of load (PoL). Tapped-inductor technology provides a simple and feasible method to extend the voltage ratio. Previous scholars have explored this feasibility. In refs.[39, 45, 47, 52] D. A. Grant etc. proposed a classification scheme to categorize the topologies of Tapped-inductor converter. Their scheme systemically and logically lists many possible circuit variants of basic Tapped-inductor converter derived from Buck, Boost and Buck-Boost converter. In [95] K.W. Cheng explored the Tapped-inductor converters derived from the topologies Quadratic Buck, Cuk, switch-capacitor Buck and so on. One of the main drawbacks of Tapped-inductor converter is high voltage spike on the transistors during switching transition. This spike is caused by not full coupling of the tapped inductor. To overcome this problem, many kinds of snubbers and soft switching technologies are proposed[44, 49, 51, 96-98]. The critical mode operation is investigated in [37, 49, 96, 99]. The modeling and control of Tapped-inductor converter is also investigated primarily in Refs [43, 46]. Although lots of work on Tapped-inductor converter have been carried out previously, the comparison in detail between Tapped-inductor converter and conventional converter does not appear in literatures. Most of the above researches on tapped inductor are mainly focused on the static performance. The research of closed-loop operation of Tapped-inductor converter especially applying modern nonlinear control into Tapped-inductor converter has not been explored enough.

1.2.4 Review of works on control methods based on energy storage

Switching device, topology and control form the three main aspects of power electronics technology. Although PID control is still the mainstream in industry application nowadays, but nonlinear control technologies will be much widely applicable to DC-DC converter because of the continuous improvement of digital signal processor (DSP) and Analog-to-Digital (AD) sampling technology.

The theories of classical PID compensation on DC converters are mainly based on the linearized state-space average model [100, 101]. The well designed PID controller can achieve good performance in a certain range around the predetermined static operation point. Usually this range cannot be very wide. Outside this range the preset PID controller will degrade and cannot assure the stability.

Based on the original nonlinear model, nonlinear control algorithms provide alternative ways to implement closed-loop operation of DC-DC converter. Nonlinear controller can provide global asymptotical stability and can still achieve good performance under a large signal disturbance. So far, the nonlinear control methods applied in DC converters include sliding mode control, back step control, feedback linearization, boundary control and passivity-based control [102-111].

In the stability design of nonlinear control methods, energy plays an important role. Some nonlinear control methods are based on the physical energy of system [67]. Passivity-based control (PBC) is a famous control methods and provokes widespread interests in the past twenty years. The basic idea of PBC is to utilize the intrinsic dissipation of nature system and control the injected energy to drive the energy stored in system to the desired level. It also extends into the field of control of power conversion. But the application of PBC are mainly concentrated in classical DC-DC converters, such as Buck, Boost, Buck-Boost and phase-shift full bridge converter. The application of PBC to Tapped-inductor DC-DC converters has not been reported.

1.3 Structure of the thesis

The structure of this thesis is as follows.

Chapter 2 systematically reviews a series of concepts related to the energy stored in DC-DC converters. Based on the works of previous scholars, the characteristics of energy storage are now further explored for the higher order converters including Cuk, Zeta and Sepic. The implication of energy storage on the overall efficiency of these higher order converters is examined.

Chapter 3 extends the definitions of the concepts of buffer energy and buffer energy factor on the basis of active power and non-active power. The redefined buffer energy and buffer energy factor can be applied to depict and analyze

non-active energy of both DC and AC systems. They can be also used explicitly to compare the performance of different DC-DC converters.

Chapter 4 uses Tapped-inductor Boost converter as an example to illustrate the energy storage and energy factors, buffer energy and buffer energy factors of Tapped-inductor converters. The basic principles of operation of Tapped-inductor DC-DC converters are reviewed. Then detailed comparisons between Tapped-inductor Boost and conventional Boost are carried out, which include the comparison of voltage gain, component stress and efficiency. Experimental results present solid verifications to the analysis of performance of Tapped-inductor Boost converter. Similar methods can be extended to other Tapped-inductor DC-DC converters.

Chapter 5 uses passivity-based control to implement closed-loop operation for Tapped-inductor Boost converter. The models of Tapped-inductor Boost converter are elaborated in detail. The overall performances of control are analyzed. Comparisons between peak-current mode control and passivity-based control are carried out.

Chapter 2 Definition and application of Buffer Energy and Energy Factor

This chapter reviews a series of novel concepts related to the energy stored in DC-DC converters. Based on the works in Refs[63, 79, 84, 85], the characteristics of energy storage are now further explored for the higher order converters including Cuk, Zeta and Sepic. The implication of energy storage on the overall efficiency of these higher order converters is examined.

Temporary energy storage is the mechanism for energy conversion in switched-mode power conversion. The classical switched-mode power converters have been fully explored for voltage conversion and control analysis, but its energy handling for each component has not been fully explored. Energy factor has been put forward as a goodness factor and examined in electric machines in papers [81-83] in which the energy factor is used to evaluate the switch reluctance motor. The previous study on energy of DC converter is mainly restricted to the power factor correction externally through a cascaded circuit [91, 112, 113] rather than through the circuit and parameter analysis. The concept of energy factor has been introduced into DC-DC converter as stored energy ratio and indicated the implication in efficiency and control of DC-DC converter by Cheng [79, 84] and Luo [63, 85]. In [79, 84] the characteristics of storage energy for classical and isolated DC-DC converters have identified the relationship of the efficiency and the storage energy. On the other hand, in Refs[63, 85] the energy factor has also been developed for the small signal analysis.

The characteristics of storage energy in three classical higher order dc converters including Cuk, Zeta and Sepic have not been explored. These converters involved a number of passive components and their energy factors under different inductor conduction mode are interesting. Under discontinuous mode, higher order converters are much more complex than the basic converters such as Buck, Boost and Buck-Boost. That is because the higher order converters have two inductors and two capacitors. They have more than one case of discontinuous mode.

2.1 Definition of buffer energy and energy factor

This section presents the basic definitions of buffer energy, energy factor and their associate concepts for DC-DC power conversion. The circuits are assumed to operate under ideal condition including negligible loss and linear magnetic and electric characteristics for inductor and capacitor.

2.1.1 Energy storage E_S

The energy storage of DC-DC converter is defined as the total energy stored in the circuit.

The energy storage components in DC-DC converter can store energy are mainly inductor, capacitor and transformer. During the operation of DC-DC converters, these components absorb and deliver energy periodically. The formulations of energy storage of inductor and capacitor are shown as (2-1) and (2-2), respectively.

$$E_{SL} = \frac{1}{2} L i^2 \tag{2-1}$$

$$E_{SC} = \frac{1}{2} C v^2 \tag{2-2}$$

For transformer, its energy is stored in magnetizing inductor and leakage inductor. So energy storage of transformer can be calculated by (2-1), too.

From (2-1) and (2-2), it can be found that energy storage is time-varying and often has the same period as switching period.

2.1.2 Buffer Energy E_B

For DC-DC converter, the energy stored in inductor or capacitor varies periodically subject to the switching frequency. Buffer energy is defined as the maximum variation of energy storage during one cycle.

The formulation of buffer energy is shown as (2-3).

$$E_B = E_{S\max} - E_{S\min} \tag{2-3}$$

2.1.3 Energy Factor F_E

Energy factor is defined as the ratio of averaged stored energy to output energy in one cycle. The formulation of energy factor of DC-DC converter is shown as (2-4),

where V_o, I_o and T_s are the output voltage, output current and period of the switching cycle, respectively, of the DC system.

$$F_E = \frac{\overline{E}_S}{V_o I_o T_s} \tag{2-4}$$

Energy factor can evaluate the inertia of power converter. High energy factor means slow response of circuit.

2.1.4 Buffer Energy Factor F_{EB}

Buffer energy factor is defined as the ratio of buffer energy to output energy in one cycle. The formulation of buffer energy factor of DC-DC converter is shown as (2-5).

$$F_{EB} = \frac{E_B}{V_o I_o T_s} \tag{2-5}$$

Buffer energy factor reflects the ripple energy ratio which will be discussed later. It can evaluate the magnitude of variation of stored energy. When converter operates, it absorbs energy from source, and delivers energy to load. The stored energy varies cycle by cycle. High buffer energy factor indicates high EMI and low efficiency.

2.2 The characteristics of energy stored in basic converters

The basic second order converters include Buck, Boost and Buck-Boost converters. This section describes the steady-state characteristics of energy stored in these three converters based on the novel concepts proposed in previous section. The methods to calculate the buffer energy and energy factor under steady state are presented.

2.2.1 Energy factors of Buck Converter

- Continuous conduction mode (CCM)

The circuit of Buck converter is shown in Fig. 2-1. The waveforms of current of inductor and voltage of capacitor under CCM are also shown in this figure.

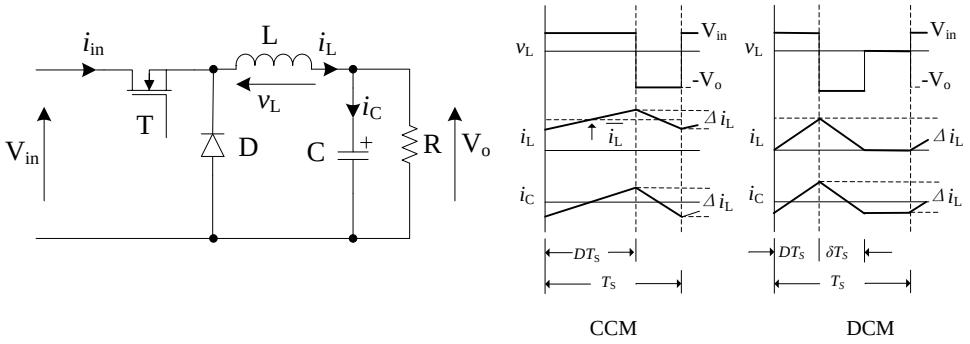

Fig. 2-1 The circuit and waveforms under CCM of Buck converter

- Inductor

The current of inductor vibrates during one cycle. The average inductor current is equal to the output current. According to the previous definition, the average energy storage of inductor of Buck converter in one cycle is

$$\overline{E}_{SL} = \frac{1}{2} L \bar{i}_L^2 = \frac{1}{2} L I_o^2 \tag{2-6}$$

Then the energy factor of inductor can be expressed as

$$F_{EL} = \frac{\overline{E}_{SL}}{V_o I_o T_s} = \frac{L I_o}{2 V_o T_s} = \frac{K}{4} \tag{2-7}$$

where K is a parameter of circuit. It is defined as (2-8).

$$K = \frac{2L}{RT_s} \tag{2-8}$$

Under steady state, in one cycle, the current of inductor increases from a minimum to a maximum and then returns to a minimum. Assume the variation is linear; therefore the buffer energy of inductor can be expressed as (2-9),

$$E_{BL} = \frac{1}{2} L (i_{L\max}^2 - i_{L\min}^2) \tag{2-9}$$

where $i_{L\max}$ and $i_{L\min}$ are the peak and trough values, respectively. If the current waveform has an average current $\overline{i_L}$, under continuous mode, then the expression of buffer energy can be reduced to (2-10).

$$E_{BL} = L\overline{i_L}\Delta i_L \tag{2-10}$$

where Δi_L is the peak-to-peak current ripple of inductor. For Buck converter, this current ripple can be expressed as (2-11).

$$\Delta i_L = \frac{(V_{in} - V_o)DT_s}{L} \tag{2-11}$$

Since

$$\overline{i_L} = I_o \tag{2-12}$$

$$\frac{V_o}{V_{in}} = D = M \tag{2-13}$$

where *D* is the duty ratio, *M* is the voltage conversion ratio. Hence the buffer energy of inductor is simplified as (2-14).

$$E_{BL} = (1-D)V_o I_o T_s \tag{2-14}$$

Then the buffer energy factor is

$$F_{EBL} = \frac{E_{BL}}{V_o I_o T_s} = 1 - D = 1 - M \tag{2-15}$$

- Capacitor

The average energy storage of inductor of Buck converter in one cycle is

$$\overline{E}_{SC} = \frac{1}{2}C\overline{v}_C^2 = \frac{1}{2}CV_o^2 \tag{2-16}$$

Then the energy factor of capacitor can be expressed as (2-17).

$$F_{EC} = \frac{\overline{E}_{SC}}{V_o I_o T_s} = \frac{CR}{2T_s} \tag{2-17}$$

The buffer energy of capacitor is

$$E_{BC} = \frac{1}{2}C(v_{C\max}^2 - v_{C\min}^2) \tag{2-18}$$

The average voltage of capacitor is equal to the output voltage of Buck converter. Then the expression of buffer energy can be reduced to (2-19).

$$E_{BC} = CV_o \Delta v_C \tag{2-19}$$

where Δv_C is the peak-to-peak voltage ripple of capacitor. For Buck converter, this voltage ripple can be expressed as (2-20)[114].

$$\Delta v_C = \frac{1}{C}\int_{+ic} i_C dt = \frac{V_o(1-D)T_s^2}{8LC} \tag{2-20}$$

Hence the buffer energy can be transformed into (2-21) equivalently.

$$E_{BC} = \frac{(1-D)V_o^2 T_s^2}{8L} \tag{2-21}$$

Then the buffer energy factor is

$$F_{EBC} = \frac{E_{BC}}{V_o I_o T_s} = \frac{1-M}{4K} \tag{2-22}$$

- Discontinuous conduction mode (DCM)

The waveforms of current and voltage of Buck converter under DCM are shown in Fig. 2-1.

➢ Inductor

Under DCM, the current ripple of inductor is very large. The average energy storage is

$$\overline{E}_{SL} = \frac{1}{2}L\bar{i}_L^2 = \frac{1}{2}LI_o^2 \tag{2-23}$$

Then the energy factor of inductor can be expressed as (2-24)

$$F_{EL} = \frac{\overline{E}_{SL}}{V_o I_o T_s} = \frac{LI_o}{2V_o T_s} = \frac{K}{4} \tag{2-24}$$

Assuming the variation linear, therefore the buffer energy of inductor under steady state can be expressed as (2-25).

$$E_{BL} = \frac{1}{2}L(i_{L\max}^2 - i_{L\min}^2) = \frac{1}{2}L\Delta i_L^2 \tag{2-25}$$

Under DCM, the voltage conversion ratio is

$$\frac{V_o}{V_{in}} = M = \frac{2}{1+\sqrt{1+4K/D^2}} \tag{2-26}$$

$$\frac{K}{D^2} = \frac{1-M}{M^2} \tag{2-27}$$

Then the current ripple of inductor can be expressed as (2-28).

$$\Delta i_L = \frac{(V_{in}-V_o)DT_s}{L} = 2I_o\frac{M}{D} \tag{2-28}$$

Hence the buffer energy can be simplified as (2-29).

$$E_{BL} = 2LI_o^2M^2/D^2 \tag{2-29}$$

The buffer energy factor can be obtained as (2-30).

$$F_{EBL} = \frac{E_{BL}}{V_oI_oT_s} = 1-M \tag{2-30}$$

- Capacitor

The average energy storage of capacitor is

$$\overline{E}_{SC} = \frac{1}{2}C\overline{v}_C^2 = \frac{1}{2}CV_o^2 \tag{2-31}$$

Then the energy factor of capacitor can be expressed as (2-32).

$$F_{EC} = \frac{\overline{E}_{SC}}{V_oI_oT_s} = \frac{CR}{2T_s} \tag{2-32}$$

Under DCM, the voltage of capacitor is still continuous. Hence the buffer energy of capacitor can be obtained by (2-33).

$$E_{BC} = CV_o\Delta v_C \tag{2-33}$$

The ripple of voltage of capacitor can be obtained by integrating the positive part of current waveform of capacitor. The detail is shown in (2-34).

$$\Delta v_C = \frac{1}{C}\int_{+i_C} i_C dt = \frac{(D+\delta)T_s(\Delta i_L - I_o)^2}{2C\Delta i_L} \tag{2-34}$$

Substitute (2-34) into (2-33), we can obtain the buffer energy of capacitor under

DCM as (2-35).

$$E_{BC} = \frac{1}{4}(2 - \frac{D}{M})^2 V_o I_o T_s \tag{2-35}$$

Then the buffer energy factor of capacitor under DCM can be expressed as (2-36)

$$F_{EBC} = \frac{E_{BC}}{V_o I_o T_s} = \frac{1}{4}(2 - \sqrt{\frac{K}{1-M}})^2 \tag{2-36}$$

The above results of calculation are summarized in TABLE 2-1 for comparison.

2.2.2 Energy factors of Boost and Buck-Boost Converter

The buffer energy and energy factors of Boost and Buck-Boost converter can be deducted by the same procedure to the Buck converter in section 2.2.1. The results are also put together in TABLE 2-1.

Special attention should be paid on the deduction of buffer energy factor of capacitor in Boost and Buck-Boost converters under DCM. That is because the current of capacitor has five cases shown in Fig. 2-2. This property does not appear in Buck converter.

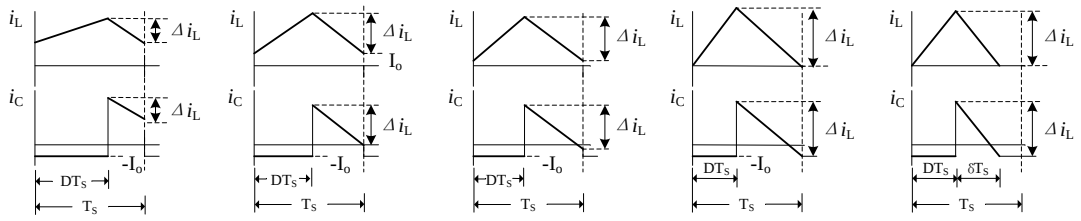

	(a)	(b)	(c)	(d)	(e)
	CCM 1	**Boundary**	**CCM 2**	**Boundary**	**DCM**
Boost	$K > (1-D)^2$	$K = (1-D)^2$	$K > D(1-D)^2$ $K < (1-D)^2$	$K = D(1-D)^2$	$K < D(1-D)^2$
Buck-Boost	$K > (1-D)^2 / D$	$K = (1-D)^2 / D$	$K > (1-D)^2$ $K < (1-D)^2 / D$	$K = (1-D)^2$	$K < (1-D)^2$

Fig. 2-2 Waveforms of current of capacitor in Boost and Buck-Boost converters under different modes

From the above figures it can be found that case b and case d are two critical conditions. Case a is corresponding to continuous mode. Case c and case e are two discontinuous modes which are DCM mode 1 and DCM mode 2. The differences of modes affect the calculation of buffer energy and energy factor of capacitor. Hence the buffer energy and energy factor of capacitor must be calculated separately. In fact DCM mode 1 (case c) is the intermediate mode. Separate calculation of energy factor on this mode can make sure the continuity [79]. The results of three modes of Buck-Boost converter can be found in TABLE 2-1.

2.2.3 Comparison of energy factors of basic converters

TABLE 2-1 put together all the energy factors and buffer energy factors of the three converters under both CCM and DCM.

In this table, R, L and C are resistance, inductance and capacitance, respectively. T_s is the switching period. $K=2L/(RT_s)$, D is the duty ratio. M is the voltage conversion ratio. The expression of M for the three converters under CCM and DCM can be found in Ref[114].

- Comments on energy factors

Energy factor represents the ratio of stored energy to output energy. To export certain amount of energy (or power), the DC-DC converter must store a corresponding amount of energy first. The ratio of stored energy to output energy is different for different converters.

TABLE 2-1 Energy factors and buffer energy factors of basic converters

Converters	Modes	Energy factor (F_E)			Buffer energy factor (F_{EB})		
		Inductor (F_{EL})	Capacitor (F_{EC})	Ratio (F_{EL}/F_{EC})	Inductor (F_{EBL})	Capacitor (F_{EBC})	Ratio (F_{EBL}/F_{EBC})
Buck	CCM	$\frac{K}{4}$	$\frac{CR}{2T_s}$	$\frac{L}{CR^2}$	$1-M$	$\frac{1-M}{4K}$	$4K$
	DCM					$\frac{1}{4}(2-\sqrt{\frac{K}{1-M}})^2$	$\frac{4(1-M)^2}{(2\sqrt{1-M}-\sqrt{K})^2}$
Boost	CCM1	$\frac{KM^2}{4}$	$\frac{CR}{2T_s}$	$\frac{LM^2}{CR^2}$	$1-\frac{1}{M}$	$1-\frac{1}{M}$	1
	CCM 2					$\frac{(1-D)^2D}{4K}[1+\frac{K}{(1-D)^2}]^2$	$\frac{4D(1-D)^2}{M^2[(1-D)^2+K)]^2}$
	DCM					$\frac{1}{4}(2-\sqrt{\frac{KM}{M-1}})^2$	$\frac{4(M-1)}{M(2-\sqrt{\frac{KM}{M-1}})^2}$
Buck-Boost	CCM1	$\frac{K(1+M)^2}{4}$	$\frac{CR}{2T_s}$	$\frac{L(1+M)^2}{CR^2}$	1	$\frac{M}{1+M}$	$\frac{1+M}{M}$
	CCM 2					$\frac{1}{4K}(1-D+\frac{KD}{1-D})^2$	$\frac{4K}{(1-D+\frac{KD}{1-D})^2}$
	DCM					$\frac{1}{4}(2-\sqrt{K})^2$	$\frac{4}{(2-\sqrt{K})^2}$

From TABLE 2-1, it can be found that the energy factors of capacitor are the same for three converters. They only depend on the circuit parameters and are not affected by the voltage conversion ratio. On the other hand, the ratios of energy stored by inductor are different for the three converters. Only the energy factor of Buck converter has no relationship with voltage gain. The energy factors of inductor of Boost and Buck-Boost converter increases along with the increase of voltage conversion ratio. Obviously, Buck-Boost converter has the highest energy factor, while Buck converter has the lowest energy factor. That indicates that to deliver the same power, Buck-Boost converter has to store the most energy, while the energy that Buck converter needs to store is the least. From this table, we can also find that the ratio of inductor's energy factor to capacitor's energy factor depends on the circuit parameters including L, C and R. In Boost and Buck-Boost converters, this ratio is also related to the voltage conversion ratio M. When M increases, the ratio also increases.

- Comments on buffer energy factors

Buffer energy factor can reflect the amplitude of variation of energy stored in converter. During operation of DC-DC converter, the stored energy varies over a cycle. The variation of energy will induce extra loss to the circuit including copper loss and core loss, and also cause more severe EMI. From TABLE 2-1, it can be found that buffer energy factor is related to circuit parameter K (equal to $2L/(RT_s)$, see equation (2-8)), voltage gain M and duty ratio D.

- Buck converter

The total buffer energy factor F_{EB} is the summation of buffer energy factor of inductor and capacitor. Fig. 2-3 shows the F_{EB} of Buck converter as a function of voltage gain M for various values of K. It can be seen that for the Buck converter, F_{EB} decreases as M increases and K increases. For $K \geq 1$, the relationship is linear. For $K<1$, the characteristic exhibits a portion of nonlinearity because of the discontinuous conduction mode.

The ratios of buffer energy factor of inductor to that of capacitor are shown in Fig. 2-4. The buffer energy of inductor is larger than capacitor when K is a high value. That indicates that, during the operation of DC-DC converter, the variation of energy

storage of inductor is bigger than that of capacitor. Under DCM ($K \leq 0.1$), the value of F_{EBL}/F_{EBC} decreases as M increases. That means, under DCM, the capacitor suffers bigger variation of energy storage than inductor.

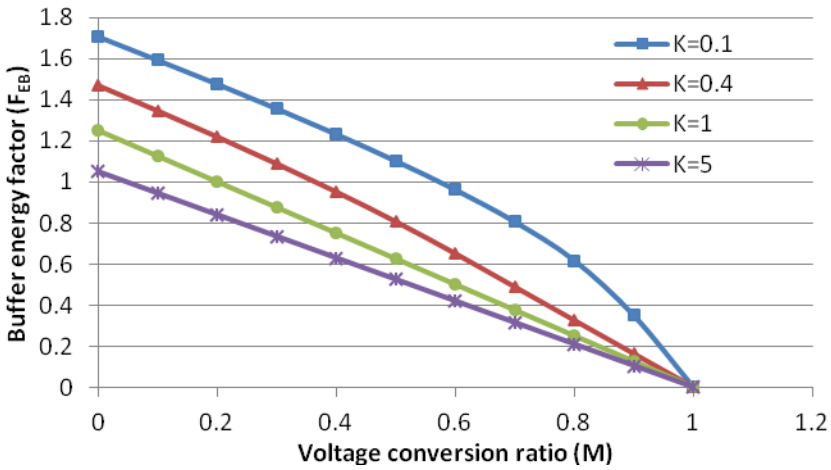

Fig. 2-3 Buffer energy factor of Buck converter against voltage gain

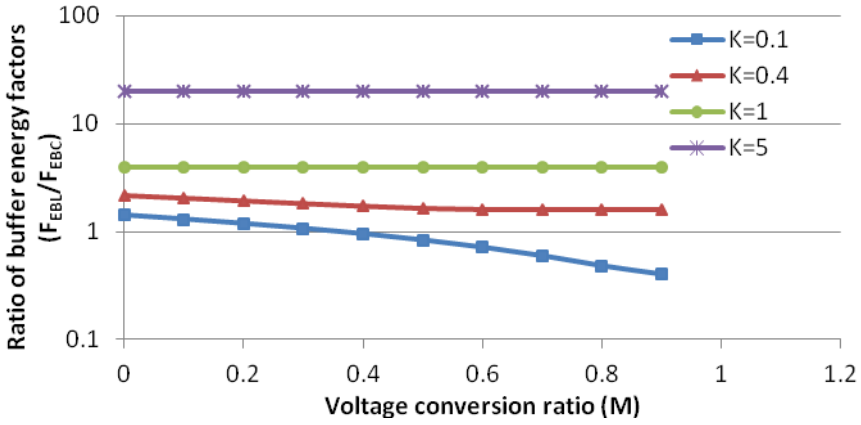

Fig. 2-4 Ratio of buffer energy factor of Buck converter against voltage gain

- Boost converter

Fig. 2-5 shows the F_{EB} for Boost converter against voltage gain M. Its characteristic is different from that of Buck converter. F_{EB} of Boost converter increases as M increases and K decreases. Fig. 2-6 shows the ratio F_{EBL}/ F_{EBC} against M. The ratio increases as M increases and K increases. And the ratio is always smaller than one. That means the buffer energy of capacitor is always bigger than that of inductor, especially under small voltage gain and small value of K.

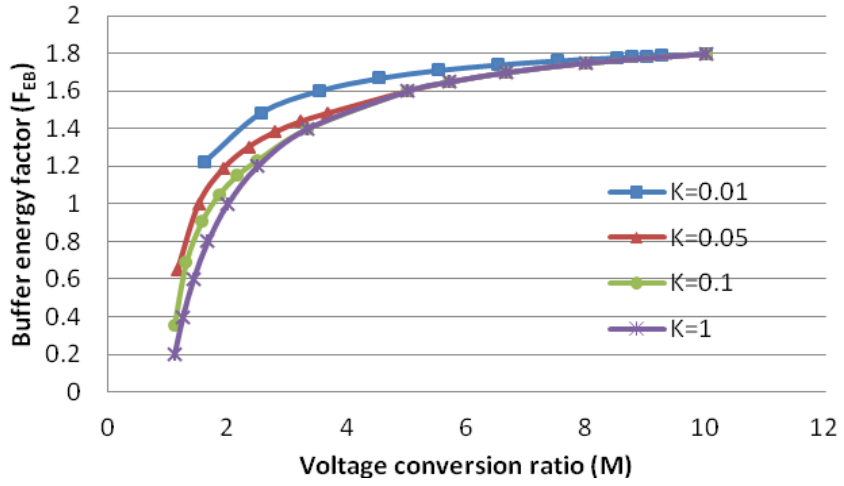

Fig. 2-5 Buffer energy factor of Boost converter against voltage gain

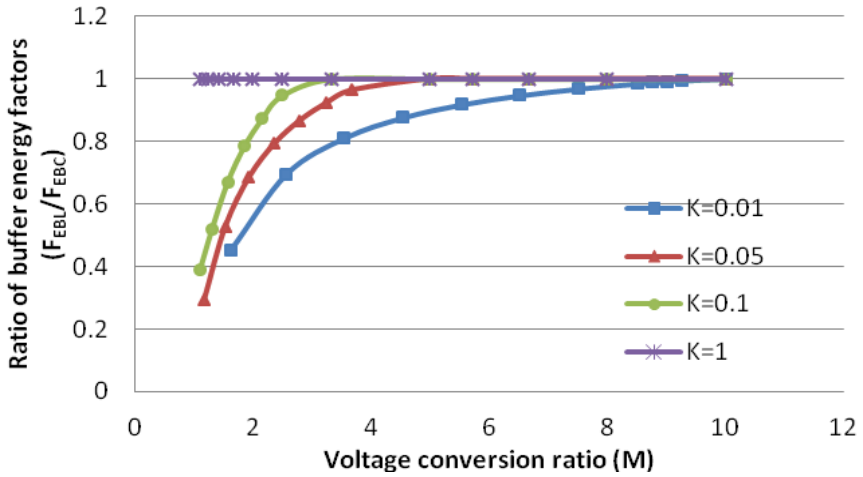

Fig. 2-6 Ratio of buffer energy factor of Boost converter against voltage gain

- Buck-Boost converter

Fig. 2-7 shows the F_{EB} for Buck-Boost converter against voltage gain M. F_{EB} of Buck-Boost converter increases as M increases and K decreases. That means the Buck-Boost converter stores more energy under higher voltage gain and smaller K value. Fig. 2-8 shows the ratio F_{EBL}/F_{EBC} against M. The ratio decreases as M increases and K decreases. And the ratio is always bigger than one. That means the buffer energy of inductor is always bigger than that of capacitor, especially under small voltage gain and big value of K.

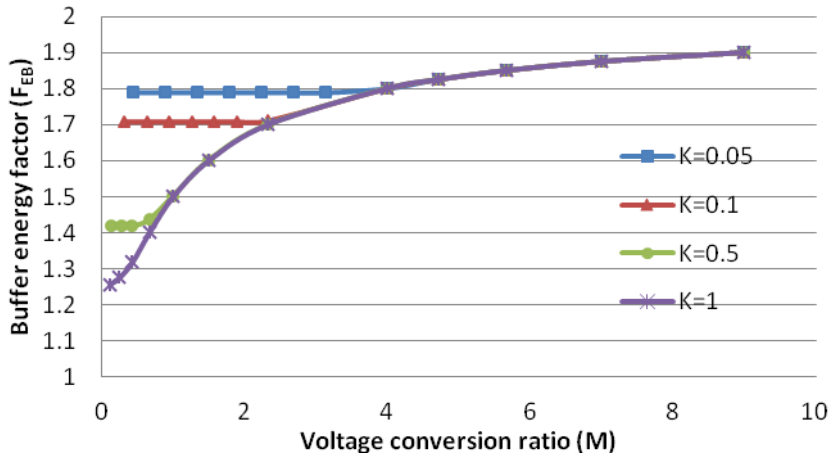

Fig. 2-7 Buffer energy factor of Buck-Boost converter against voltage gain

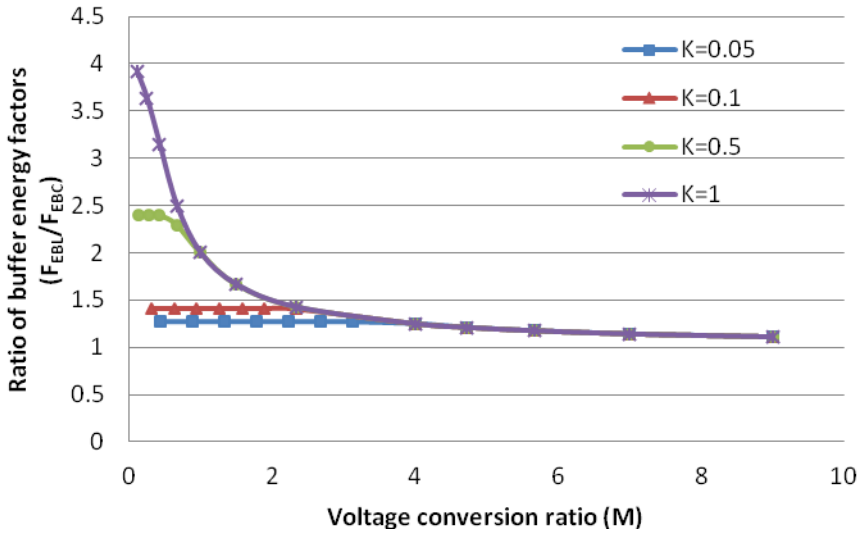

Fig. 2-8 Ratio of buffer energy factor of Buck-Boost converter against voltage gain

In general, for all the three converters, buffer energy factor increases as *K* decreases. That means the variation of energy storage increases as *L* decreases, *R* increases and switching period increases. These are reasonable as it implies the less storage energy being processed.

2.3 The characteristics of energy stored in high order converters

The basic high order converters include Cuk, SEPIC and Zeta converters. This section describes the steady-state characteristics of energy stored in these three

converters based on the novel concepts proposed in section 2.1. These high order converters have four energy-storage components: two inductors and two capacitors. The increased numbers of energy-storage components raise the complexity of analysis. The methods to calculate the buffer energy and energy factors for the three converters are presented.

2.3.1 Energy factors of Cuk Converter

As shown in Fig. 2-9, Cuk converter is a combination of Boost and Buck converters [100, 101]. The operation of Cuk converter has continuous mode (CCM) and discontinuous mode (DCM). Fig. 2-10 shows the process from CCM to DCM. It is noted that the DCM of Cuk converter is obviously more complex than the basic second order converters. Here only researches the case that inductor L_2 works under DCM. It has two modes under DCM as shown in Fig. 2-10.

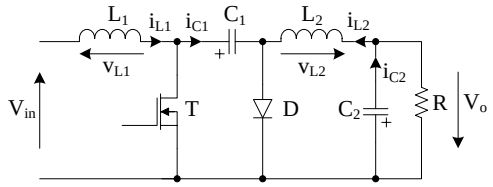

Fig. 2-9 Circuit of Cuk converter

- Continuous conduction mode (CCM)

Fig. 2-10 (a) shows the typical waveforms of Cuk converter under CCM.

The average energy storages of the four energy-storage components are shown as (2-37) ~ (2-40).

$$\overline{E}_{SL1} = \frac{1}{2} L_1 I_{in}^2 \tag{2-37}$$

$$\overline{E}_{SC1} = \frac{1}{2} C_1 (V_{in} + V_o)^2 \tag{2-38}$$

$$\overline{E}_{SL2} = \frac{1}{2} L_2 I_o^2 \tag{2-39}$$

$$\overline{E}_{SC2} = \frac{1}{2} C_2 V_o^2 \tag{2-40}$$

Then the energy factors of these components can be obtained through dividing the average energy storage by output energy of the converter in one cycle. The results

are shown as (2-41) ~ (2-44).

$$F_{EL1} = \frac{\overline{E}_{SL1}}{V_o I_o T_s} = \frac{1}{4} K_1 M^2 \tag{2-41}$$

$$F_{EC1} = \frac{RC_1}{2T_s}(1+\frac{1}{M})^2 \tag{2-42}$$

$$F_{EL2} = \frac{1}{4} K_2 \tag{2-43}$$

$$F_{EC2} = \frac{RC_2}{2T_s} \tag{2-44}$$

where K_1 and K_2 are constants determined by the parameters of circuit. They are defined as follows. L_1 and L_2 are inductances of the two inductors of Cuk converter, respectively. R is the resistance of load. T_s is the switching period. Such definitions for K_1, K_2 and K hold true for the analysis of Zeta and Sepic converters.

$$K_1 = 2L_1/(RT_s) \tag{2-45}$$

$$K_2 = 2L_2/(RT_s) \tag{2-46}$$

$$K = K_1 K_2/(K_1 + K_2) \tag{2-47}$$

Next the method to obtain buffer energy factor will be presented. The current ripple and average current of inductor L_1 under CCM can be expressed as

$$\Delta i_{L1} = V_{in} D T_s / L_1 \tag{2-48}$$

$$\bar{i}_{L1} = I_{in} \tag{2-49}$$

The buffer energy and energy factor of inductor L_1 can be obtained as following expressions.

$$E_{BL1} = L_1 \bar{i}_{L1} \Delta i_{L1} = D V_o I_o T_s \tag{2-50}$$

$$F_{EBL1} = \frac{E_{BL1}}{V_o I_o T_s} = D \tag{2-51}$$

The buffer energy factors of component L_2, C_1, and C_2 of Cuk converter under CCM can be worked out by the same procedure as that of L_1. The results are listed in TABLE 2-2.

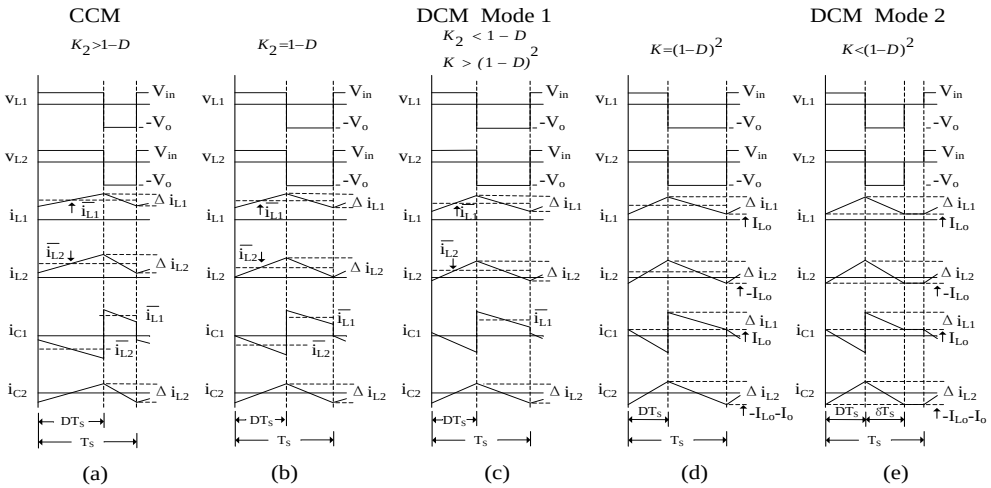

Fig. 2-10 Operation waveforms of Cuk converter under different mode

K_1, K_2 and K are defined as (2-45) ~ (2-47) respectively.

- Discontinuous conduction mode (DCM)

The inductor currents of Cuk converter for discontinuous mode analysis should be considered for the interaction between the two inductors L_1 and L_2. The Cuk converter is symmetrical for input and output when bi-directional switch scheme is used. The analysis is firstly started with the discontinuous mode of output inductor, i.e. L_2 (The case for discontinuous mode of L_1 is similar and will not be repeated here). Secondly, when the basic converters go into discontinuous mode, the inductor current will be zero during off time. But when Cuk converter goes into discontinuous mode, the inductor current can be reversed. This leads to more than one situation for the DCM of Cuk converter. As Fig. 2-10 shows, if L_2 works in discontinuous mode, then during off time, its current should be initially zero, and then decreases until the diode stops conduction. The waveforms in Fig. 2-10 show the course to the discontinuous mode.

There are three situations of DCM of Cuk converter. The critical points between these situations are: 1) at the end of off time, i_{L2} touches zero; 2) i_{L2} reverses, but i_D reaches zero at the end of off time. Fig. 2-10 (b) and (d) show these two critical situations. So there are totally two discontinuous modes for the Cuk converter and their start points are the above two critical situations, which can be determined by the circuit parameters.

Now parameters about storage energy for the two discontinuous modes of Cuk

converter shown in Fig. 2-10 are calculated below.

➢ Mode 1

This mode is between critical situations b) and d) in Fig. 2-10. The critical condition from CCM to this mode is

$$\Delta i_{L2} = 2I_o \tag{2-52}$$

Then by waveform analysis, the critical condition can be simplified as (2-53).

$$K_2 = 1 - D \tag{2-53}$$

✧ Inductor L_1:

As Fig. 2-10 (c) shows, the situation of L_1 is the same as that under CCM. Therefore

$$F_{EBL1} = D \tag{2-54}$$

✧ Inductor L_2:

The maximum variation of storage energy is

$$E_{BL2} = L_2 i_{L2\max}^2 / 2 \tag{2-55}$$

Since

$$i_{L2\max} = I_o + \Delta i_{L2} / 2 \tag{2-56}$$

Substituting (2-56) into (2-55), it follows that

$$E_{BL2} = \frac{1}{2} L_2 I_o^2 (1 + \frac{1-D}{K_2})^2 \tag{2-57}$$

$$F_{EBL2} = (1 + K_2 - D)^2 / (4K_2) \tag{2-58}$$

✧ Capacitor C_1:

As Fig. 2-10 (c) shows that，

$$\overline{V}_{C1} = V_{in} + V_o \tag{2-59}$$

ΔV_{C1} can be obtained through integrating the area below the horizontal axes of i_{C1}.

$$\Delta V_{C1} = \frac{1}{C_1} (\frac{I_o}{\Delta i_{L2}} + \frac{1}{2})^2 \cdot \frac{1}{2} \cdot DT_s \cdot \Delta i_{L2} \tag{2-60}$$

Substituting (2-59) and (2-60) into (2-4), one can get

$$F_{EBC1} = \frac{(K_2 + 1 - D)^2}{4K_2(1-D)} \tag{2-61}$$

✧ Capacitor C_2:

As Fig. 2-10 (c) shows, under this mode, the situation of C_2 is the same as that under CCM. So

$$F_{EBC2} = (1-D)/(4K_2) \tag{2-62}$$

➢ Mode 2

This mode emerges after the critical situation (d) occurs in Fig. 2-10. The critical condition from DCM mode 1 to this mode is

$$K = (1-D)^2 \tag{2-63}$$

There is a flat part in the waveforms of i_{L1} and i_{L2}. The value I_{Lo} of the flat part can be expressed by circuit parameters[114]. Here only the results of I_{Lo} and voltage conversion ratio are provided.

$$I_{Lo} = V_{in} D T_S (D/L_2 - \delta/L_1)/2 \tag{2-64}$$

$$V_o / V_{in} = D/\delta \tag{2-65}$$

where $\delta = \sqrt{K}$.

✧ Inductor L_1:

As Fig. 2-10 (e) shows, the buffer energy of inductor L_1 can be expressed as

$$E_{BL1} = \frac{1}{2} L_1 [(I_{Lo} + \Delta i_{L1})^2 - I_{LO}^2] \tag{2-66}$$

Substitute (2-64) and (2-66) into (2-4), one can get

$$F_{EBL1} = 1 - \delta + (D + \delta - 1)K/K_2 \tag{2-67}$$

✧ Inductor L_2:

$$E_{BL2} = \frac{1}{2} L_2 (\Delta i_{L2} - I_{LO})^2 \tag{2-68}$$

Substitute (2-64) and (2-68) into (2-4), then

$$F_{EBL2} = K_2 K[\delta / K + (2 - D - \delta) / K_2]^2 / 4 \tag{2-69}$$

✧ Capacitor C_1:

Similar to the calculation in Mode 2, the ripple of voltage of capacitor C_1 can be obtained by calculation of the area in waveform of i_{C1} under the horizontal-axis. According to the principle of similar triangles, so

$$\Delta V_{C1} = \frac{1}{C_1} \cdot (\frac{\Delta i_{L2} - I_{Lo}}{\Delta i_{L2}})^2 \cdot \frac{1}{2} \cdot DT_S \cdot \Delta i_{L2} \tag{2-70}$$

$$\overline{V}_{C1} = V_{in} + V_o \tag{2-71}$$

Substituting (2-64) and (2-71) into (2-4):

$$F_{EBC1} = \frac{\delta(D+\delta)}{K_2}(1 - \frac{D+\delta}{2} + \frac{K_2 \delta}{2K})^2 \tag{2-72}$$

✧ Capacitor C_2:

$$\overline{V}_{C2} = V_o \tag{2-73}$$

ΔV_{C2} can be calculated by the waveform area of C_2 above the horizontal axis. That is:

$$\Delta V_{C2} = \frac{1}{C_2} \cdot \frac{1}{2}(D+\delta)T_S \cdot \Delta i_{L2} \cdot (\frac{\Delta i_{L2} - I_o - I_{Lo}}{\Delta i_{L2}})^2 \tag{2-74}$$

Substituting (2-64) and (2-74) into (2-4), then

$$F_{EBC2} = (1 - D/2 - \delta/2)^2 (1 + D/\delta) K / K_2 \tag{2-75}$$

Results of buffer energy factor of all reactive components under different modes are listed in TABLE 2-2. Their sum under each mode is the total buffer energy factor for the whole circuit.

TABLE 2-2 Buffer energy factors of components in Cuk converter

Cuk	F_{EBL1}	F_{EBL2}	F_{EBC1}	F_{EBC2}
CCM	D	$1-D$	1	$\frac{1-D}{4K_2}$
DCM Mode 1	D	$\frac{(1+K_2-D)^2}{4K_2}$	$\frac{(1+K_2-D)^2}{4K_2(1-D)}$	$\frac{1-D}{4K_2}$
DCM Mode 2	$1-\delta+(D+\delta-1)\frac{K}{K_2}$	$\frac{K_2K}{4}\left(\frac{\delta}{K}+\frac{2-D-\delta}{K_2}\right)^2$	$\frac{\delta(D+\delta)}{K_2}\left(\frac{2-D-\delta}{2}+\frac{K_2\delta}{2K}\right)^2$	$\left(1-\frac{D+\delta}{2}\right)^2\cdot\frac{D+\delta}{\delta}\frac{K}{K_2}$

TABLE 2-3 Buffer energy factors of components in Zeta converter

Zeta	F_{EBL1}	F_{EBL2}	F_{EBC1}	F_{EBC2}
CCM	D	$1-D$	$1-D$	$\frac{1-D}{4K_2}$
DCM Mode 1	D	$\frac{(1+K_2-D)^2}{4K_2}$	$\frac{D(1+K_2-D)^2}{4K_2(1-D)}$	$\frac{1-D}{4K_2}$
DCM Mode 2	$1-\delta+(D+\delta-1)\frac{K}{K_2}$	$\frac{K_2K}{4}\left(\frac{\delta}{K}+\frac{2-D-\delta}{K_2}\right)^2$	$\frac{\delta D}{K_2}\left(\frac{2-D-\delta}{2}+\frac{K_2\delta}{2K}\right)^2$	$(1-\frac{D+\delta}{2})^2\cdot\frac{D+\delta}{\delta}\frac{K}{K_2}$

TABLE 2-4 Buffer energy factors of components in Sepic converter

Sepic	F_{EBL1}	F_{EBL2}	F_{EBC1}	F_{EBC2}
CCM	D	$1-D$	$1-D$	D or $\frac{(1-D)^2}{4K}\cdot[1+\frac{DK}{(1-D)^2}]^2$
DCM Mode 1	D	$\frac{(1+K_2-D)^2}{4K_2}$	$\frac{(1+K_2-D)^2}{4K_2}$	
DCM Mode 2	$1-\delta+(D+\delta-1)\frac{K}{K_2}$	$\frac{K_2K}{4}\left(\frac{\delta}{K}+\frac{2-D-\delta}{K_2}\right)^2$	$\frac{\delta^2}{K_2}\left(\frac{2-D-\delta}{2}+\frac{K_2\delta}{2K}\right)^2$	$\frac{(2\delta-K)^2}{4K}$

2.3.2 Buffer energy factors of Zeta and Sepic Converter

Typical Zeta and Sepic converters are shown in Fig. 2-11 and Fig. 2-12. Their operational waveforms are similar to that of the Cuk converter[114]. The process from CCM to DCM also resembles that of Cuk converter. They also have two modes under DCM.

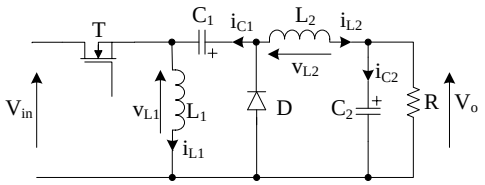

Fig. 2-11 Circuit of Zeta converter

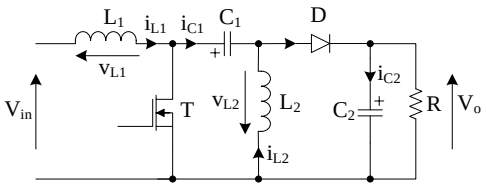

Fig. 2-12 Circuit of Sepic converter

The buffer energy factor of the reactive components of Zeta and Sepic converters can be easily deduced based on the results of Cuk converter. Their expressions under different modes are listed in TABLE 2-3 and TABLE 2-4. Their sums under each mode are the total buffer energy factors for the whole circuits.

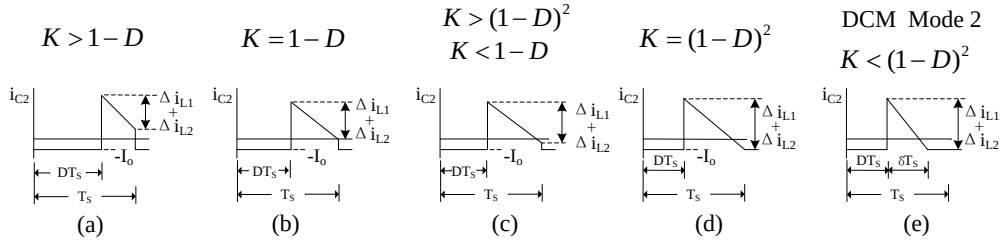

Fig. 2-13 Operation waveforms of capacitor C_2 in Sepic under different modes

The boundary conditions between different modes of Zeta and Sepic converters are the same as those of Cuk converter shown in Fig. 2-10. Special attention should be paid to the voltage waveform of C_2 in Sepic. It is different from that in Cuk and Zeta converters. This will cause the boundary conditions between states of C_2 in Sepic to be different from those in Cuk and Zeta converters. The operation of C_2 in Sepic still has three states as illustrated by Fig. 2-13. In the five states in Fig. 2-13, (b) and (d) are boundary states. State (e) corresponds to the DCM mode 2. But states (a) and (c) can be taken place at any moment during CCM and DCM Mode 1. It depends on the value of *K* and *D*. In fact, based on Fig. 2-13, the boundary condition for state (b), which is the transition from (a) to (c), can be calculated as follows:

$$\bar{i}_{L1} - \frac{1}{2}\Delta i_{L1} + \bar{i}_{L2} - \frac{1}{2}\Delta i_{L2} - I_o = 0 \tag{2-76}$$

Simplifying (2-76), the boundary condition for the transitional state (b) is:

$$K = 1 - D \tag{2-77}$$

It can be seen that this boundary condition is different from $K_2 = 1 - D$, which is

the boundary condition from CCM to DCM Mode 1 in Cuk and Zeta converter.

The buffer energy factor of C_2 in Sepic can be easily deduced like the buffer energy factor of other reactive components. Its results are listed in TABLE 2-4.

2.4 The consolidation of the energy factor

Fig. 2-14 ~ Fig. 2-16 show the buffer energy factor of Cuk, Zeta and Sepic converters as a function of duty ratio D. For simplicity, K=K_2 are assumed. This assumption is justified when K_2 is much smaller than K_1. K_1, K_2 and K are defined as (2-45) ~ (2-47) respectively. It is also noted that L_1 works in CCM.

All three converters have continuity characteristics between different operation modes. The boundary conditions between different operation modes are the same for all three converters. Fig. 2-14 ~ Fig. 2-16 also illuminate the continuity of the curves.

Fig. 2-14 shows the characteristics of buffer energy factor (F_{EB}) of the Cuk converter. It can be seen that for Cuk converter, buffer energy factor is always larger than 2. It decreases as K increases. For $K \geq 1$, the relationship between buffer energy factor and D is linear. F_{EB} decreases as D increases. For $K < 1$, the characteristic exhibits a portion of nonlinearity because of the discontinuous inductor conduction mode. The lower limit of buffer energy factor is 2 and is independent of K. It occurs even when the transistor is always turned on.

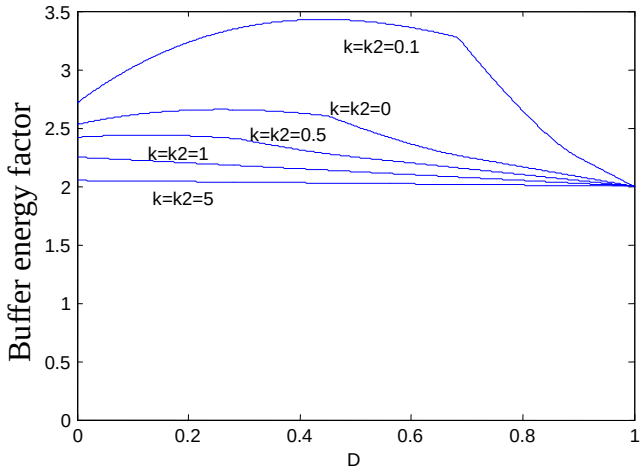

Fig. 2-14 Buffer energy factor of the Cuk converter

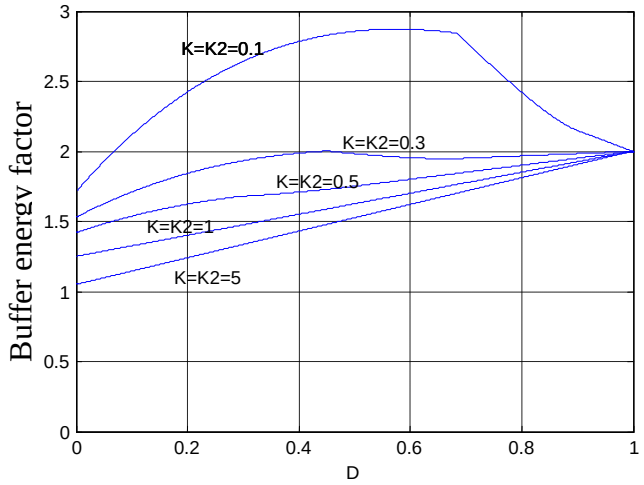

Fig. 2-15 Buffer energy factor of the Zeta converter

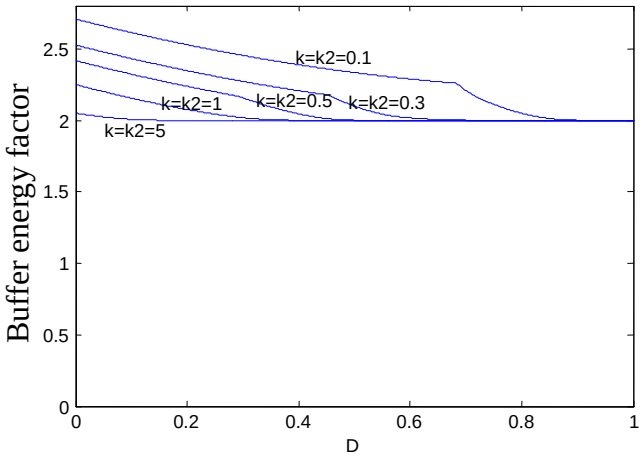

Fig. 2-16 Buffer energy factor of the Sepic converter

The characteristic of buffer energy factor of Zeta converter is shown in Fig. 2-15, which is different from that of the Cuk converter. Buffer energy factor of Zeta also decreases when K increases. F_{EB} varies linearly with D when $K \geq 1$. It reaches maximum value of 2 at $D=1$. For $K<1$, the nonlinear portion of the curve is again due to discontinuous mode. And the maximum value of buffer energy factor does not occur at $D=1$, but occurs when D is at certain value between 0 and 1.

Fig. 2-16 shows characteristics of buffer energy factor of Sepic. It can be seen that the buffer energy factor of Sepic is always not less than 2. It decreases as K and D increase. For $K \geq 1$, a large portion of buffer energy factor maintains the value of 2. For $K < 1$, the characteristic exhibits a portion of nonlinearity again because of the

discontinuous mode. Buffer energy factor reaches the maximum value when the transistor is always turned on.

In general, for all the three converters, buffer energy factor increases as K decreases. This is the universal property shared by the three basic first order converters (Buck, Boost and Buck-Boost converters).

2.5 Experimental results

Fig. 2-17 and Fig. 2-18 show the experimental results of efficiency against buffer energy factor for Cuk and Zeta converter. The circuits for experiments are the same as Fig. 2-9 and Fig. 2-11, L_1=L_2=340μH, C_1=C_2=220μF, f_s=100kHz, the load is set as R=10.07Ω, output voltage is set as V_o=30V and output power is set as 90W. Then the values of K_1, K_2 and K can be calculated out. They are K_1=K_2=6.8, K=3.4. Low $R_{ds(on)}$ MOSFET IRFB4227PBF is used. The converters work under the continuous mode. Duty ratio is varied to give different buffer energy factors for the experiments. The buffer energy factor covers 2.0096-2.0284 for the Cuk converter and 1.272-1.754 for the Zeta converter. Beyond this range it will be very difficult to operate due to either a very large voltage or current in the circuits. Fig. 2-17 and Fig. 2-18 show that the efficiency decreases as buffer energy factor increases for most values of buffer energy factor as expected.

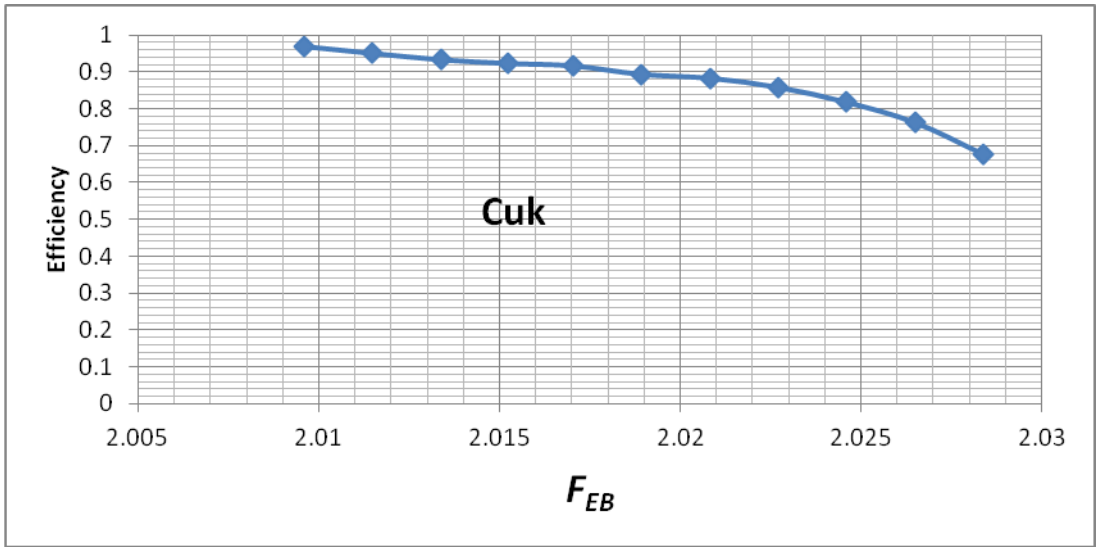

Fig. 2-17 Efficiency against Buffer energy factor of Cuk converter

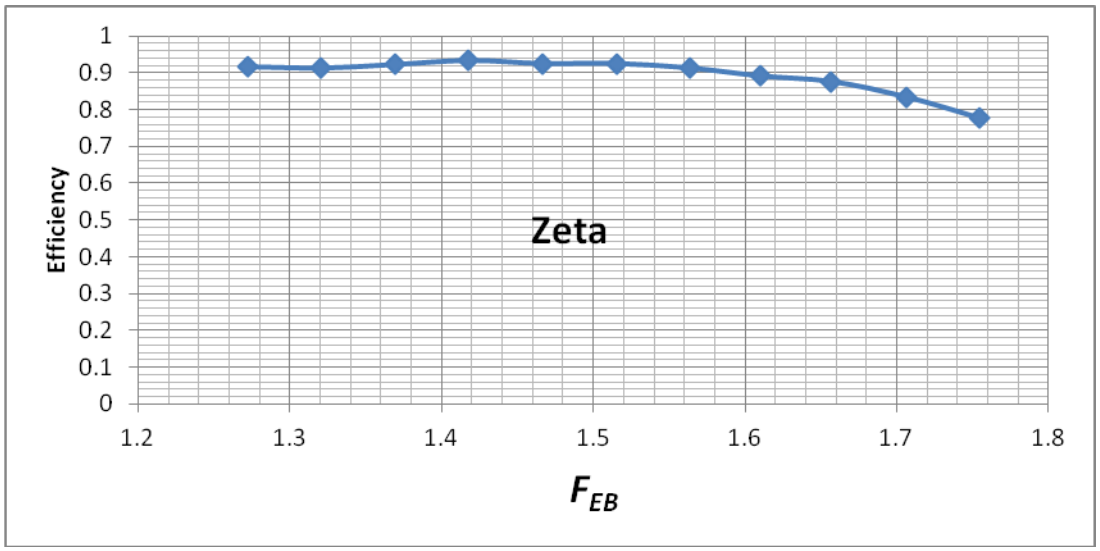

Fig. 2-18 Efficiency against buffer energy factor of Zeta converter

2.6 The energy factors for isolated DC-DC converters

One benefit of isolated DC-DC converter is to extend the voltage conversion ratio by adjusting the turns ratio of the transformer. The classical isolated DC-DC converters include Forward and Flyback converter which are derived from the Buck and Buck-Boost converters, respectively. In the isolated DC-DC converter, besides inductor and capacitor, the magnetizing inductor of transformer can also store energy. This section analyzes the energy factors of Forward and Flyback converters under CCM. Through these two examples, the differences of behaviour of energy storage between isolated and non-isolated converters are presented.

By the definitions in (2-1)~(2-5) and methods presented in the above section, the energy factors and buffer energy factors of Forward and Flyback converters can be obtained. The results are listed in TABLE 2-5.

TABLE 2-5 Comparison of energy factors between isolated and non-isolated converters

Converters	Modes	Energy factor (F_E)			Buffer energy factor (F_{EB})		
		Inductor (F_{EL})	Capacitor (F_{EC})	Transformer (F_{ETR})	Inductor (F_{EBL})	Capacitor (F_{EBC})	Transformer (F_{EBTR})
Forward	CCM	$\frac{K}{4}$	$\frac{CR}{2T_s}$	$\frac{M^2}{N^4 K_M}$	$1-\frac{M}{N}$	$\frac{1-M/N}{4K}$	$\frac{1}{N^2 K_M}$
Buck	CCM	$\frac{K}{4}$	$\frac{CR}{2T_s}$	Not applicable	$1-M$	$\frac{1-M}{4K}$	Not applicable
Flyback	CCM	Not applicable	$\frac{CR}{2T_s}$	$\frac{K_M}{4}(1+\frac{M}{N})^2$	Not applicable	$\frac{M}{N+M}$	1
Buck-Boost	CCM	$\frac{K}{4}(1+M)^2$	$\frac{CR}{2T_s}$	Not applicable	1	$\frac{M}{1+M}$	Not applicable

In TABLE 2-5, N is the ratio of the secondary turns to the primary turns of transformer. The constant K for Tapped-inductor Boost converter is defined as (2-78). K_M is determined by (2-79).

$$K = 2L/(RT_s) \tag{2-78}$$

$$K_M = 2L_M/(RT_s) \tag{2-79}$$

where L_M is the inductance referred to the primary side.

Firstly Forward converter is compared with Buck converter. The energy factors of inductor and capacitor are the same for the two kinds of converters. But Forward converter has one more energy-storage component which is transformer. The amount of energy stored in transformer depends on the magnetizing inductor L_M, turns ratio N and voltage gain M. The amount of energy storage increases as M increases, N and L_M decrease. That means the magnetizing inductor should be large enough to decrease energy storage to a low level. In terms of buffer energy, for $N>1$, the buffer energy of inductor and capacitor in Forward converter are both higher than those in Buck converter. For $N<1$, the buffer energies of inductor and capacitor in Forward converter are both less than those in Buck converter. The transformer of Forward converter also has buffer energy factor which depends on the magnetizing inductor and turns ratio.

Secondly Flyback converter is compared with Buck-Boost converter. The

energy factors of capacitor are the same for the two converters. As the transformer in Flyback converter is in fact a coupled inductor, the energy factor of transformer has the same style with that of inductor of Buck-Boost converter. The only difference is the turns ratio. The buffer energy factor of transformer in Flyback converter is the same as that of inductor in Buck-Boost converter. They are both equal to one.

2.7 Conclusion

This chapter presents the concepts and corresponding definitions of ***Energy Storage*** ($\boldsymbol{E_S}$), ***Energy Factor*** ($\boldsymbol{F_E}$), ***Buffer Energy*** ($\boldsymbol{E_B}$)and ***Buffer Energy Factor*** ($\boldsymbol{F_{EB}}$). $\boldsymbol{E_S}$ and $\boldsymbol{F_E}$ are used to indicate the amount of energy stored in DC-DC converters during operation. $\boldsymbol{E_B}$ and $\boldsymbol{F_{EB}}$ are used to indicate the magnitude of variation of energy storage in DC-DC converter.

These novel concepts can be applied to evaluate different topologies of DC-DC converters. Through the comparison of Buck, Boost and Buck-Boost converter, it can be found that the Buck-Boost converter has the highest F_E, while Buck converter has the lowest F_E. That indicates that to deliver the same power. Buck-Boost converter has to store the most energy, while energy that Buck converter needed to store is the least. It can be also found that the ratio of inductor's F_E to capacitor's F_E depends on the circuit parameters including *L*, *C* and *R*. In Boost and Buck-Boost converter, this ratio is also related to the voltage conversion ratio *M*. When *M* increases, the ratio also increases.

F_{EB} can reflect the magnitude of variation of energy stored in converter. For Buck, Boost and Buck-Boost converters, the total buffer energy factor F_{EB} (sum of that of inductor and capacitor) increases as inductor *L* and frequency f_s decreases, and resistor of load *R* increases. That means the magnitude of variation of energy storage increases as *L* and f_s decreases, and *R* increases.

The analysis based on energy is also carried out for higher order DC-DC converters which include Cuk, Sepic and Zeta converters. For all the three converters, in general, F_{EB} increases as inductor *L* and frequency f_s decreases, resistor of load *R* increases. This is the universal property shared by the three basic first order converters (Buck, Boost and Buck-Boost converters).

Small buffer energy factor indicates that the power loss will be relatively low and efficiency is expected to be high. Experimental results for Cuk and Zeta

converter confirm the relationship between buffer energy factor and efficiency.

Chapter 3 Extension of definition of buffer energy and buffer energy factor

This chapter extends the definitions of the concepts of ***buffer energy*** and ***buffer energy factor*** which are introduced in Chapter 2 . The extension is on the basis of the theory of active power and non-active power. Explicit formulations are presented for them. The redefined buffer energy and buffer energy factor can be applied to depict and analyze non-active energy of both DC and AC systems. They can also be used explicitly to compare the performance of different DC-DC converters.

3.1 Background

In Chapter 2 the definitions of buffer energy and buffer energy factor have been presented. Using these definitions the energy behaviour inside DC-DC converters can be described. But the exchange of energy between converter and power source cannot be analyzed based on the definitions. This chapter extends the definitions of these two novel concepts. After the development, buffer energy and buffer energy factor can be applied to analyse the whole DC systems which not only include single component but also the whole circuit. By the extension study in this chapter, buffer energy and energy factor are more suitable to be viewed as the counterparts of reactive power and power factor, respectively, in DC systems.

DC-DC power converter has L and C for energy storage. In each switching cycle, energy absorbed from front-end source is stored in the converter during the on time of switching devices. Such energy is released to the output during the transistor off time and can be considered as non-active energy. The time derivative of non-active energy is the non-active power. The non-active power is the counterpart of the reactive power for the conventional AC system. Such power deteriorates the efficiency, and imposes extra stress in components and power quality.

Traditional concepts of reactive power and power factor cannot be applied directly to evaluate the non-active power of DC-DC converters. Although the improved definition of power factor [86] reflects the amount of active power in DC-DC converters, it cannot indicate the amount of non-active power. Along with increasing developments of new energy source, the analysis of power and energy for DC system is increasingly important. It is necessary to develop a method to measure

the effectiveness of the power being handled by DC-DC converters. New concepts are needed to investigate the non-active power and energy processing in DC-DC converters.

On the other hand, stored energy has a close relationship with the stability of DC-DC converter. Some control methods for DC-DC converter are based on energy storage [65, 67, 73, 115, 116]. Passivity based control is one of such control methods [67, 73, 115, 116]. It uses naturally stored energy of the system as the Lyapunov energy function, and utilizes the intrinsic passivity of the physical system to formulate the control methods. Ref [107] uses state-energy plane to deal with right-half-plane zero problem and implement boundary control. The ripples of inductor current and capacitor voltage reflect the variation of energy storage which can also be used to build a controller for DC-DC converters. Such controller is referred as ripple based control [117, 118].

This chapter aims to define and clarify the static energy behaviour of DC system, especially DC-DC converters. Some scholars have initiated this work. Lawrenson has proposed a goodness factor for switched reluctance motor (SRM) to express the ratio of active power processed by SRM [80]. Papers [82, 83] elaborated the concept of DC power factor and use such definition in the analyses of SRM. Similar concepts for DC-DC converters were firstly put forward in references [79, 84]. In [79] the concepts of Variation of Energy Storage (VES) and Maximum Storage Energy Factor (MSEF) for DC-DC converters have been introduced. The VES is defined as the difference between the maximum energy and minimum energy stored in the inductor or capacitor of DC-DC converters during one cycle under steady state. MSEF is defined as the ratio of the VES to the input energy of the whole circuit in one cycle. On the other hand, references [63, 85] also proposes similar concepts such as Stored Energy and Energy Factor. In these papers the concepts have been applied to the modelling and control of DC-DC converters. All the above concepts around energy proposed by the above scholars provide new measurements on the performance of DC-DC converters. However their concepts and definitions cannot provide enough information of non-active power in DC-DC converters, and can only be applied to DC-DC converters instead of all electrical systems.

This chapter systematically introduces two novel concepts which are ***buffer energy*** and ***energy factor*** to describe the non-active energy and evaluate the

performance of DC-DC converters. Explicit definitions are presented for them. The proposed buffer energy and energy factor can be applied to depict and analyze non-active energy of both DC and AC systems. They can be used explicitly to compare the performance of different DC-DC converters. It can be proved that they are the extension of the concepts of VES and MSEF respectively proposed in reference [79].

The structure of this chapter is as follows. Section 3.2 will define the instantaneous non-active power and introduce the concepts and definitions of buffer energy and energy factor. Section 3.3 studies the relations between energy factor and efficiency. Section 3.4 describes the application of buffer energy and energy factor. Section 3.5 presents the experimental results of energy factors of different converters. Section 3.6 concludes the study.

3.2 Extension of definition of buffer energy and buffer energy factor

The concepts of active power and reactive power are widely used to analyze the energy usage in electrical systems. Active power is the average value of instantaneous power. It describes essentially the energy being consumed or released by the system and hence is applicable to all electrical systems. But conventional definition for reactive power cannot be directly applied to non-sinusoidal systems including DC system. Lots of works have been done to improve the definition of reactive power and make it suitable for non-sinusoidal systems [86, 90, 93, 119, 120]. Reference [86] presents a novel method to decompose current into active component and non-active component. The method is adopted in this thesis to define instantaneous non-active power and non-active energy. Then buffer energy and energy factor are introduced to address and measure non-active energy in DC-DC converters.

For the one-port network shown as Fig. 3-1 (a), u and i are input voltage and current respectively. According to [86] the input current i can be divided into two orthogonal components which are active current i_a and non-active current i_q. Active current i_a is the component consumed by an equivalent resistor. Hence it should be directly proportional to the input voltage at any instant. This component is called the active current because it is responsible for the supply of the active power P. The

non-active current is the remaining component which is obtained by subtracting the active current from the input current. It is called non-active current because the average power in one cycle T caused by this component is zero. The formulas of active and non-active currents are shown in (3-1) and (3-2) respectively.

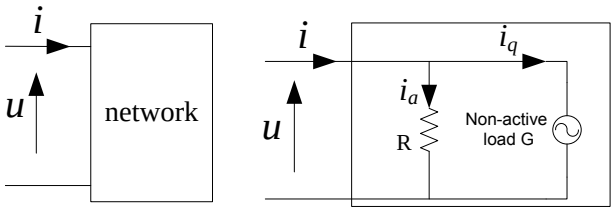

(a) (b)

Fig. 3-1 Network of circuit. (a) One port network. (b) The equivalent network

$$i_a = k \cdot u \tag{3-1}$$

$$i_q = i - i_a \tag{3-2}$$

k is a constant to be determined. As mentioned before, the average power in one cycle caused by non-active current i_q should be zero. This can be used to determine the formula of k as (3-3),

$$k = \int_0^T uidt \Big/ \int_0^T u^2 dt \tag{3-3}$$

where T is the period of cycle. The active power and non-active power can be defined as (3-4) and (3-5)respectively.

$$P = \frac{1}{T}\int_0^T uidt = \frac{1}{T}\int_0^T ui_a dt \tag{3-4}$$

$$q = u \cdot i_q \tag{3-5}$$

Obviously P in (3-4) is the average active power or active power for short. The quantity q in (3-5) can be regarded as non-active power. It is a kind of instantaneous power.

From the above definitions it can be found that non-active power is different from reactive power. In the following example a circuit comprising of a resistor R and an inductor L connected in series is being considered. If the input voltage is sinusoidal AC voltage, then the input voltage and current can be expressed as (3-6), in which ω is the angular frequency, φ is the impedance angle, which is equal to

$\tan^{-1}(\omega L/R)$. U and I are the RMS values of input voltage and current respectively. Following formulations through (3-1) ~ (3-5), the non-active power of the circuit can be obtained as (3-7). The reactive power Q of the circuit is shown as (3-8). From (3-7) and (3-8) it can be found that the definition of non-active power proposed in this thesis is different from reactive power. Furthermore, the common definition of reactive power is only for the case that voltage and current are both sinusoidal and with the same frequency. But non-active power is suitable for voltage and current with all kinds of waveforms.

$$\begin{bmatrix} u \\ i \end{bmatrix} = \sqrt{2} \cdot \begin{bmatrix} U\cos(\omega t) \\ I\cos(\omega t - \varphi) \end{bmatrix} \tag{3-6}$$

$$q_{in} = u \cdot i_q = UI\sin\varphi\sin(2\omega t) \tag{3-7}$$

$$Q = UI\sin\varphi \tag{3-8}$$

Based on the above definitions, the system in Fig. 3-1 (a) can be taken as equivalent to the circuit comprising of one resistor R and one non-active load G in parallel connection. The equivalent circuit is illustrated in Fig. 3-1 (b). In this figure, the admittance of the equivalent resistor is k. The non-active load is in fact an imaginary non-active power supply which can consume or release non-active power.

As mentioned above, the average value of q in one cycle must be zero. That means the energy absorbed and released by G in one cycle are equal. Then the energy absorbed or released by G in one cycle T is defined as ***buffer energy***. It is denoted by E_b and its formula can be obtained as (3-9). Buffer energy is to-and-fro energy. Its average value in one cycle is zero. The accompanying concept ***buffer power*** P_b is defined as (3-10). Buffer power is the DC counterpart of reactive power which is widely used in AC sinusoidal system.

$$E_b = \frac{1}{2}\int_0^T |q|dt \tag{3-9}$$

$$P_b = E_b / T \tag{3-10}$$

The ratio of buffer power P_b to the input active power P of the whole system under consideration is defined as ***energy factor***. It is denoted by F_E. The formula of F_E can be obtained as:

$$F_E = \frac{E_b}{P \cdot T} = \frac{P_b}{P} \tag{3-11}$$

The application of E_b and F_E based on a Buck converter is studied as given below. For clarity, Fig. 3-2 is the circuit of the Buck converter used for this example.

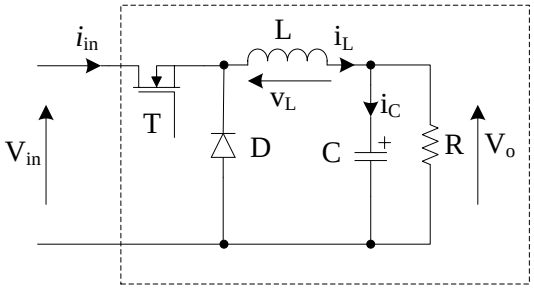

Fig. 3-2 Circuit of Buck converter

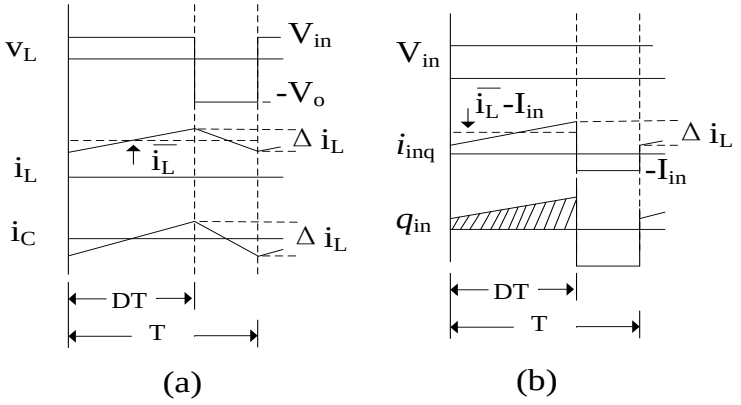

Fig. 3-3 (a) The waveforms of Buck converter under CCM; (b) The waveforms of input voltage, non-active current and non-active power of Buck converter.

The waveforms of Buck converter operating under CCM (continuous conduction mode) are shown in Fig. 3-3 (a). According to (3-3), k can be formulated as (3-12). Active input current i_{ina} is equal to I_{in} which is the average value of input current. Non-active current i_{inq} and instantaneous input non-active power q_{in} are illustrated as Fig. 3-3 (b). The shaded area in the waveform of q_{in} in the figure is the input buffer energy E_{bin}. E_{bin} can be obtained as $(1\text{-}D)V_{in}I_{in}T$. The energy factor of whole circuit F_{Ein} can be obtained as (3-13).

$$k = I_{in} / V_{in} \tag{3-12}$$

$$F_{Ein} = E_{bin} / (P_{in} \cdot T) = 1 - D \tag{3-13}$$

In (3-13) P_{in} is the input average power which is also the input active power

based on the definition given in (3-14). Based on the above mathematics, the buffer energy of each single component in Fig. 3-2 can also be obtained from (3-14) ~ (3-16). Their energy factors can be obtained according to (3-11). The results are listed in TABLE 3-1.

$$E_{bL} = \int_0^{DT} v_L i_L dt = (1-D)V_{in} I_{in} T \tag{3-14}$$

$$E_{bC} = \frac{1-D}{4K} V_{in} I_{in} T \tag{3-15}$$

$$E_{bR} = 0 \tag{3-16}$$

In (3-15), K=2L/(RT). The buffer energy and energy factor for Buck converter under discontinuous conduction mode (DCM) are also derived. The results are shown in TABLE 3-1. It can be proved that the buffer energy and energy factors of transistor and diode are zero. Special attention should be paid on that the energy factor of the whole circuit is not simply the direct sum of the energy factor of each component. This is similar to the fact that the power factor of the complete circuit is not equal to the sum of the power factors of each component.

TABLE 3-1 Energy Factor for Whole Circuits and Each Components of Buck Converter

	CCM			DCM		
	F_{Ein}	F_{EL}	F_{EC}	F_{Ein}	F_{EL}	F_{EC}
Buck	$1-D$	$1-D$	$\frac{1-D}{4K}$	$(1-\frac{D}{2})^2$	$1-M$	$(1-\frac{D}{2M})^2$
Boost	$\frac{D(1-D)^2}{4K}$	D	D	$\frac{(2D-KM^2)^2}{4(M-1)KM}$	$1-\frac{1}{M}$	$(1-\frac{D}{2(M-1)})^2$
Buck-Boost	$1-D$	1	D	$(1-\frac{D}{2})^2$	1	$(1-\frac{D}{2M})^2$

$K=2L/(RT_s)$, M is the energy conversion ratio under discontinuous mode.

In TABLE 3-1 M is the voltage conversion ratio under DCM, it has different expressions for different

$$M = 2/(1+\sqrt{1+4K/D^2}) \tag{3-17}$$

For Boost converter,

$$M = (1+\sqrt{1+4D^2/K})/2 \tag{3-18}$$

and for Buck-Boost converter,

$$M = D/\sqrt{K} \tag{3-19}$$

From TABLE 3-1 it can be found that the energy factors of inductor and capacitor of Buck, Boost and Buck-Boost converter are the same as the MSEF (Maximum storage energy factor) proposed in reference [79] which is a new goodness factor for DC-DC converter. In that paper the Variations of Energy Storage (VES) are defined as the difference between the maximum energy and minimum energy stored in an inductor or capacitor of the DC-DC converter during one cycle at steady state. They can be expressed as (3-20) and (3-21).

$$S_L = \tfrac{1}{2} L(i_{\max}^2 - i_{\min}^2) = LI_L \Delta i_L \tag{3-20}$$

$$S_C = \tfrac{1}{2} C(v_{\max}^2 - v_{\min}^2) = CV_C \Delta v_C \tag{3-21}$$

Based on these definitions, the ratios of VES to output energy is formulated as (3-22). The MSEF is defined as (3-23).

$$R_{SL} = \frac{S_L}{V_o I_o T_S}, R_{SC} = \frac{S_C}{V_o I_o T_S} \tag{3-22}$$

$$MSEF = \sum_{L,C} (R_{SL} + R_{SC}) \tag{3-23}$$

In fact, VES and MSEF defined in Ref[79] are special cases of buffer energy and energy factor when they are applied to energy-storage components at steady state. Under steady state, the average energy absorbed by inductor and capacitor is zero. This means the power consumed by inductor or capacitor is thoroughly non-active. According to such definition, the buffer energy is in fact the difference between maximum energy and minimum energy stored in an inductor or capacitor, which is exactly the VES defined in [79]. The ratios R_{SL} and R_{SC} defined in (3-22) are equal to the energy factors for inductor and capacitor proposed in this thesis if the converter is under idealised condition. In other words, (3-20) ~ (3-23) provide alternative methods to obtain buffer energy and energy factor of energy-storage components.

It can be shown that the concepts of buffer energy and energy factor proposed in this thesis do have advantages that VES and MSEF do not possess. This is because buffer energy and energy factor can be applied not only to energy-storage

components but also to all kinds of components. It is applicable not only to single component but also to the whole circuit (like power factor). It is applicable not only to steady state but also to dynamic state. Lastly it is applicable not only to DC system as it is equally applicable to AC system.

3.3 Relationship between efficiency and energy factor

Buffer energy will cause extra loss to the converters. It will increase the RMS value of the devices' current which causes an increase of power loss in parasitic resistors, and buffer energy also imposes core loss on magnetic components and polarization loss on capacitors. Buck converter is used in the exercise to illustrate the extra power loss caused by buffer energy. Simplified equivalent circuit of Buck converter as shown in Fig. 3-4 is adopted to demonstrate the influence of buffer energy. The inductor comprises an equivalent resistor in series with an ideal inductor. Only the on-state resistor is considered for the transistor and its value does not change with temperature. Only the on-state voltage drop and equivalent resistor are taken into account for the diode. Equivalent series resistor (ESR) will be considered for capacitor. The waveforms of inductor's current and capacitor's voltage are illustrated in Fig. 3-3 (a). The above parasitic parameters are assumed to be small and do not affect the principal operation and waveforms of the circuit.

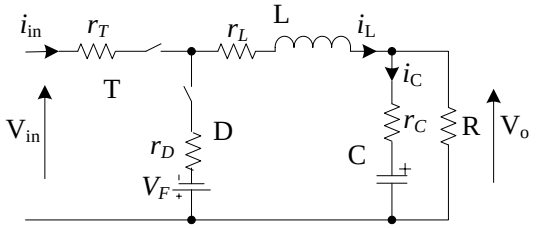

Fig. 3-4 Buck converter with simplified equivalent parasitic resistors

The current of inductor i_L comprises of DC component I_L and ripple δi_L, which are shown in (3-24).

$$i_L = I_L + \delta i_L \tag{3-24}$$

The energy loss of inductor in one cycle can be expressed as (3-25).

$$E_{loss\_L} = \int_t^{t+T_s} {i_L}^2 r_L d\tau = \int_t^{t+T_s} {I_L}^2 r_L d\tau + \int_t^{t+T_s} {\delta i_L}^2 r_L d\tau \tag{3-25}$$

From (3-25), it can be found that the copper loss comprises two parts. The first part is caused by average current which is necessary for power output, and the second part is caused by ripple which can be restrained. The second part can be named as ripple copper loss and is referred as $E_{riploss}$. It can be easily proved that under CCM the ripple energy loss of inductor can be obtained as (3-26).

$$E_{riploss\_L} = \int_t^{t+T_s} \delta i_L{}^2 r_L d\tau = r_L \Delta i_L^2 T_s / 12 \tag{3-26}$$

Substituting (3-9) ~ (3-11) into (3-26), $E_{riploss}$ can be expressed as

$$E_{riploss\_L} = \frac{1}{12} r_L (\frac{E_{bL}}{LI_L})^2 T_s = \frac{1}{12} r_L (\frac{F_{EL} V_o I_o T_s}{LI_L})^2 T_s \tag{3-27}$$

The ripple loss rate ξ_L of inductor can be defined as (3-28).

$$\xi_L = \frac{E_{riploss\_L}}{V_o I_o T_s} = \frac{r_L R T_s^2}{12 L^2} F_{EL}^2 \tag{3-28}$$

Under CCM the ripple loss rate of capacitor, transistor and diode can also be obtained. They are listed in TABLE 3-2.

TABLE 3-2 Relationship between ripple loss rate and Energy Factor under CCM

	ξ_L	ξ_C	ξ_T	ξ_D
Buck	$\frac{r_L}{3RK^2} F_{EL}^2$	$\frac{r_C}{3RK^2} F_{EL}^2$	$D\frac{r_T}{3RK^2} F_{EL}^2$	$\frac{(1-D) r_D}{3RK^2} F_{EL}^2$
Boost	$\frac{(1-D)^2 r_L}{3RK^2} F_{EL}^2$	$\frac{(1-D)^3 r_C}{3RK^2} F_{EL}^2 + \frac{D r_C}{(1-D)R}$	$\frac{D(1-D)^2 r_T}{3RK^2} F_{EL}^2$	$\frac{(1-D)^3 r_D}{3RK^2} F_{EL}^2$
Buck-Boost	$\frac{(1-D)^2 r_L}{3RK^2} F_{EL}^2$	$\frac{(1-D)^3 r_C}{3RK^2} F_{EL}^2 + \frac{D r_C}{(1-D)RT_S}$	$\frac{D(1-D)^2 r_T}{3RK^2} F_{EL}^2$	$\frac{(1-D)^3 r_D}{3RK^2} F_{EL}^2$

K=2L/(RT_s), R is the resistance of load.

TABLE 3-3 The Loss Calculation of Boost Converter (Unit: W)

Po	55.1	82.4	109.4	135.9	162.1	187.8	213.6	237.9	262.1	286.1
DC Loss	0.567	1.304	2.343	3.685	5.347	7.296	9.573	12.10	14.99	18.32
Switching Loss	0.915	1.312	1.699	2.072	2.471	2.846	3.211	3.557	3.906	4.220
Ripple Loss	0.468	0.674	0.963	1.339	1.808	2.366	3.028	3.766	4.623	5.614
Total Loss	1.951	3.290	5.005	7.096	9.626	12.51	15.81	19.42	23.52	28.16

From TABLE 3-2 it can be seen that the ripple energy loss can be expressed by energy factor, i.e. the energy loss caused by ripple can be computed by energy factor. Usually the conduction loss of certain components includes the loss caused by both the average current and ripple current. TABLE 3-2 indicates that buffer energy has potential influence on efficiency.

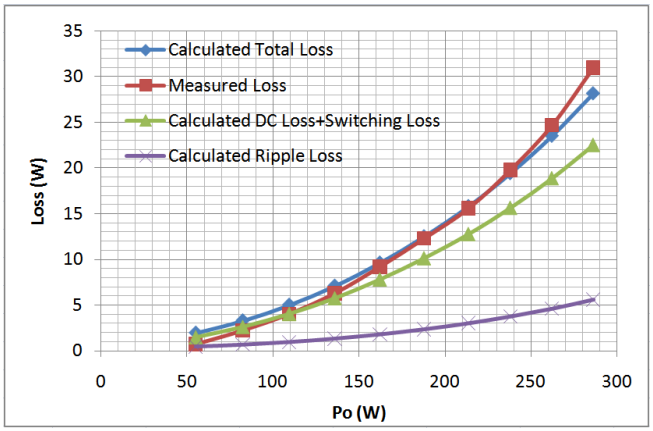

(a)

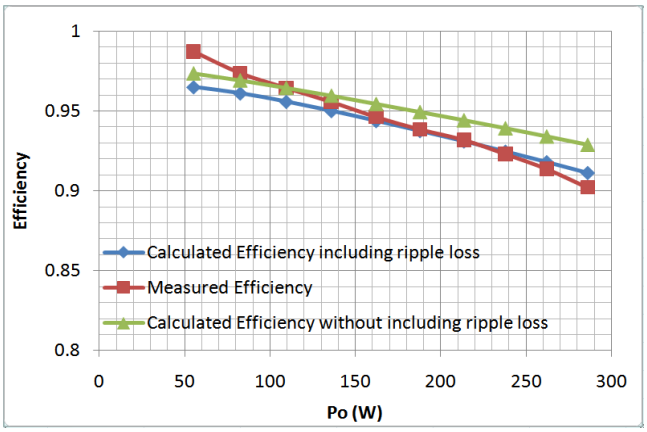

(b)

Fig. 3-5 The loss and efficiency of Boost converter. (a) Loss; (b) Efficiency.

Here an example is used to illustrate the influence of buffer energy on the efficiency. In this example a prototype of Boost converter is built with synchronous rectifier technology. To exaggerate the effect of buffer energy, small inductor is used in the prototype. The parameters of the circuit are as follows. Inductor L=100μH, $r_{L(DC)}$=0.11Ω, $r_{L(40kHz)}$=0.252Ω. The MOSFET IRFB38N20DPBF is used. The $r_{DS(on)}$ is 0.054 Ω. Output capacitor C=440μF, with r_C=0.164 Ω. The input voltage is kept as 30V. Duty ratio is kept as 0.492. Switching frequency is 40kHz. Under these

conditions the ripple current of inductor is very large (about 3.5A), and the converter works under CCM. The load is varied from 55.1W to 286.1W. From TABLE 3-1 it can be seen that in this circuit F_{EL} is equal to 0.492. By substituting F_{EL} into TABLE 3-2, one can get the ***ripple loss*** in TABLE 3-3. Fig. 3-5 shows the ripple loss and its contribution to the efficiency. From Fig. 3-5 it can be found that the predicted efficiency including ripple loss is closer to the measured efficiency than that without including ripple loss.

3.4 Comparison of basic converters by energy factor

TABLE 3-4 lists the input energy factors of Buck, Boost and Buck-Boost converters.

TABLE 3-4 Input Energy Factor of Three Basic Converters under CCM

		Buck	Boost	Buck-Boost
F_{Ein}	CCM	$1-D$	$D(1-D)^2/(4K)$ †	$1-D$
	DCM	$(1-\frac{D}{2})^2$	$\frac{(2D-KM^2)^2}{4(M-1)KM}$	$(1-\frac{D}{2})^2$

†$K=2L/(RT)$, T is the switching period, M is the voltage conversion ratio.

Fig. 3-6 shows the characteristic of the energy factors of the above three converters under CCM and DCM. In Fig. 3-6 (a), the circuit parameters of the three converters are the same. They are R=10Ω, L=50μH, C=47μF, f_s=100kHz. These values ensure the converters are operating under CCM. From Fig. 3-6 (a) it can be seen that the input energy factor of Boost converter is much smaller than the input energy factors of Buck and Buck-Boost converters. In Fig. 3-6 (b), the load resistor of the three converters are changed into R=50Ω. With this load, the converters will enter DCM when the duty ratio is smaller than certain values. Fig. 3-6 (b) shows the input energy factors of the three converters under DCM. It can be seen that under DCM the input energy factor of Boost converter is still the lowest. Energy factor is a measurement of non-active power. Fig. 3-6 shows that Boost converter absorbs much less non-active power from front-end supply. It is reasonable as Boost converter has an input inductor as filter. That is why the energy factor of Boost converter depends on the value of inductor (K depends on inductor).

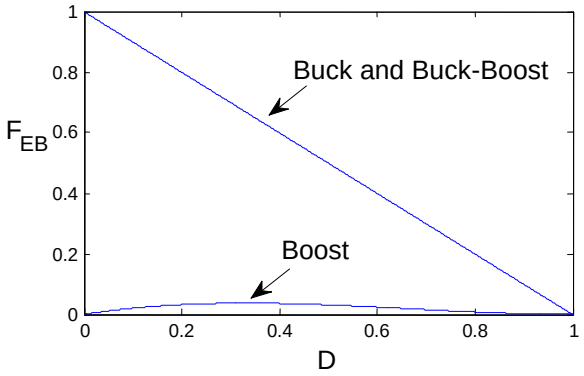

(a)

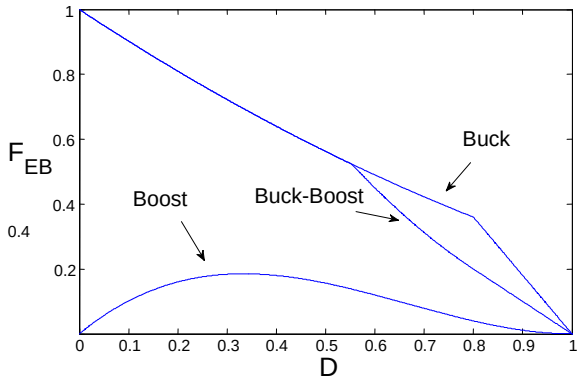

(b)

Fig. 3-6 The input energy factors of three basic converters against duty ratio. (a) CCM; (b) DCM

Cuk, Zeta and Sepic are fourth order converters. Their circuits and waveforms of operation can be found in references [114, 121]. Each circuit has two inductors L_1 and L_2. L_1 is at input side and L_2 is at output side. TABLE V lists the input energy factors of the three converters under CCM and DCM respectively [122]. In this table, T is the switching period.

Fig. 3-7 (a) shows the characteristics of the input energy factors of three fourth order converters under CCM against duty ratio. The simulation parameters are R=10Ω, L_1=L_2=100 μH, C_1=C_2=100 μF and f_s=100kHz. These values ensure that the converters operate under CCM. From Fig. 3-7 (a) it can be found that SEPIC and Cuk converters have the same characteristics of input energy factor against duty ratio. The input energy factors of SEPIC and Cuk converters are much smaller than the energy factor of Zeta converter over a large range of duty ratio. It is reasonable as SEPIC and Cuk converters both have an input inductor. They absorb less non-active energy from front-end power supply when compared to Zeta converter.

TABLE 3-5 Input Energy Factors of Three High Order Converters

F_{Ein}	Cuk	Zeta	Sepic
CCM	$\frac{(1-D)^2}{4DK_1}$ †	$1-D$	$\frac{(1-D)^2}{4DK_1}$
DCM	$\frac{L_{12}(D+\delta)}{4L_1D}\cdot(2-D-\delta)^2$ †	$\frac{(2-D)^2}{4}$	$\frac{L_{12}(D+\delta)}{4L_1D}\cdot(2-D-\delta)^2$

†$K_1=2L_1/(RT)$, $L_{12}=L_1//L_2=L_1L_2/(L_1+L_2)$, $\delta=\sqrt{2L_{12}/(RT)}$.

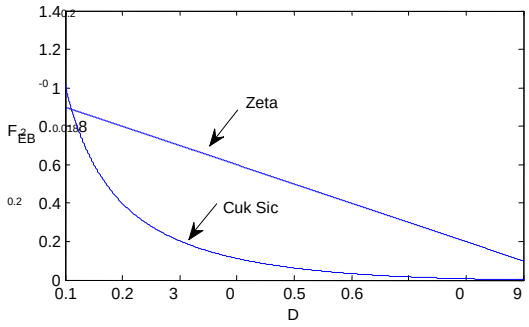

(a)

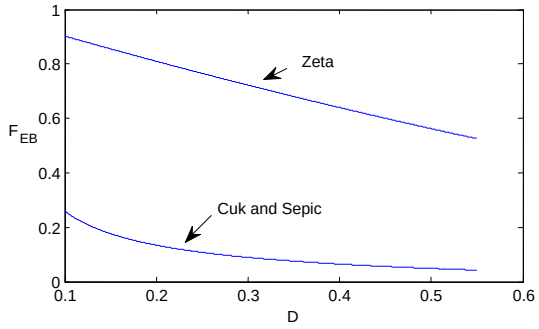

(b)

Fig. 3-7 The input energy factors of Cuk, Sepic and Zeta converters vs. duty ratio. (a) CCM; (b) DCM

Fig. 3-7 (b) shows the input energy factor of the three converters under DCM against duty ratio. As the three converters all have two inductors, the simulation parameters now are changed to R=10Ω, L_1=100μH, L_2=10μH, C_1=C_2=100μF and f_s=100kHz. To make sure the inductor L_2 operate under DCM, the duty ratio cannot be larger than 0.6 according to the boundary conditions of these converters [114, 121]. From Fig. 3-7 (b) it is found that under DCM input energy factors of SEPIC and Cuk converters are much smaller than the energy factor of Zeta converter again. But their difference is larger than that under CCM. That means under DCM the quality of harmonic and distortion for input current and input power of Zeta

converter further deteriorates because of its input transistor.

TABLE 3-6 presents the energy factors of components (L_1, L_2, C_1, and C_2) of the Cuk, Sepic and Zeta converters under CCM. Energy factors of each single component can indicate the characteristics of non-active energy circulating inside the converters. The non-active energy circulating inside the converters will cause power loss and the reduction in voltage conversion ratio. Fig. 3-8 shows the sum of energy factors of all components for the Cuk, SEPIC, and Zeta converters under CCM respectively. The simulation parameters are R=10Ω, L_1=L_2=100μH, C_1=C_2=100μF, f_s=100kHz. From Fig. 3-8 it is found that the Cuk converter has the highest amount of non-active circulating energy while Zeta converter has the least amount. This indicates that Zeta converter has the best internal energy handling characteristic even though its input current is discontinuous all the time which is bad for filtering.

TABLE 3-6 Energy factors of components in high order converters under CCM

	F_{EL1}	F_{EL2}	F_{EC1}	F_{EC2}	Sum of F_E of all components
Cuk	D	$1-D$	1	$(1-D)/(4K_2)$	$2+(1-D)/(4K_2)$
Zeta	D	$1-D$	D	$(1-D)/(4K_2)$	$1+D+(1-D)/(4K_2)$
Sepic	D	$1-D$	$1-D$	D	2

Apart from static analysis of DC-DC converter, the buffer energy and energy factor and their correlative concepts defined in this thesis can be applied to dynamic analysis of DC-DC converter. For example, during transient period the inductor and capacitor absorb or release not only non-active energy but also active energy until steady state is reached. Under steady state the inductor and capacitor only consume non-active energy. Indeed such characteristics can be used to indicate whether the converter goes into steady state. The fact that the value of k defined in (3-3) for inductor is zero means the converter has entered into steady state. Otherwise the converter is in transient state.

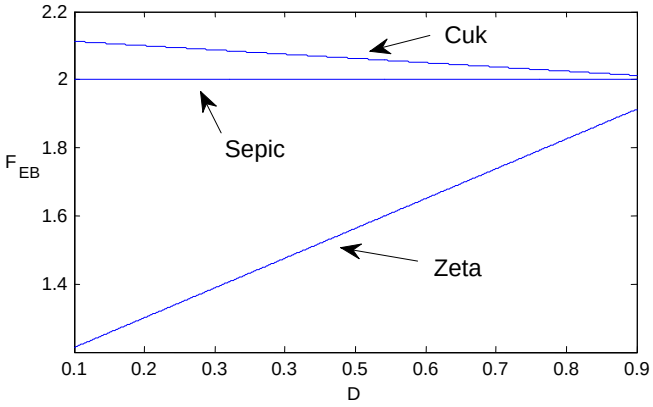

Fig. 3-8 The sum of energy factors of all components under CCM vs. duty ratio

3.5 Experimental results

Too much buffer energy can degrade the performance of power supply and the front-end equipments. Two sets of experiments are used to illustrate how the energy factors of Buck and Boost converters are measured.

The parameters of experimental prototype of Buck converter are as follows: L=100 μH, C=100 μF, R=2.5Ω, f_s=20kHz, and duty ratio D=0.5. These chosen values ensure the converters operate under CCM. The output power is 60.6W. The output voltage and output current are 12.29V and 4.94A respectively. The input voltage and input average current are 28.2V and 2.64A respectively. In the experiment the input voltage and current are recorded by HIOKI 8855 (a data logger). The sampling interval is 5 μs. These data are used to obtain the energy factor of Buck converter according to (3-1)~(3-11). Fig. 3-9 (a) illustrates the input voltage v_{in}, current i_{in} and energy factor F_{Ein} of Buck converter from initial state to steady state. From Fig. 3-9 (a) it can be found that the input energy factor of Buck converter with 50% duty ratio is about 0.5. This is consistent with the theoretical value according to TABLE 3-1.

Fig. 3-9 (b) illustrates v_{in}, i_{in} and F_{Ein} of Boost converter from initial state to steady state. The parameters of the prototype of Boost converter are as follows. L=100 μH, C=100 μF, R=15.68Ω, f_s=20kHz, duty ratio D=0.5. These values ensure the converters operate under CCM. The output power is 60.9W. The output voltage and output current are 29.62V and 2.06A respectively. The input voltage and input average current are 16.2V and 4.11A respectively.

From Fig. 3-9 (b) it is found that the input energy factor of Boost converter with

50% duty ratio is about 0.123. This is again consistent with the theoretical value according to TABLE 3-3. This result also proves that at the same power level, Boost converter has a lower energy factor than Buck converter, which means Boost converter absorbs less non-active power from front-end power supply than Buck converter at the same power level.

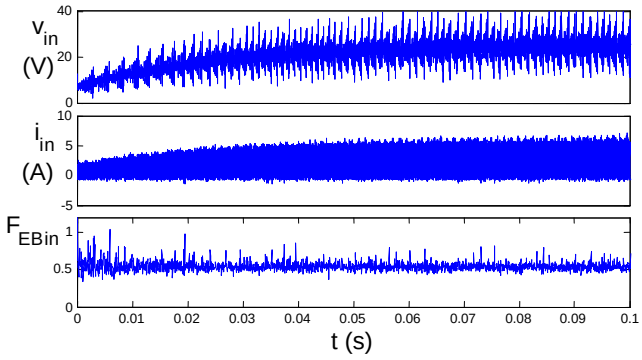

(a)

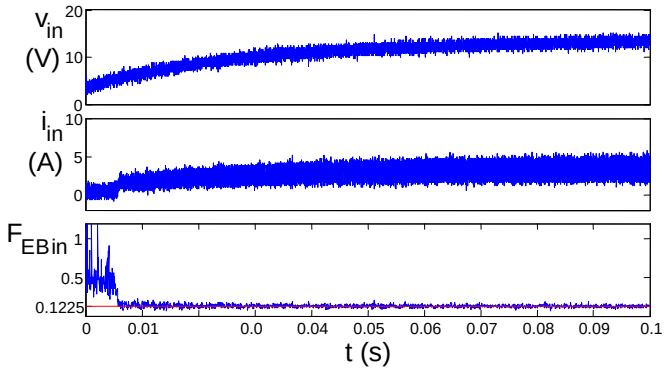

(b)

Fig. 3-9 Experimental results of input voltage, current and energy factor. (a) Buck converter and (b) Boost converter.

Fig. 3-10 presents the measured energy factors of inductor and capacitor of Boost converter under steady state. According to the definition in Section 3.2, the theoretical values of the energy factors of the inductor and capacitor of Boost converter are both equal to the duty ratio *D*. In this experiment *D* is 0.5. From Fig. 3-10 it can be found that the measured energy factors of inductor and capacitor are both about 0.4. This value is slightly smaller than the theoretical value of 0.5. This error is induced by the voltage loss caused by transistor, diode and parasitical components of the inductor and capacitor.

Fig. 3-11 presents the measured energy factors of inductor and capacitor of the Boost converter against duty ratio. The theoretical values of the energy factors of inductor and capacitor are both equal to the duty ratio *D*. From Fig. 3-11 it can be found that the measured results are very close to the theoretical values.

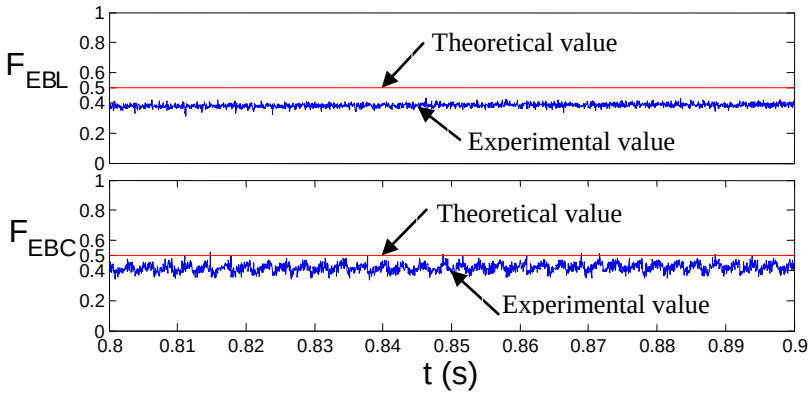

Fig. 3-10 Energy factors of inductor and capacitor of Boost converter.

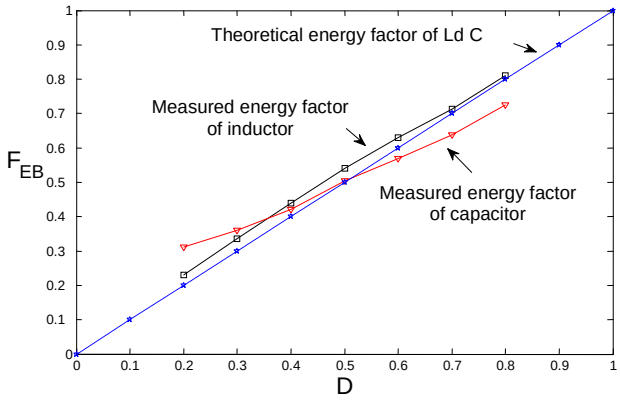

Fig. 3-11 Measured energy factors of inductor and capacitor of Boost converter against duty ratio

3.6 Conclusions

The novel concepts referred as buffer energy and buffer energy factor proposed in Chapter 2 are reviewed in this chapter. Their explicit and more general definitions are proposed based on the non-active energy circulating in circuits. By the proposed definitions, the buffer energy and buffer energy factor can be used to analyze both DC and AC systems. The analysis of energy process shows that the buffer energy and buffer energy factor can be used as a measurement of the performance of electrical

system, especially for DC-DC converters. They are different from traditional reactive power and power factor. Their advantage is that they can indicate the amount of non-active energy (or power) in DC-DC converters whereas conventional reactive power and power factor cannot.

The buffer energy factors of some basic converters have been researched in detail. Theoretical results explain Boost converter has much lower energy factor than Buck and Buck-Boost converters, which indicate that much less non-active power is absorbed by Boost converter from the front-end power supply. For the same reason SEPIC and Cuk converters have lower energy factor than Zeta converter. But among these three converters, Zeta converter has the least amount of non-active circulating energy inside the converter.

Experimental results show that buffer energy factor can be measured. The measured results are consistent with theoretical analysis. Buffer energy can also be measured based on the experiments described in this thesis. Buffer energy, buffer energy factor and their related concepts proposed in this thesis have promising application in both static and dynamic analyses and design of DC-DC converters.

Chapter 4 Static performance and energy factor of Tapped-inductor converters

This chapter uses Tapped-inductor Boost converter as an example to introduce the basic principle of operation. Then detailed comparisons between Tapped-inductor Boost and conventional Boost are carried out, which include the comparison of voltage gain, component stress and efficiency. Experimental results present solid verification of the analysis of performance of Tapped-inductor Boost converter. Similar methods can be extended to other Tapped-inductor DC-DC converters.

4.1 Introduction

The Tapped-inductor DC-DC converter extends the application of its traditional counterparts. For the applications which need very high/low voltage gain without isolation requirement, the Tapped-inductor DC-DC converter is an attractive choice. For these applications, unlike conventional DC-DC converter, Tapped-inductor converter can avoid the duty ratio falling into extreme range to achieve very high/low voltage gain through controlling the tapped turns ratio of winding. The after-effect is that the efficiency and reliability are improved in the applications of extreme voltage gain.

Tapped-inductor technology provides a simple and feasible method to extend the voltage conversion ratio. Previous scholars have explored this feasibility. In Refs[39, 45, 47, 52] D. A. Grant revised the converter and categorize the topologies of Tapped-inductor converter. The nomenclature of circuit variants of basic Tapped-inductor converter derived from Buck, Boost and Buck-Boost converter are diode tapped, transistor tapped and rail-tapped. In [95] K.W. Cheng explored the concept of Tapped-inductor converters and generates the topologies of Quadratic Buck, Cuk, switch-capacitor Buck and so on. Because of the discontinuous current in the tapping, high voltage spike may occur in the transistor and diodes that deteriorate the converter performance. Snubbers and soft-switching are proposed to solve the problem[44, 49, 51, 96-98]. The critical mode operation is investigated in Refs [37, 49, 96, 99]. The modeling and control of are also investigated presented in Refs[43, 46]. Most of the works are presented as independent studies and there is no comparative study between Tapped-inductor converter and conventional converter in

detail. They are mostly in terms of circuit analysis during static state. The research of closed-loop and small signal analysis of Tapped-inductor converter especially applying modern nonlinear control into Tapped-inductor converter has not been explored enough.

Nowadays, along with the increase usage of DC electronic equipment, DC distribution system gains more applications such as telecommunication system, data center, and vehicles (ship, airplane). In the DC distribution systems, DC-DC power converters are used for DC voltage matching. High performance power converters are needed to reduce the power loss and hence simple topology and low component count are preferred. Many DC line may operated under low voltage. The associated energy source or devices such as photovoltaic, fuel cell, battery and super capacitor are also low voltage for individual cells. High voltage gain step up converter are needed for the connection of various units together. Tapped-inductor Boost converter is a feasible choice.

This chapter uses Tapped-inductor Boost converter as an example to introduce the basic principle of operation. Then detailed comparisons between Tapped-inductor Boost and conventional Boost have been carried out, which include the comparison of voltage gain, component stress and efficiency. Experimental results verify the analysis results and confirm the performance of Tapped-inductor Boost converter. Similar methods can be extended to other Tapped-inductor DC-DC converters.

The output voltage of Boost converter is higher than input voltage. The voltage gain depends on the duty ratio. Theoretically it can reach infinitely large voltage gain. But practically large voltage gain cannot be obtained by conventional Boost converter. It is because of three main reasons. Firstly, very high duty ratio (e.g. >0.9) is not easy to implement reliably because of the limit of switching speed. Secondly, the components in the circuit have parasitic resistance. The input current during high conversion ratio is large. It will cause extra voltage drop. The voltage drop is severe when the duty ratio is high because of high input current and peak diode current. Thirdly, the high pulsation currents occur in the diode and capacitor that cause additional loss.

4.2 The topologies of Tapped-inductor converters

Ref. [39] synthetically presents the introduction of most kinds of

Tapped-inductor DC-DC converters. The possible topologies of Tapped-inductor converters which is derived from basic DC-DC converters can be found in [39]. Several novel topologies derived from high order converters are listed in TABLE 4-1.

TABLE 4-1 Topologies of some novel Tapped-inductor converters

	Diode to tap	Switch to tap	Switch and diode to tap
Cuk	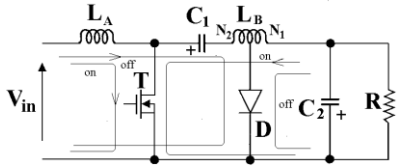	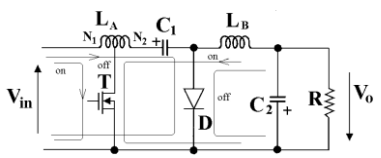	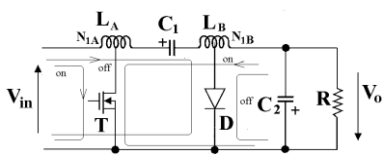
Quadratic Buck	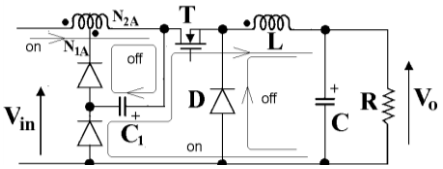	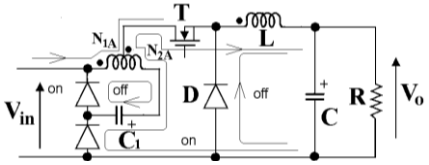	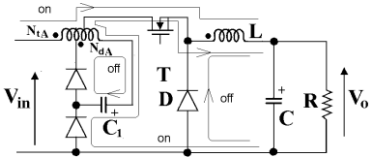

4.3 The voltage gain and efficiency of conventional Boost converter

One of the advantages of Tapped-inductor converter is high efficiency under extreme duty ratio. Conventional DC-DC converters suffer low efficiency under extreme high or low voltage conversion ratio. Here Boost converter is used as an example to explain this point.

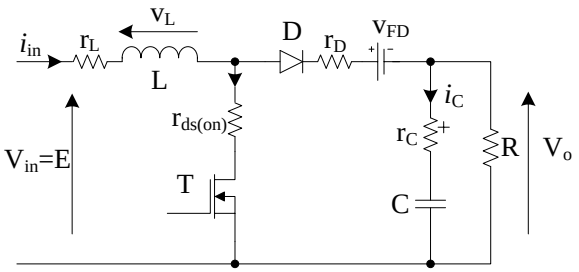

Fig. 4-1 Classical Boost converter with parasitic parameters

Fig. 4-1 is the boost converter with parasitic parameters. In the figure, r_{L} is the ESR of inductor, $r_{\mathrm{ds(on)}}$ is the on-state resistor of MOSFET, r_{D} is the body resistor of diode, r_{C} is the ESR of capacitor, V_{FD} is the forward voltage drop of diode. R is the resistance of load. L is the inductance of input inductor; C is the capacitance of output capacitor. V_{in} is the input voltage which is equal to E. V_{o} is the output voltage. The dynamic model of this converter is as follows. In the model, current of inductor and voltage of capacitor are chosen as the state variables. They are represented by x_1 and x_2, respectively. u is the duty ratio.

$$\begin{cases} \dot{x}_1 = -\dfrac{1}{L}[r_L + r_{ds}u + (1-u)(r_D + r_C \,//\, R)]x_1 - (1-u)\dfrac{1}{L}\dfrac{R}{R+r_C}x_2 + \dfrac{E}{L} - (1-u)\dfrac{V_{FD}}{L} \\ \dot{x}_2 = (1-u)\dfrac{R}{(r_C+R)C}x_1 - \dfrac{1}{(r_C+R)C}x_2 \end{cases} \tag{4-1}$$

At steady state, the states are represented by $\bar{x}_1$ and $\bar{x}_2$.

$$\dot{\bar{x}}_1 = 0, \qquad \dot{\bar{x}}_2 = 0 \tag{4-2}$$

Substitute (4-2) into (4-1). The voltage conversion ratio ξ under steady state can be obtained as follows.

$$\xi(\bar{u}) = \frac{V_o}{E} = \frac{\bar{x}_2}{E} = \frac{(1-\bar{u})[1-(1-\bar{u})\frac{V_{FD}}{E}]}{[r_L + r_{ds}\bar{u} + (1-\bar{u})(r_D + r_C // R)]\frac{1}{R} + (1-\bar{u})^2 \frac{R}{R+r_C}} \tag{4-3}$$

And

$$\bar{x}_1 = \frac{\bar{x}_2}{(1-\bar{u})R} \tag{4-4}$$

So the efficiency η can be predicted as

$$\eta(\bar{u}) = \frac{V_o^2 / R}{E \cdot \bar{x}_1} = \frac{[1-(1-\bar{u})\frac{V_{FD}}{E}](1-\bar{u})^2}{[r_L + r_{ds}\bar{u} + (1-\bar{u})(r_D + r_C // R)]\frac{1}{R} + (1-\bar{u})^2 \frac{R}{R+r_C}} \tag{4-5}$$

Using the data in TABLE 4-2, the relationship between voltage conversion ratio and duty ratio is plotted as Fig. 4-2.

TABLE 4-2 the parameters used in the simulation of voltage gain and efficiency

	r_L (mΩ)		r_{ds} (mΩ)	r_D (mΩ)	r_C (mΩ)	V_{FD} (V)	E (V)	R (Ω)	L (μH)		C (μF)	N	
Boost	50		25	20	50	0.4	24	100	144		220	23	
Tapped-inductor Boost	r_{L1} 24	r_{L2} 26							L_1 33	L_2 39		*N1* 11	*N2* 12

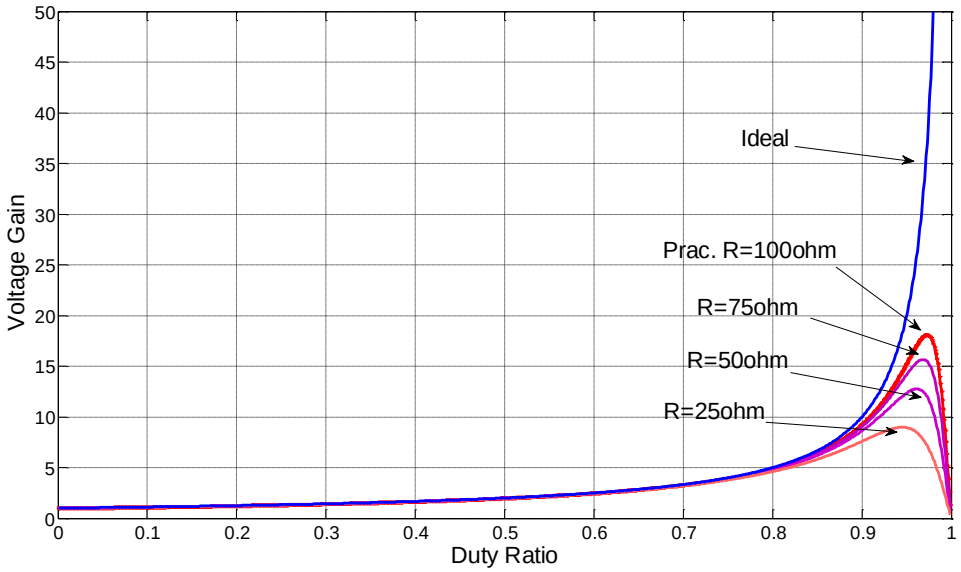

Fig. 4-2 The practical voltage conversion ratio of classical Boost converter with various loads

From Fig. 4-2, it can be found that the practical Boost converter cannot attain infinite voltage gain because of the existence of parasitic parameters. In fact the maximum voltage gain decreases along with the increase in load.

On the other hand, the duty ratio above 0.9 imposes a big challenge to the electronic driver circuits as it is not reliable in most cases.

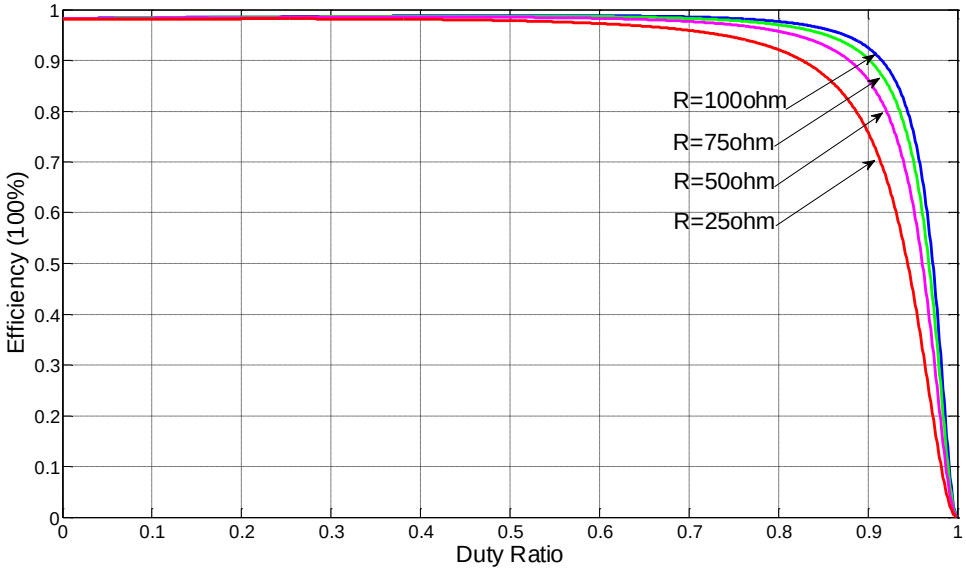

Fig. 4-3 The theoretical efficiency of classical Boost converter with various loads

From Fig. 4-3, it can be found that, the efficiency decreases with the increase of duty ratio. The efficiency also decreases when the load increases.

Under steady state, if the output voltage is set to 160V, then according to (4-3), the duty ratio should be 0.8559. According to (4-5), the efficiency will be 96.07%. If the load increases to 25Ω, then the efficiency will be 86%. This result does not include the switching loss and the extra loss caused by temperature' influence on the r_{ds} of MOSFET. So the practical efficiency will be decreased more severely.

4.4 The voltage gain and efficiency of Tapped-inductor converter

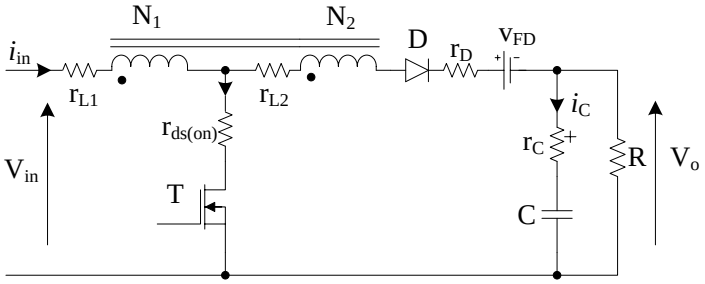

Fig. 4-4 The circuit diagram of Tapped-inductor Boost converter

Fig. 4-4 is the Tapped-inductor Boost converter with parasitic parameters. In the figure, r_{L1} and r_{L2} are the ESR of primary and secondary windings, respectively. $r_{ds(on)}$ is the on-state resistor of MOSFET, r_D is the body resistor of diode, r_C is the ESR of capacitor, V_{FD} is the forward voltage drop of diode. R is the resistance of load. L is the inductance of input inductor; C is the capacitance of output capacitor. V_{in} is the input voltage which is equal to E. V_o is the output voltage. The dynamic model of Tapped-inductor Boost converter with parasitic parameters are shown in (4-6)~(4-10). In the model, the flux of magnetic core and voltage of capacitor are chosen as the state variables. They are represented by φ and v_C, respectively. u is the duty ratio.

On-state:

$$i_{Lon} = \frac{N_1 \varphi}{L_1} \tag{4-6}$$

$$\begin{cases} \dot{\varphi} = \dfrac{E}{N_1} - \dfrac{r_{L1} + r_{ds}}{L_1}\varphi \\ \dot{v}_C = -\dfrac{v_C}{(r_C + R)C} \end{cases} \tag{4-7}$$

i_{Lon} is the on-state current through primary winding. N_1 and L_1 are the turns and

inductance of primary winding, respectively.

Off-state:

$$i_{Loff} = \frac{N_1^2 \varphi}{(N_1 + N_2)L_1} \tag{4-8}$$

$$\begin{cases} \dot{\varphi} = -(r_{L1} + r_{L2} + r_D + \dfrac{Rr_C}{R + r_C}) \dfrac{N_1^2 \varphi}{(N_1 + N_2)^2 L_1} - \dfrac{R}{(N_1 + N_2)(R + r_C)} v_C + \dfrac{E - V_{FD}}{(N_1 + N_2)} \\ \dot{v}_C = \dfrac{N_1^2 R}{(N_1 + N_2)(R + r_C) C L_1} \varphi - \dfrac{1}{(R + r_C) C} v_C \end{cases} \tag{4-9}$$

i_{Loff} is the off-state current through both primary and secondary windings. N_2 is the turns of secondary winding.

Then the average state space model is shown below.

$$\begin{cases} \dot{\varphi} = -[u(r_{L1} + r_{ds}) + (1-u)(r_{L1} + r_{L2} + r_D + \dfrac{Rr_C}{R + r_C}) \dfrac{N_1^2}{(N_1 + N_2)^2}] \dfrac{1}{L_1} \varphi \\ \quad - (1-u) \dfrac{R}{(N_1 + N_2)(R + r_C)} v_C + \dfrac{(uN_2 + N_1)E - (1-u)N_1 V_{FD}}{N_1 (N_1 + N_2)} \\ \dot{v}_C = \dfrac{(1-u)N_1^2 R}{(N_1 + N_2)(R + r_C) C L_1} \varphi - \dfrac{1}{(r_C + R) C} v_C \end{cases} \tag{4-10}$$

At steady state, we have

$$\dot{\varphi} = 0 \tag{4-11}$$

$$\dot{v}_C = 0 \tag{4-12}$$

Then average output voltage

$$V_o = \bar{v}_o = \bar{v}_C \tag{4-13}$$

Substituting (4-11) and (4-12) into (4-10), we can obtain the voltage conversion ratio and flux under steady state as (4-14) and (4-15).

$$\xi(\bar{u}) = \frac{V_o}{E} = \frac{[1 + \bar{u}\frac{N_2}{N_1} - (1-\bar{u})\frac{V_{FD}}{E}](1-\bar{u})}{\bar{u}\frac{r_{L1} + r_{ds}}{R}(1 + \frac{N_2}{N_1})^2 + (1-\bar{u})(r_{L1} + r_{L2} + r_D + \frac{Rr_C}{R + r_C})\frac{1}{R} + (1-\bar{u})^2 \frac{R}{(R + r_C)}} \tag{4-14}$$

$$\bar{\varphi} = \frac{(N_1 + N_2)L_1}{(1-\bar{u})N_1^2 R} V_o \tag{4-15}$$

So

$$\bar{i}_{Lon} = \frac{N_1 \overline{\varphi}}{L_1} \tag{4-16}$$

$$\bar{i}_{Loff} = \frac{N_1^2 \overline{\varphi}}{(N_1 + N_2) L_1} \tag{4-17}$$

$$\bar{i}_{in} = \bar{u}\bar{i}_{Lon} + (1-\bar{u})\bar{i}_{Loff} = \frac{\bar{u}N_1N_2 + N_1^2}{(N_1 + N_2)L_1}\overline{\varphi} = \frac{\bar{u}N_2 + N_1}{(1-\bar{u})N_1 R} V_o \tag{4-18}$$

Then the efficiency is

$$\eta(\bar{u}) = \frac{V_o^2 / R}{E \cdot \bar{i}_{in}} = \frac{[1 - \frac{N_1 - N_1\bar{u}}{N_1 + N_2\bar{u}} \cdot \frac{V_{FD}}{E}](1-\bar{u})^2}{\bar{u}\frac{r_{L1} + r_{ds}}{R}(1 + \frac{N_2}{N_1})^2 + (1-\bar{u})(r_{L1} + r_{L2} + r_D + \frac{Rr_C}{R + r_C})\frac{1}{R} + (1-\bar{u})^2 \frac{R}{(R + r_C)}} \tag{4-19}$$

Fig. 4-5 and Fig. 4-6 show the voltage gain and efficiency of Tapped-inductor converter against duty ratio. The parameters used for simulation are the same as those in conventional Boost converter which are shown in TABLE 4-2. Special attention should be paid on the ESR of inductor. As the tap divides the inductor into to two parts: L_1 (L_p) and L_2 (L_s). So the ESR is also assumed to be divided into two parts according to the turns ratio. That is to say r_{L1}:r_{L2}=N_1:N_2.

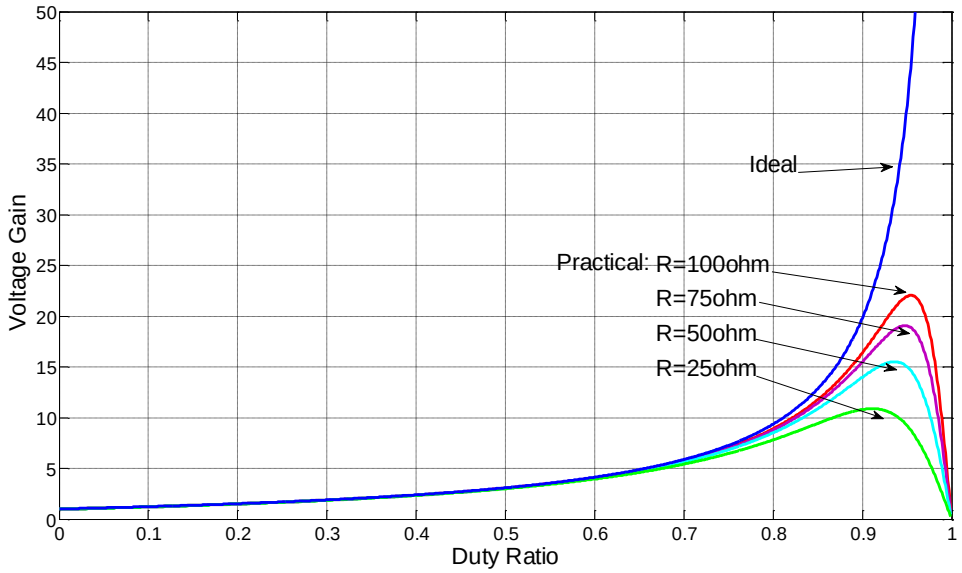

Fig. 4-5 The voltage gain of Tapped-inductor Boost converter with various loads

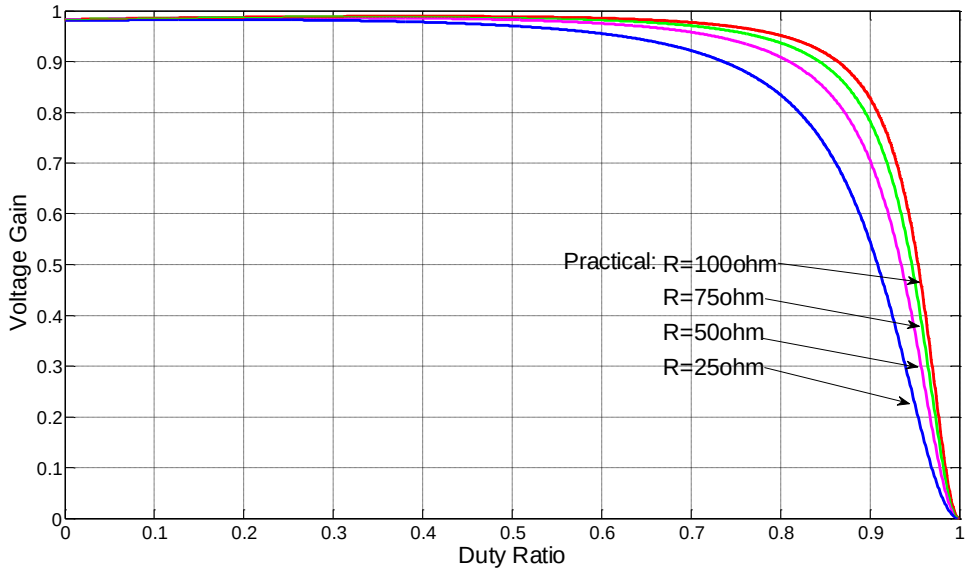

Fig. 4-6 The theoretical efficiency of Tapped-inductor Boost converter with various loads

4.5 Comparison between Tapped-inductor and conventional Boost converter

4.5.1 Comparison of voltage gain and efficiency

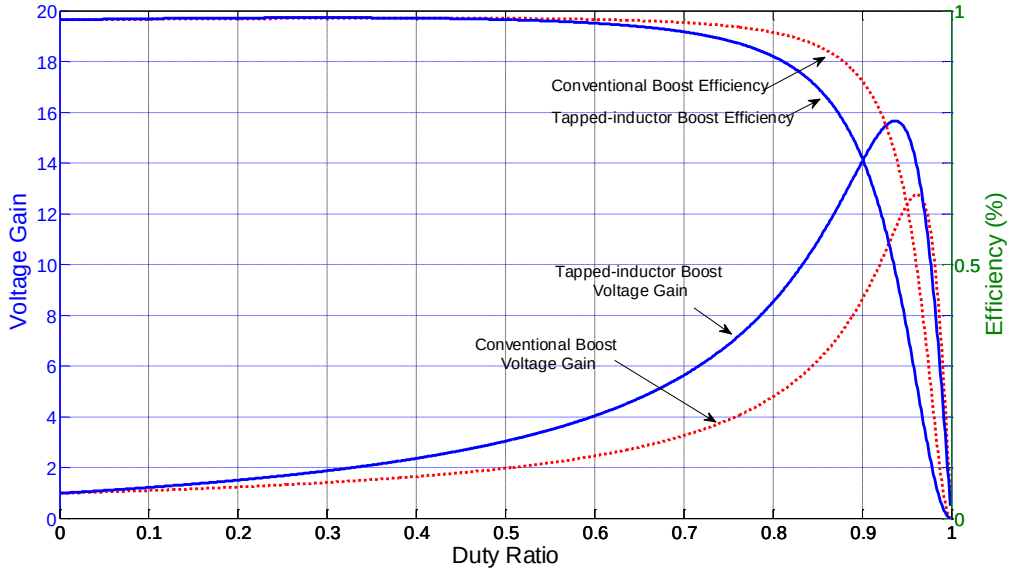

Fig. 4-7 Comparison of voltage gain and efficiency between conventional Boost and Tapped-inductor Boost converter

From Fig. 4-7 it can be found that: at the left side of peak voltage gain, under the same duty ratio, the voltage gain of Tapped-inductor Boost converter is higher

than the conventional Boost converter; but the efficiency of Tapped-inductor Boost is lower than the conventional Boost converter. For the application to pump a 24V energy source (e.g. battery stack) to a 160V DC distribution bus, the conventional Boost converter needs a duty ratio of 0.87, whereas the Tapped-inductor Boost converter only needs a duty ratio of 0.75. The theoretical efficiencies are 90% and 95%, respectively.

Fig. 4-8 shows the relationship between efficiency and voltage gain for the both converters. In the figure, the region above the efficiency of 0.5 is the nominal operation condition. In Fig. 4-8, the parts of curves with efficiency lower than 0.5 indicate that the converters operate under extremely high duty ratio and it is not reliable.

From this figure, it can be found that with the same voltage gain, the efficiency of Tapped-inductor converter is higher than the efficiency of conventional Boost converter.

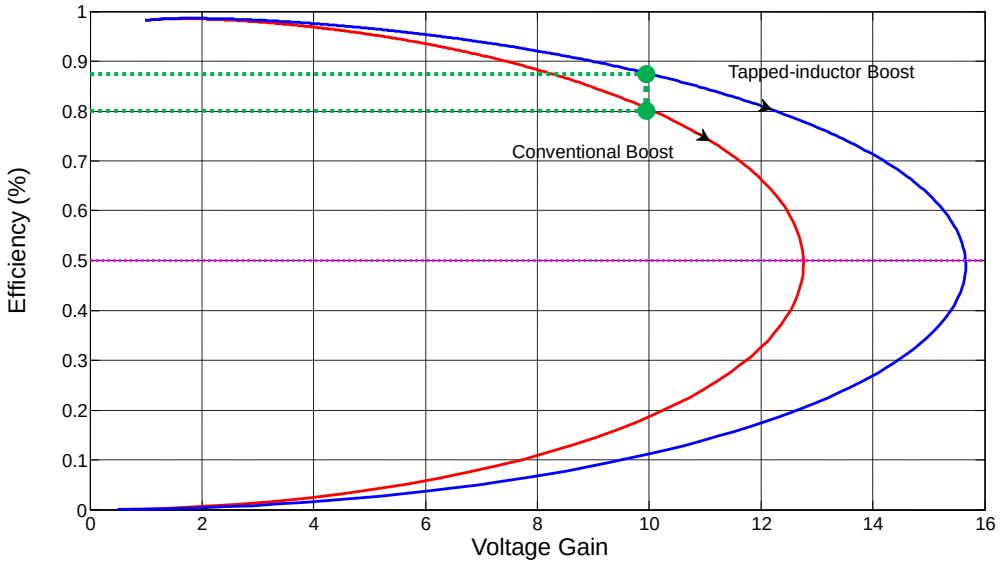

Fig. 4-8 The relations between efficiency and voltage gain of conventional Boost and Tapped-inductor Boost converters

4.5.2 Comparison of stress of components

In this section, the stresses of components are considered under the condition of the same size inductor and the same voltage gain. The ripple analysis for the

Tapped-inductor converter and the conventional converter are examined. Boost converter is chosen for the case study.

The figures below show two types of Boost converter with ideal components (no parasitic parameters).

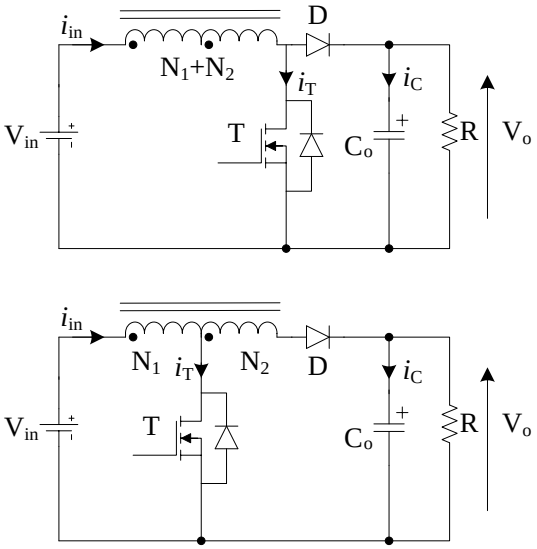

Fig. 4-9 Circuit diagram of conventional Boost and Tapped-inductor Boost converters with same circuit parameters

Under the same input voltage, output voltage and load resistor, the waveforms are shown in Fig. 4-10. In Fig. 4-10, k is a constant which is equal to N_2/N_1, D is duty ratio, and T_s is the switching period. The stresses of each component are compared in TABLE 4-3.

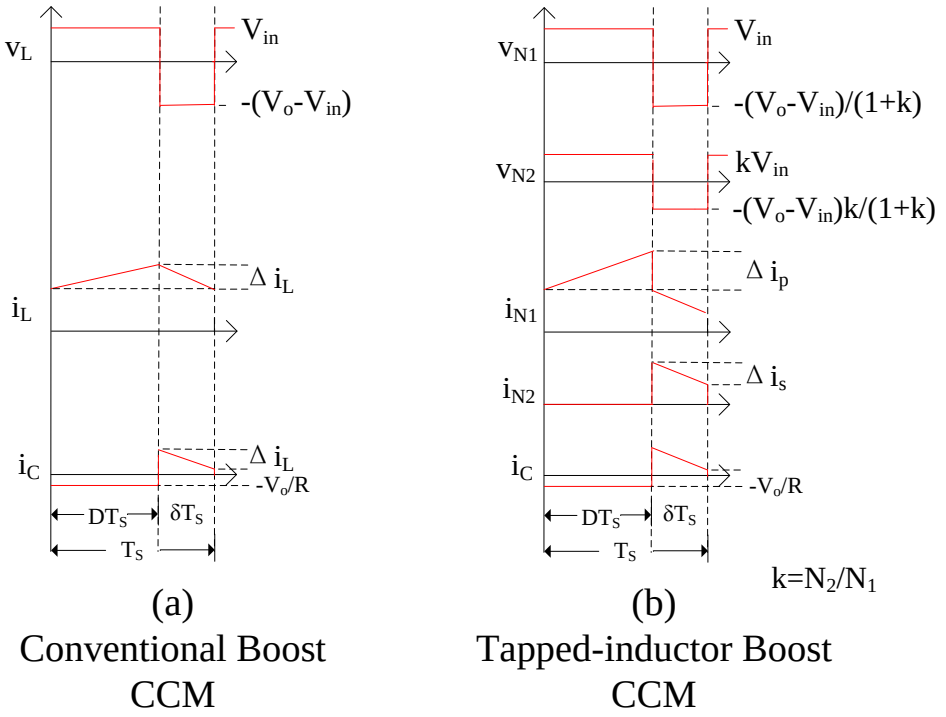

Fig. 4-10 The waveforms of conventional Boost and Tapped-inductor Boost converter operating under CCM

TABLE 4-3 Comparison of stress of components between conventional Boost and Tapped-inductor Boost converter

Comp-onents	Type	Maximum voltage	Average current	Rms current
T	Conventional	V_o	$(M-1)I_o$	$I_o\sqrt{[\frac{(M-1)^2}{3K^2M^6}+1]M(M-1)}$
	Tapped-inductor	$\frac{1+k/M}{1+k}V_o$	$(M-1)I_o$	$I_o\sqrt{[\frac{(1+k)^4(M-1)^2}{3M^2K^2(M+k)^4}+1](M-1)(M+k)}$
D	Conventional	V_o	I_o	$I_o\sqrt{\frac{(M-1)^2}{3K^2M^5}+M}$
	Tapped-inductor	$(1+k/M)V_o$	I_o	$I_o\sqrt{\frac{(1+k)^3(M-1)^2}{3M^2K^2(M+k)^3}+\frac{M+k}{1+k}}$
L_1	Conventional	$Max(V_{in},V_o-V_{in})$	MI_o	$I_o\sqrt{\frac{(M-1)^2}{3K^2M^4}+M^2}$
	Tapped-inductor	$Max(V_{in},\frac{V_o-V_{in}}{1+k})$	MI_o	$I_o\sqrt{\frac{(1+k)^4(M-1)^2}{3M^2K^2(M+k)^2}+(M+k)^2}$
L_2	Conventional	Not applicable	Not applicable	Not applicable
	Tapped-inductor	$Max(kV_{in},\frac{M-1}{1+k}kV_{in})$	I_o	Same to diode
C	Conventional	V_o	0	$I_o\sqrt{\frac{(M-1)^2}{3K^2M^5}+M-1}$
	Tapped-inductor	V_o	0	$I_o\sqrt{\frac{(1+k)^3(M-1)^2}{3M^2K^2(M+k)^3}+\frac{M-1}{1+k}}$

The stresses of two kinds of Boost converter are listed in TABLE 4-3. The total inductance is *L*. *M* is the voltage gain which is expressed as (4-20).

$$V_o / V_{in} = M \tag{4-20}$$

The boundary condition between continuous mode (CCM) and discontinuous mode (DCM) of Tapped-inductor Boost converter is

$$K = D(1-D)^2 \cdot \frac{1+k}{1+kD} \tag{4-21}$$

where

$$K = 2L/(RT_s) \tag{4-22}$$

If *K* is larger than the right hand side of the equation, the Tapped-inductor Boost converter operates under CCM. Otherwise it operates under DCM.

From the above table, it can be found that, the voltage stress of MOSFET in Tapped-inductor Boost is smaller than in conventional Boost converter. But the voltage stress of diode in Tapped-inductor Boost is higher than in conventional Boost converter. The average currents of each component in both converters are the same. But the rms current of components in Tapped-inductor is higher than that of the conventional Boost converter. This means the current ripple of Tapped-inductor Boost is higher than that of the conventional one.

The output voltage ripple is mainly determined by the current of output capacitor. The rms value of current of capacitor as shown in TABLE 4-3 cannot be determined by observation for which one is larger. It is affected by the value of *K* (K=$2L/RT_s$), which is decided by the circuit parameters.

4.5.3 Comparison of energy factors of components

As elaborated in Chapter 2 and Chapter 3 , energy factor reflects the amount of buffer energy in DC-DC converter. Too much buffer energy will cause large extra loss to the converter. This section aims to compare the energy factor of Tapped-inductor Boost converter with conventional Boost converter.

A current step exists in the inductor of Tapped-inductor converter. But the flux

of the whole inductor is continuous. So the energy storage is also continuous. Following the equations (2-1) ~ (2-5) in Chapter 2 , the energy factor of Tapped-inductor Boost converter under CCM can be derived as TABLE 4-4.

The storage energy:

$$E_S = \frac{1}{2}Li^2 = \frac{1}{2}R_m\phi^2 = \frac{1}{2}\frac{N^2}{L}\phi^2 \tag{4-23}$$

where ϕ is the flux. R_m is the magnetic resistor, which is the same for both on state and off state.

$$\phi = \frac{Li}{N} = \frac{Ni}{R_m} \tag{4-24}$$

$$\phi_{\min} = \frac{L_1 i_{p\min}}{N_1} \tag{4-25}$$

$$\phi_{\max} = \frac{L_1 i_{p\max}}{N_1} \tag{4-26}$$

For the inductor

$$\begin{aligned} E_{bL} &= E_{S\max} - E_{S\min} = \frac{1}{2}L_1(i_{p\max}^2 - i_{p\min}^2) \\ &= L_1 I_{pa}\Delta i_p = \frac{M-1}{M}V_o I_o T_s \end{aligned} \tag{4-27}$$

$$F_{EbL} = 1 - \frac{1}{M} \tag{4-28}$$

For the capacitor

$$E_{bC} = V_o\int_{T_s}^{T_s+DT_s} i_C dt = V_o I_o D T_s = V_o I_o T_s \frac{M-1}{M+k} \tag{4-29}$$

$$D = \frac{V_o - V_{in}}{V_o + kV_{in}} = \frac{M-1}{M+k} \tag{4-30}$$

$$F_{EbC} = \frac{M-1}{M+k} \tag{4-31}$$

TABLE 4-4 Comparison of energy factor between conventional Boost and Tapped-inductor Boost converters

	Energy Factor of components	
	Inductor	Capacitor
Conventional Boost	$1-1/M$	$1-1/M$
Tapped-inductor Boost	$1-1/M$	$\frac{M-1}{M+k}$

TABLE 4-4 compares the buffer energy factor between conventional Boost converter and Tapped-inductor Boost converter. From TABLE 4-4 it can be found that, under the same voltage gain, the buffer energy factor of inductor is the same for both converters. But the buffer energy factor of the capacitor in the tapped inductor Boost converter is less than the conventional Boost converter. This means the flux ripple of inductor is the same for the both converters. But the output voltage ripple of Tapped-inductor Boost converter is smaller than that of the conventional Boost converter. This is reasonable because, comparing to conventional Boost converter, the Tapped-inductor Boost converter can operate under a smaller duty ratio to achieve the same voltage gain.

4.6 The model of Tapped-inductor converters

Unlike conventional DC-DC converter, Tapped-inductor converter has the discontinuous current between different taps and terminals of the inductor during the switching transition interval. This difference increases the difficulty of modeling and controller design for Tapped-inductor converter. This section uses Tapped-inductor Boost converter as an example to illustrate the difference of modeling between Tapped-inductor converter and convention DC-DC converter.

4.6.1 State space average model

The configurations of tapped Boost converter are as follows.

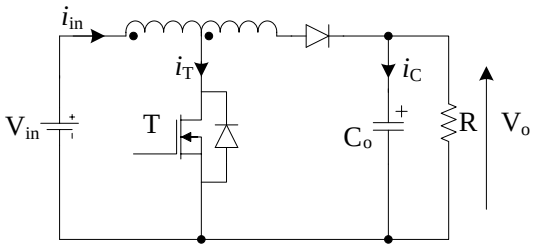

Fig. 4-11 The circuit diagram of Tapped-inductor Boost converter

- Modeling based on magnetizing current

As mentioned above, the terminal current of inductor is discontinuous. But the magnetic flux and magnetic motive force (MMF) of inductor are continuous. So the magnetizing current transferred to primary side is also continuous. Now the magnetizing current transferred to primary side is adopted to build the state space averaged model for the Tapped-inductor Boost converter.

- On-state:

The on-state state space equation is shown as (4-32). In (4-32), i_m is the magnetizing current transferred to the primary side. L_{on} is the inductance of primary windings.

$$\begin{bmatrix} \dot{i}_m \\ v_C \end{bmatrix} = \begin{bmatrix} 0 & 0 \\ 0 & -\frac{1}{RC} \end{bmatrix} \cdot \begin{bmatrix} i_m \\ v_C \end{bmatrix} + \begin{bmatrix} \frac{1}{L_{on}} \\ 0 \end{bmatrix} \cdot V_{in} \tag{4-32}$$

- Off-state:

When the switch is turned off, the circuit is changed from on-state to off-state; the current of inductor reduces by the ratio of total number of turns to the primary turns. If the leakage inductance is negligible, the current of inductor is fully magnetizing current. Transferring this magnetizing current to the primary side, we can obtain a continuous primary-side magnetizing current i_m. Then the state space equation during off period is shown in (4-33) below. L_{on} is the inductance of primary windings.

$$\begin{bmatrix} \dot{i}_m \\ v_C \end{bmatrix} = \begin{bmatrix} 0 & -\frac{1}{L_{on}(1+k)} \\ \frac{1}{C(1+k)} & -\frac{1}{RC} \end{bmatrix} \cdot \begin{bmatrix} i_m \\ v_C \end{bmatrix} + \begin{bmatrix} \frac{1}{L_{on}(1+k)} \\ 0 \end{bmatrix} \cdot V_{in} \tag{4-33}$$

- Average model in one cycle

Using the standard state-space average method [100, 101] based on duty ratio, we can obtain the local average states and averaged state space model shown in (4-34).

$$\begin{bmatrix} \dot{i}_m \\ v_C \end{bmatrix} = \begin{bmatrix} 0 & -\frac{1-D}{L_{on}(1+k)} \\ \frac{1-D}{C(1+k)} & -\frac{1}{RC} \end{bmatrix} \cdot \begin{bmatrix} i_m \\ v_C \end{bmatrix} + \begin{bmatrix} \frac{1+kD}{L_{on}(1+k)} \\ 0 \end{bmatrix} \cdot V_{in} \tag{4-34}$$

This is the large signal state space average model. By linearizing this model, we can obtain the linearized small signal model.

- Linearized small signal model

The equilibrium point can be obtained by letting the left hand side of equal sign in (4-34) equal to zero. When the Tapped-inductor Boost converter goes into steady state, its steady operational point should be one of the equilibrium points. Now assume the steady operating point is (I_m, V_C), and the corresponding duty ratio is D. The static state (I_m, V_C) can be expressed by the D as equation (4-35).

$$\begin{cases} V_C = \frac{1+kD}{1-D} V_{in} \\ I_m = \frac{(1+k)(1+kD)}{R(1-D)^2} V_{in} \end{cases} \tag{4-35}$$

Around this static operating point, the averaged model shown in (4-34) can be linearized. The linearized model is obtained as (4-36).

$$\begin{bmatrix} \dot{\hat{i}}_m \\ \hat{v}_C \end{bmatrix} = \begin{bmatrix} 0 & -\frac{1-D}{L_{on}(1+k)} \\ \frac{1-D}{C(1+k)} & -\frac{1}{RC} \end{bmatrix} \cdot \begin{bmatrix} \hat{i}_m \\ \hat{v}_C \end{bmatrix} + \begin{bmatrix} \frac{V_{in}}{L_{on}(1-D)} \\ \frac{(1+kD)V_{in}}{RC(1-D)^2} \end{bmatrix} \cdot \hat{d} \tag{4-36}$$

This model is small-signal linearized state space averaged model of Tapped-inductor Boost converter. The small-signal state variables are voltage of capacitor $\hat{v}_C$ and magnetizing current of inductor transferred to primary side $\hat{i}_m$. It should be paid more attention that the magnetizing current transferred to primary side cannot be obtained directly during off time, but it is needed to obtain through turns ratio relationship. This model can be applied to implement the peak current mode control for Tapped-inductor Boost converter, which is elaborated in Chapter 5 .

- Modelling based on the flux

As mentioned above, for the Tapped-inductor converter, the terminal current of inductor is discontinuous during the switching transition. But the magnetic flux of inductor is continuous. So the magnetic flux can be used to build the state space averaged model of Tapped-inductor converter which is shown below.

$$\begin{cases} \dot{\varphi} = -\dfrac{1-u}{N_1+N_2}v_C + \dfrac{uk+1}{N_1+N_2}E \\ \dot{v}_C = \dfrac{(1-u)N_1}{(1+k)CL_1}\varphi - \dfrac{1}{RC}v_C \end{cases} \tag{4-37}$$

More accurate model based on magnetic flux has been obtained as (4-10) in section 4.4. That model comprises of the main parasitic parameters of each component in a Tapped-inductor Boost converter.

To apply the model using flux to build controller, a flux observer is necessary to implement the closed-loop operation.

- Modelling based on the input current

The benefit of using input current to build model is that, compared with magnetizing current, the input current can be measured conveniently. Like conventional DC-DC converters, it only needs a sampling resistor in series connection with Tapped-inductor to measure the input current.

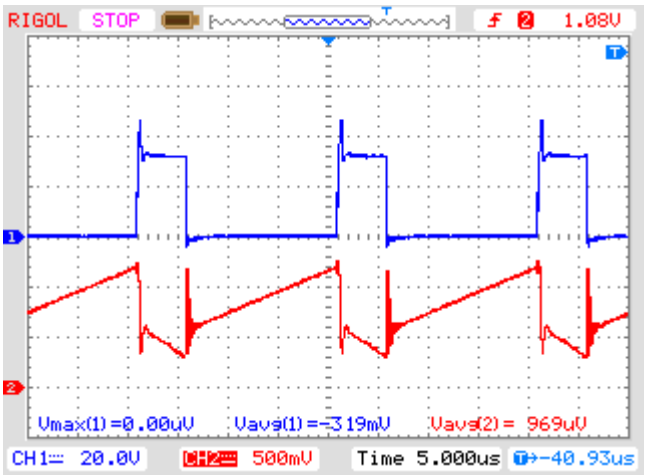

Fig. 4-12 The waveform of V_{ds} of MOSFET and current of inductor

CH1:40V/div, CH2:5A/div

The input current is the same to the current of inductor. Their waveforms are shown in Fig. 4-12. The local averaged input current is the average value in one

cycle of input current. The local averaged input current is called input current for short. The relationship between input current and magnetizing current is shown in (4-38).

$$i_m = \frac{1+k}{1+ku} i_{in} \tag{4-38}$$

k is the turns ratio of secondary side to primary side, and *u* is the duty ratio.

Substitute (4-38) into (4-37), we can obtain the model of Tapped-inductor Boost converter based on input current.

$$\begin{bmatrix} \dot{i}_{in} \\ v_C \end{bmatrix} = \begin{bmatrix} 0 & -\frac{(1-u)(1+ku)}{L_{on}(1+k)^2} \\ \frac{(1-u)}{(1+ku)C} & -\frac{1}{RC} \end{bmatrix} \cdot \begin{bmatrix} i_{in} \\ v_C \end{bmatrix} + \begin{bmatrix} \frac{1+(3+k)ku-ku^2}{L_{on}(1+k)^2} \\ 0 \end{bmatrix} \cdot V_{in} \tag{4-39}$$

4.7 Experimental results

A 250W Tapped-inductor Boost converter prototype is built to compare with the conventional Boost converter with the same power level.

Fig. 4-13~Fig. 4-16 shows the waveforms of the experiments with prototype of Tapped-inductor Boost converter. During the experiments, load resistor is kept at 100Ω. The duty ratio varies from 0.1 to 0.85. Input voltage is set as 12V when duty ratio is 0.25 (low power) and 16V for other values of duty ratio. Fig. 4-13 is the result under duty ratio of 0.25. The output voltage and power are 31.07V and 9.6W, respectively. From the figure it can be found that the Tapped-inductor converter works under discontinuous mode. After the current decreases to zero, reverse recovery of diode occurs. The duty ratios for Fig. 4-14~Fig. 4-16 are 0.6, 0.75 and 0.8, respectively. The corresponding output voltages are 60.86V, 101.86V and 124.32V. And the output powers are 37W, 103.8W, and 154.6W, respectively.

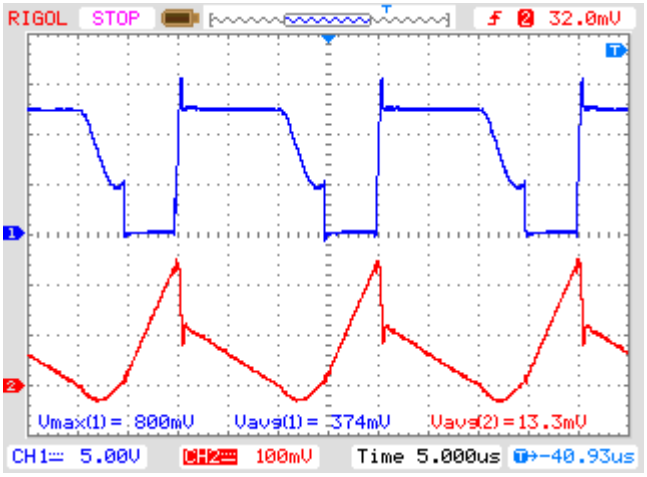

Fig. 4-13 The waveforms of V_{ds} of MOSFET and current of inductor (P_o=9.6W)

CH1:10V, CH2:1A/div

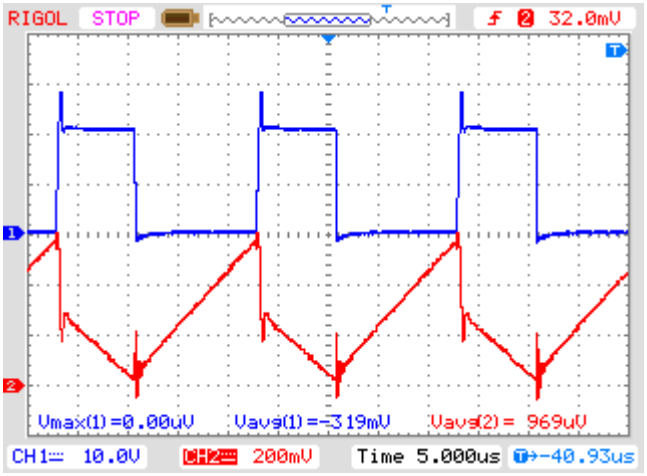

Fig. 4-14 The waveforms of V_{ds} of MOSFET and current of inductor (P_o=37W).

CH1:20V/div, CH2:2A/div

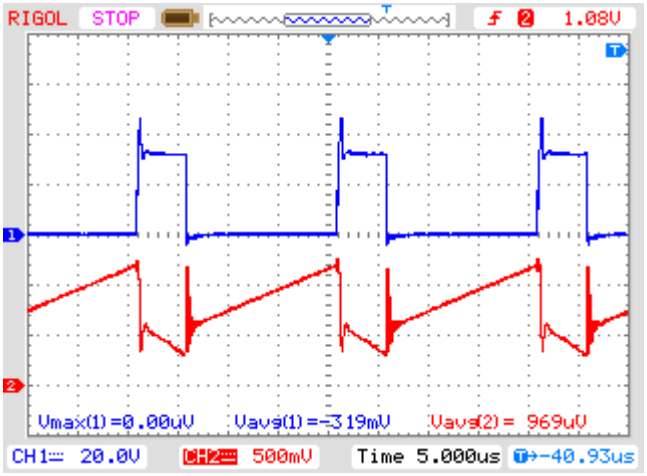

Fig. 4-15 The waveforms of V_{ds} of MOSFET and current of inductor (P_o=103.8W)

CH1:40V/div, CH2:5A/div

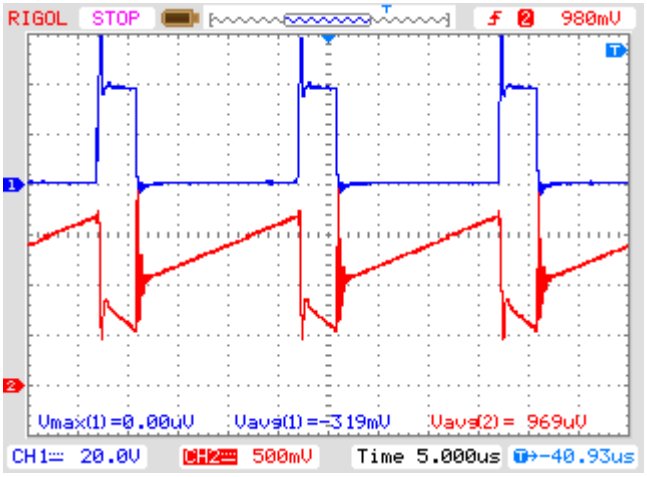

Fig. 4-16 The waveforms of V_{ds} of MOSFET and current of inductor (P_o=154.6W)
CH1:40V/div, CH2:5A/div

Fig. 4-17 shows the measured voltage gain of both conventional Boost and Tapped-inductor Boost converters. The experimental conditions are the same for these two converters. They are: V_{in}=16V, R=100Ω, the duty ratio is varied from 0.1 to 0.8. The circuit parameters are the same for the two converters except the inductor. The inductor of conventional Boost is 144.3μH, while the Tapped-inductor Boost has primary inductor of 33μH and secondary inductor of 39μH. From this figure, it can be found that, under the same duty ratio, the voltage conversion ratio of Tapped-inductor Boost is obviously higher than that of conventional Boost.

Fig. 4-18 compares the measured and predicted voltage gains of both Boost and Tapped-inductor Boost converter. From this figure it can be found that they are matched well.

Fig. 4-19 exhibits the measured efficiency of the both converters. The experimental conditions are the same for the two converters. They are: V_{in}=16V, P_o=100W. By adjusting the duty ratio, voltage gain is varied from 1 to 6 and 1 to 8 for conventional Boost and Tapped-inductor Boost, respectively. From this figure, it can be found that, under the same voltage gain, the efficiency of Tapped-inductor Boost is obviously higher than that of conventional Boost converter.

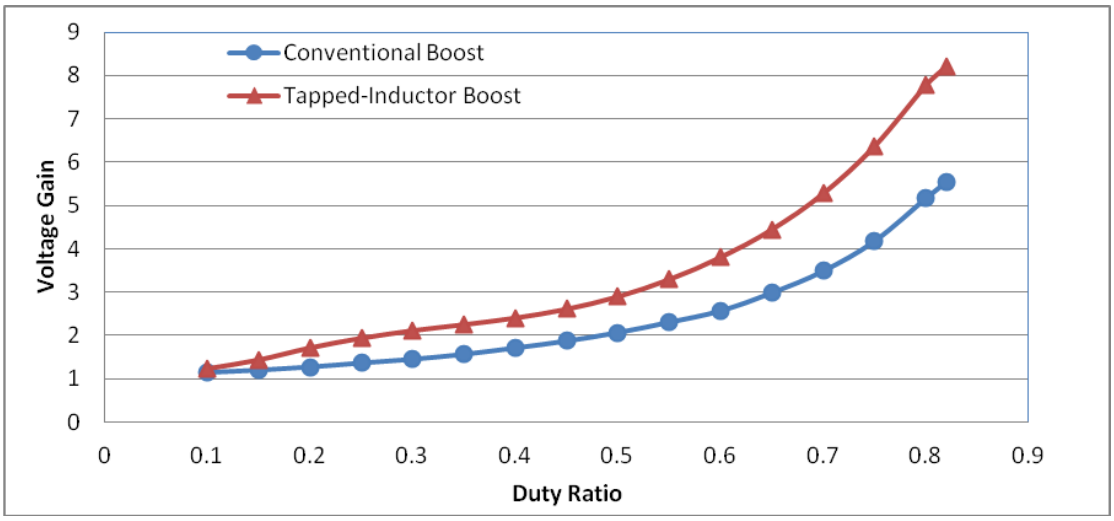

Fig. 4-17 The measured voltage gain of conventional Boost and Tapped-inductor Boost against duty ratio

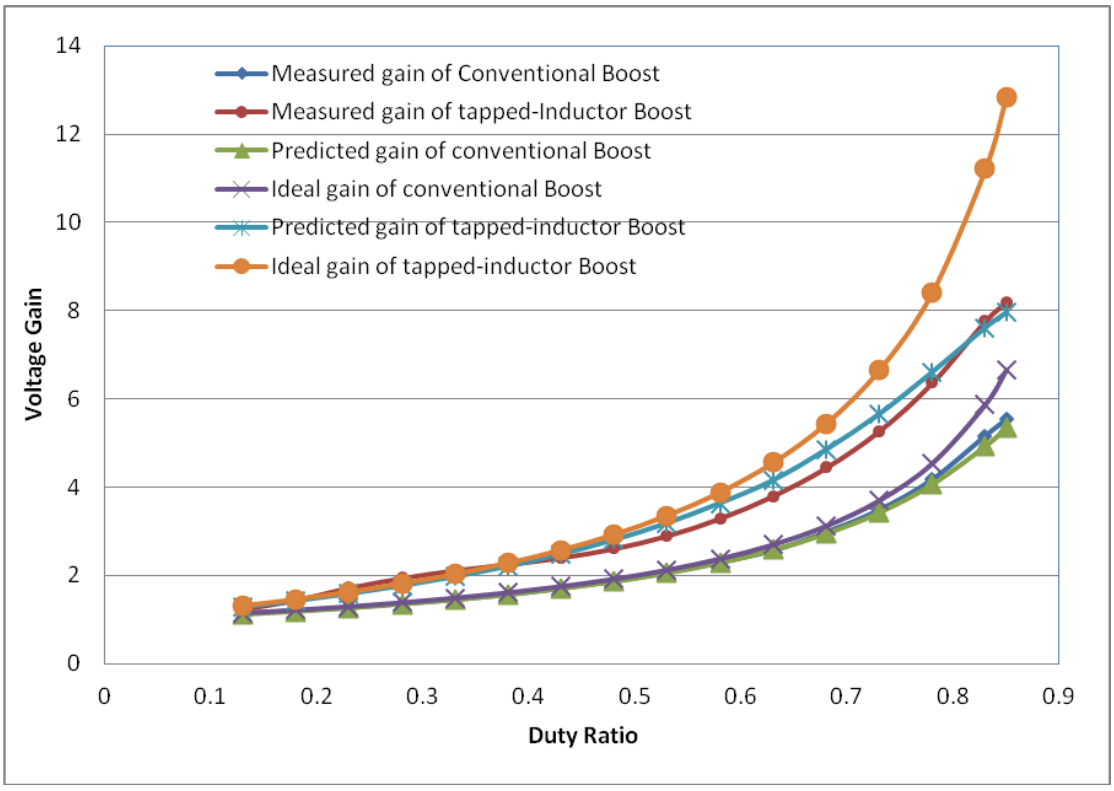

Fig. 4-18 Comparison between measured and predicted voltage gain

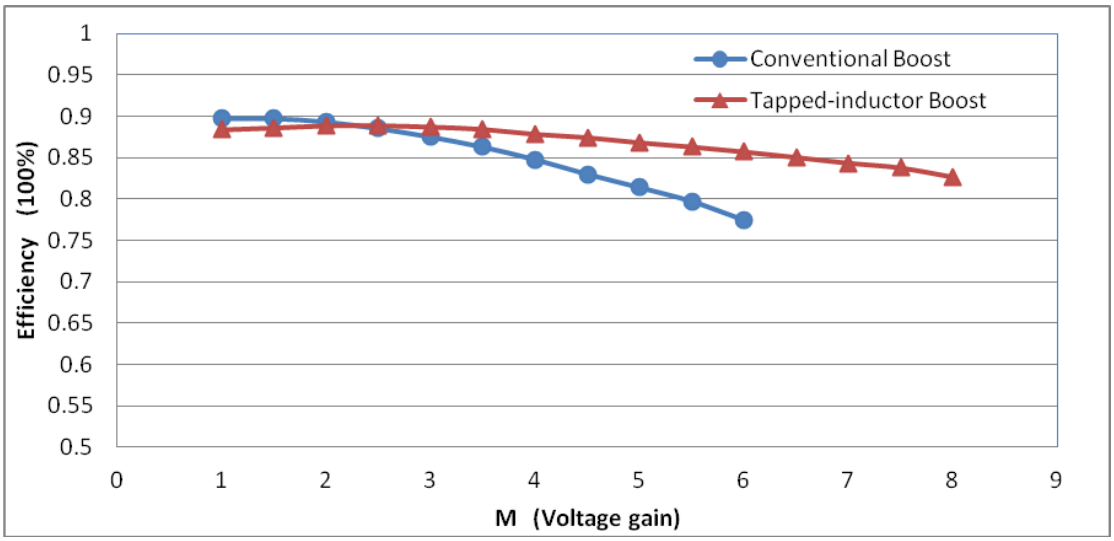

Fig. 4-19 The measured efficiency of conventional Boost and Tapped-inductor Boost converter against voltage gain

4.8 Conclusions

This chapter investigates the performance of Tapped-inductor converters under steady state. First the possible topologies of Tapped-inductor are collected based on previous research. The topologies of Tapped-inductor converter can be derived by tapping inductor of all conventional DC-DC converters. The tapping methods can be classified into five types [39]: diode to tap, switch to tap, power source to tap, Load to tap and ground to tap.

Tapped-inductor Boost converter has been chosen to compare with conventional Boost converter. The comparison are carried out under the same output voltage and output current.

Theoretical analysis illustrates that, with the existence of parasitic parameters of components in circuit, the voltage gain of Tapped-inductor Boost converter is higher than the conventional Boost converter under the same duty ratio; the efficiency of Tapped-inductor Boost converter is higher than the conventional Boost converter under the same voltage conversion ratio.

The comparison of stress of components is also carried out between Tapped-inductor Boost converter and conventional Boost converter. The maximum voltage of transistor of the former is smaller than that of the latter. But the RMS current of transistor of the former is higher than that of the latter. In terms of Diode, the maximum voltage of the former is higher than that of the latter. But the current

stress between the two converters has no explicit trend. In terms of inductor, the rms current of the former is higher than the latter.

The buffer energy factors of the two converters have been also carried out. The results of buffer energy factors of inductor and capacitor are the same for the two converters.

Experimental results proved the theoretical prediction on voltage conversion ratio of and efficiency improvement between the two converters.

Chapter 5 Passivity-based control for Tapped-inductor converter

PID has been used extensively in power converter control because of its simple and cost effect. Many cases, only electronic Analog IC can perform the duty. However, because of the demand in the higher power and higher performance and lower cost in Digital Signal Processor (DSP) and sampling technology, more advanced control method is used.

Nevertheless the theories of classical PID compensation are mainly focused on the linear model of plant. Most of the PID control relies on an approximate linearization around the static operating point of a power converter. The well designed PID controller can achieve good performance in a certain range around the predetermined static operation point. For practical applications and other special applications, the operational range may be wide. The preset PID controller will degrade and cannot assure the stability.

Based on the original nonlinear model, nonlinear control algorithms provide alternative ways to implement closed-loop operation of DC-DC converter. Nonlinear controller can provide global asymptotical stability and can still achieve good performance under a large signal disturbance. In the stability design of nonlinear control methods, the energy function of Lyapunov theory plays the key role. Although this energy function is often not necessarily related to the real energy, the physical energy sometimes can provide an intuitional choice for the Lyapunov energy function. In fact some nonlinear control methods are exactly based on the physical energy of system [67]. Ref. [59, 61, 123] proposed an energy-based control method. This control method can make sure the large-signal stability of plant, even can avoid the problem of chaos of DC-DC converters. But the drawback of this method is that the converter can only work under DCM and is not suitable for high current load. Passivity-based control (PBC) is one of such kind of control algorithms. The basic idea of PBC is to utilize the intrinsic dissipation of nature system to control the injected energy to drive the energy stored in system to the desired level. In the last ten years passivity-based control gains a good development and wide applications. It also extends into the field of control of power conversion [67-76, 115, 116, 124-129]. However the application of PBC are mainly concentrated in classical

DC-DC converters, such as Buck, Boost, Buck-Boost, phase-shift full bridge converters, and so on. Along with the rapid development and application of micro grids and DC distribution systems, Tapped-inductor DC-DC converter will play a more and more important role because of its virtue of wide conversion ratio, high efficiency and simple structure. It is significant to research the application of nonlinear algorithm especially PBC to control the Tapped-inductor DC-DC converter.

Compared to classical DC-DC converters, Tapped-inductor DC-DC converter exhibits different characteristics which bring new challenges to the design of controller. During the operation of Tapped-inductor DC-DC converter, step change of the current of inductor will occur at the instant of switching of tap. The number of steps can be increased by adding taps. Then the freedom of control can be increased. Because of the discontinuity of inductor current, the mathematical model of conventional converter is invalid for the Tapped-inductor converter. However, although the current of the inductor has step changes at the instant of switching of taps, the energy must be continuous. That means the magnetic flux and magnetizing current of the tapped inductor are continuous. This point can be used to build new models for the control of converter with tapped inductor.

This chapter uses passivity-based control to implement closed-loop operation for Tapped-inductor Boost converter. The models of Tapped-inductor Boost converter are elaborated in detail. The overall performances of control are analyzed. Comparisons among peak-current mode control, sliding mode control and passivity-based control are carried out.

5.1 Overview of passivity-based control

5.1.1 Definition of passivity

Dissipation is a common property of nature object, which implies that the stored energy of system is always less than the received energy from outside. For a dissipative system, if the injected power can be expressed by the product of input and output, then this kind of dissipative system can be called ***Passive System***. Passivity is a special kind of dissipation. The property of passivity plays a vital role in designing asymptotically stabilizing controllers for nonlinear systems. The passive property can be illustrated by (5-1) and (5-2).

$$H(t) - H(0) \le \int_0^t (u^{\mathrm{T}} \cdot y) d\tau \tag{5-1}$$

$$\dot{H} \le u^{\mathrm{T}} \cdot y \tag{5-2}$$

In these equations, H is the energy stored in systems. u and y are input and output, respectively, which may be vectors. If the "$\le$" can be changed into "$<$", then this passivity system is so-called strictly passive system.

5.1.2 Port-controlled Hamiltonian system

Most nature physical systems have the property of passivity. One important passivity system is Hamilton system. Hamilton equation is one of important method to describe mechanical system. Researches show that this methodology can be applied to electrical system including power electronics converters [130]. The port-controlled Hamiltonian systems (PCH) with dissipation can be expressed by (5-3).

$$\Sigma : \begin{cases} \dot{\mathbf{x}} = [\mathbf{J}(\mathbf{x}) - \mathbf{R}(\mathbf{x})] \dfrac{\partial H}{\partial \mathbf{x}} + \mathbf{g}(\mathbf{x})\mathbf{u} \\ \mathbf{y} = \mathbf{g}^{\mathrm{T}}(\mathbf{x}) \dfrac{\partial H}{\partial \mathbf{x}} \end{cases} \tag{5-3}$$

where $\mathbf{x}$ is the state variable. $\mathbf{J}(\mathbf{x})$ is the structure matrix. For a Hamilton system, it can be proved that $\mathbf{J}(\mathbf{x})$ is a skew-symmetric matrix [130], which is the key property to form the passivity-based control algorithm. $\mathbf{R}(\mathbf{x})$ is the damping matrix which can dissipate the stored energy. It should be positive or semi-positive definite matrix. H is the energy stored by system. It is a positive real quantity at non-zero state and is zero only at zero state. $\mathbf{g}(\mathbf{x})$ is input matrix. $\mathbf{u}$ and $\mathbf{y}$ are input and output respectively.

It is quite straightforward to check that all the average models of the basic DC-DC converters conform to the generalized Hamiltonian model given in (5-3).

It is easy to test that a system described by (5-3) is passive. By differentiating the energy function H with respect to time, the PCH system satisfies the power-balance equation as follows.

$$\frac{\partial H}{\partial t} = \left(\frac{\partial H}{\partial \mathbf{x}}\right)^{\mathrm{T}} [\mathbf{J}(\mathbf{x}) - \mathbf{R}(\mathbf{x})] \frac{\partial H}{\partial \mathbf{x}} + \left(\frac{\partial H}{\partial \mathbf{x}}\right)^{\mathrm{T}} \mathbf{g}(\mathbf{x})\mathbf{u} \tag{5-4}$$

Using the condition that $\mathbf{J}(\mathbf{x})$ is a skew-symmetric matrix, the above equation can be simplified to (5-5).

$$\frac{\partial H}{\partial t} = -(\frac{\partial H}{\partial \mathbf{x}})^{\mathrm{T}} \mathbf{R}(\mathbf{x}) \frac{\partial H}{\partial \mathbf{x}} + \mathbf{y}^{\mathrm{T}} \mathbf{u} \tag{5-5}$$

As mentioned above, $\mathbf{R}(\mathbf{x})$ is positive or semi-positive definite matrix. We can obtain the following inequality (5-6) which demonstrates the passivity of system (5-3).

$$\frac{\partial H}{\partial t} \le \mathbf{y}^{\mathrm{T}} \mathbf{u} \tag{5-6}$$

5.1.3 Energy shaping

The purpose of energy-shaping is to reshape the energy-storage function *H* for closed-loop system. When passivity property is applied to controller design, the energy storage *H* should be clarified further. In (5-3), *H* is the energy storage of original system which is also open-loop system. If input quantity ***u*** can be set to zero or negative output –***y***, then the energy storage *H* will dissipate to zero or a lower limit (if it exists). Unfortunately for most controlled system, the desired value of energy storage is not zero or the lower limit. So one of the key procedures in PBC design is the so-called energy-shaping [130]. Equations (5-7) and (5-8) illustrate the common choice for open-loop energy-storage function and reshaped closed-loop energy-storage function. The matrix **D** can be viewed as inertia matrix. It is a positive diagonal matrix [130].

$$H_{open-loop} = \frac{1}{2} \mathbf{x}^{\mathrm{T}} \mathbf{D} \mathbf{x} \tag{5-7}$$

$$H_{close-loop} = \frac{1}{2} (\mathbf{x} - \mathbf{x}_d)^{\mathrm{T}} \mathbf{D} (\mathbf{x} - \mathbf{x}_d) \tag{5-8}$$

5.1.4 Damping injection

The second key procedure in PBC design is damping injection. The main purpose of damping injection is to modify the damping matrix $\mathbf{R}(\mathbf{x})$ to make it strictly positive definite. The damping injection also provides adjustable parameters to adjust the effect of control.

5.2 PBC for Tapped-inductor Boost converter

This section uses Tapped-inductor Boost converter as example to illustrate the application of PBC to Tapped-inductor DC-DC converters.

5.2.1 Port-controlled Hamiltonian model of Tapped-inductor Boost converter

Unlike conventional DC-DC converter, Tapped-inductor converter has the discontinuous current of inductor during the transition interval. This difference increases the difficulty of modeling and controller design for Tapped-inductor converter. This section uses Tapped-inductor Boost converter as an example to illustrate the difference of modeling between Tapped-inductor converter and convention DC-DC converter.

The configuration of Tapped-inductor Boost converter is shown in Fig. 5-1.

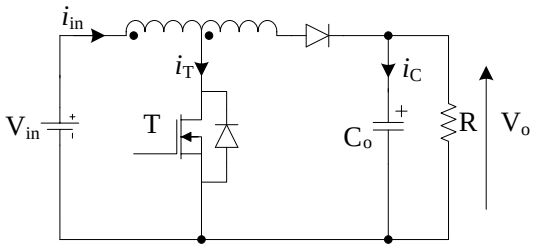

Fig. 5-1 Tapped-inductor Boost converter

Assume the turns ratio of secondary winding to primary winding is k, L_{on} is the inductance of primary winding, and i_{ms} is the magnetizing current transferred to secondary side. The switch is turned on and off alternatively in a period. The two state equations under on-switch and off-switch are described in (5-9) and (5-10), respectively.

On-switch:

$$\begin{bmatrix} \dot{i}_{ms} \\ v_C \end{bmatrix} = \begin{bmatrix} 0 & 0 \\ 0 & -\frac{1}{RC} \end{bmatrix} \cdot \begin{bmatrix} i_{ms} \\ v_C \end{bmatrix} + \begin{bmatrix} \frac{1}{(1+k)L_{on}} \\ 0 \end{bmatrix} \cdot V_{in} \tag{5-9}$$

Off-switch:

$$\begin{bmatrix} \dot{i}_{ms} \\ v_C \end{bmatrix} = \begin{bmatrix} 0 & -\frac{1}{L_{off}} \\ \frac{1}{C} & -\frac{1}{RC} \end{bmatrix} \cdot \begin{bmatrix} i_{ms} \\ v_C \end{bmatrix} + \begin{bmatrix} \frac{1}{L_{off}} \\ 0 \end{bmatrix} \cdot V_{in} \tag{5-10}$$

It should be noticed that $L_{off} = L_{on}(1+k)^2$. Then Using the standard state-space-average method [100, 101], we can obtain the state-space averaged

model of Tapped-inductor Boost converter as (5-11). u is the duty ratio.

$$\begin{bmatrix} \dot{i}_{ms} \\ v_C \end{bmatrix} = \begin{bmatrix} 0 & -\frac{(1-u)}{L_{off}} \\ \frac{(1-u)}{C} & -\frac{1}{RC} \end{bmatrix} \cdot \begin{bmatrix} i_{ms} \\ v_C \end{bmatrix} + \begin{bmatrix} \frac{1+ku}{L_{off}} \\ 0 \end{bmatrix} \cdot V_{in} \tag{5-11}$$

In fact this model can be transformed into the port-controlled Hamilton model. If the state variables are chosen as flux linkage of inductor and charge of capacitor, H represents the energy stored by the Tapped-inductor Boost converter, then the model (5-11) can be transformed into port-controlled Hamiltonian model equivalently. The state vector and energy function can be expressed as

$$\boldsymbol{\alpha} = \begin{bmatrix} \psi_L & Q_C \end{bmatrix}^{\mathrm{T}} \tag{5-12}$$

$$H = \frac{1}{2} L_{off} i_{ms}^2 + \frac{1}{2} C v_C^2 = \frac{1}{2} \boldsymbol{\alpha}^{\mathrm{T}} \mathbf{D}^{-1} \boldsymbol{\alpha} \tag{5-13}$$

where **D** is positive diagonal matrix. **D** and its inverse matrix can be expressed as (5-14).

$$\mathbf{D} = \begin{bmatrix} L_{off} & 0 \\ 0 & C \end{bmatrix}, \quad \mathbf{D}^{-1} = \begin{bmatrix} \frac{1}{L_{off}} & 0 \\ 0 & \frac{1}{C} \end{bmatrix} \tag{5-14}$$

Now the original system (5-11) can be equivalently revised to the PCH equation (5-15).

$$\dot{\boldsymbol{\alpha}} = \left(\begin{bmatrix} 0 & -(1-u) \\ (1-u) & 0 \end{bmatrix} - \begin{bmatrix} 0 & 0 \\ 0 & \frac{1}{R} \end{bmatrix} \right) \frac{\partial H}{\partial \boldsymbol{\alpha}} + \begin{bmatrix} V_{in} \\ 0 \end{bmatrix} \cdot (1+ku) \tag{5-15}$$

It can be verified that (5-15) is consistent to the standard PCH equation (5-3) by just letting:

$$\mathbf{J} = \begin{bmatrix} 0 & -\frac{1-u}{1+k} \\ \frac{1-u}{1+k} & 0 \end{bmatrix}, \quad \mathbf{R} = \begin{bmatrix} 0 & 0 \\ 0 & \frac{1}{R} \end{bmatrix}, \quad \mathbf{g} = \begin{bmatrix} V_{in} \\ 0 \end{bmatrix}, \quad U = 1+ku, \quad y = \mathbf{g}^{\mathrm{T}} \frac{\partial H}{\partial \boldsymbol{\alpha}} \tag{5-16}$$

In the equation (5-16), U is the equivalent control input, which is a function of duty ratio u. It can be concluded that the PCH system (5-15) defines a passive map: $U \rightarrow y$.

Let **x** represent the original state vector appeared in (5-11).

$$\mathbf{x} = \begin{bmatrix} i_{ms} & v_C \end{bmatrix}^{\mathrm{T}} \tag{5-17}$$

Notice that

$$\boldsymbol{\alpha} = \mathbf{D}\mathbf{x} \tag{5-18}$$

and

$$\frac{\partial H}{\partial \boldsymbol{\alpha}} = \mathbf{D}^{-1}\boldsymbol{\alpha} = \mathbf{x} \tag{5-19}$$

Substitute (5-18) and (5-19) into (5-15), an equivalent and simplified PCH equation can be obtained as (5-20).

$$\mathbf{D}\dot{\mathbf{x}} = (\mathbf{J} - \mathbf{R})\mathbf{x} + \mathbf{g} \cdot U \tag{5-20}$$

5.2.2 PBC for Tapped-inductor Boost converter

- Energy shaping

The desired state of Tapped-inductor Boost converter is shown in (5-21).

$$\mathbf{x}_d = \begin{bmatrix} i_{msd} & v_{Cd} \end{bmatrix}^{\mathrm{T}} \tag{5-21}$$

Then the PCH model shown in (5-20) can be transformed into the error dynamics as follows.

$$\mathbf{D}\dot{\tilde{\mathbf{x}}} = (\mathbf{J} - \mathbf{R})\tilde{\mathbf{x}} + \boldsymbol{\Phi} \tag{5-22}$$

where

$$\tilde{\mathbf{x}} = \mathbf{x} - \mathbf{x}_d \tag{5-23}$$

$$\boldsymbol{\Phi} = \mathbf{g} \cdot U - \mathbf{D}\dot{\mathbf{x}}_d + (\mathbf{J} - \mathbf{R})\mathbf{x}_d \tag{5-24}$$

Now the energy function of the error dynamic system (5-22) should be chosen as (5-25). With this energy function, it can be easily verified that (5-22) also defines a passive map: $\boldsymbol{\Phi} \to \tilde{\mathbf{x}}$.

$$H_e = \frac{1}{2}(\mathbf{x} - \mathbf{x}_d)^{\mathrm{T}}\mathbf{D}(\mathbf{x} - \mathbf{x}_d) \tag{5-25}$$

- Damping injection

Reforming the damping matrix **R** can make sure that the state vector converges to the desired point. The converging condition is that the reformed damping matrix is positive definite. One simple method of damping injection is shown by (5-26).

$$\mathbf{R_d} = \mathbf{R} + \mathbf{R}' = \begin{bmatrix} r_1 & 0 \\ 0 & r_2 + 1/R \end{bmatrix} \tag{5-26}$$

where

$$\mathbf{R}' = \begin{bmatrix} r_1 & 0 \\ 0 & r_2 \end{bmatrix} \tag{5-27}$$

r_1 and r_2 are adjustable parameters. Now $\mathbf{R_d}$ is positive definite.

Then the new error dynamic equation of original Tapped-inductor Boost converter should be:

$$\mathbf{D}\dot{\tilde{\mathbf{x}}} = (\mathbf{J} - \mathbf{R_d})\tilde{\mathbf{x}} + \mathbf{\Psi} \tag{5-28}$$

$$\mathbf{\Psi} = \mathbf{\Phi} + \mathbf{R}'\tilde{\mathbf{x}} = \mathbf{g} \cdot U - \mathbf{D}\dot{\mathbf{x}}_d + (\mathbf{J} - \mathbf{R})\mathbf{x}_d + \mathbf{R}'\tilde{\mathbf{x}} \tag{5-29}$$

Using the method in section 5.2.1, it can be easily verified that, with the energy function H_e (see equation (5-25)), the error dynamic system (5-28) also defined a strictly passive map: $\mathbf{\Psi} \to \tilde{\mathbf{x}}$. This indicates that:

$$\dot{H}_e \le \tilde{\mathbf{x}}^{\mathrm{T}}\mathbf{\Psi} \tag{5-30}$$

The equal sign is satisfied only at $\tilde{\mathbf{x}} = 0$.

If $\mathbf{\Psi}$ is set to zero, then according to Lyapunov theory about stability, the error dynamic system (5-28) is asymptotically stable at the equilibrium point $\tilde{\mathbf{x}} = 0$.

So the controller can be derived by setting $\mathbf{\Psi} \equiv 0$, which leads to (5-31).

$$\mathbf{g} \cdot U - \mathbf{D}\dot{\mathbf{x}}_d + (\mathbf{J} - \mathbf{R})\mathbf{x}_d + \mathbf{R}'\tilde{\mathbf{x}} = 0 \tag{5-31}$$

By substituting (5-16), (5-17), (5-21), (5-23) and (5-27) into (5-31), the controller dynamic equation can be obtained as (5-32).

$$\begin{cases} (1+ku)V_{in} - L_{off}\dot{i}_{msd} - (1-u)v_{Cd} + r_1\tilde{i}_{ms} = 0 \\ -C\dot{v}_{Cd} + (1-u)i_{msd} - \dfrac{1}{R}v_{Cd} + r_2\tilde{v}_C = 0 \end{cases} \tag{5-32}$$

The next step is to determine the reference values i_{msd} and v_{Cd}, which leads to two kinds of controllers. The first one is so-called “direct control”, which stabilizes

the capacitor voltage to a preset reference of output voltage directly. The second one is so-called "indirect control". Indirect control stabilizes the magnetizing current of inductor to a preset reference that is corresponding to a desired output voltage. The problem of indirect control is that the reference value of magnetizing current of inductor is hard to be determined for those applications with frequently varied load. Additional measure, e.g. adaptive algorithm, robust control etc., is necessary to enhance the robustness of controller.

- Direct control

The purpose of direct control is to regulate the output voltage to the expected value directly. This means the v_{Cd} should be set to the constant reference V^*. This leads to the control strategy shown in (5-33) and (5-34). For simplicity, r_2 can be set to zero. This does not affect the stability because the modified damping matrix shown in (5-26) is still negative definite.

$$v_{Cd} = V^* \tag{5-33}$$

The control strategy is:

$$\begin{cases} u = 1 - \dfrac{1}{i_{msd}}\left(\dfrac{1}{R}V^* - r_2\tilde{v}_C\right) \\ \dot{i}_{msd} = \dfrac{1}{L_{off}}[(1+ku)V_{in} - (1-u)V^* + r_1\tilde{i}_{ms}] \end{cases} \tag{5-34}$$

The controller should stabilize $\mathbf{x}$ to the desired value $\mathbf{x_d}$ under steady state. Then under steady state, the controller should be reduced as follows.

$$\dot{u} = \frac{(1-u)^2 R}{L_{off}V^*}[(1+ku)V_{in} - (1-u)V^*] \tag{5-35}$$

By letting $\dot{u} = 0$, the only equilibrium of the controller with physical meaning can be obtained as (5-36).

$$u^* = \frac{V^* - V_{in}}{V^* + kV_{in}} \tag{5-36}$$

At this equilibrium,

$$\left.\frac{d\dot{u}}{du}\right|_{u=u^*} = \frac{RV_{in}^2}{L_{on}v_C^*(v_C^* + kV_{in})} > 0 \tag{5-37}$$

Inequality (5-37) means the controller is not stable under steady state. So this controller is not a feasible controller.

- Indirect control

From above analysis it can be found that the direct control of output voltage is not feasible. This is the common problem of non-minimum phase property of Boost converter. An alternative method is indirect regulation of output voltage.

Indirect control set the inductor current to a constant reference, i.e. $i_{msd} = I^*$. Then substitute it into (5-32), the desired state can be obtained as (5-38). Here r_2 can be set to zero again. This does not affect the stability.

$$i_{msd} = I^* \tag{5-38}$$

Substituting this desired state into the second equation in (5-32), the indirect control strategy can be obtained as follows.

$$\begin{cases} \tilde{i}_{ms} = i_{ms} - I^*, \tilde{v}_C = v_C - v_{Cd} \\ \dot{v}_{Cd} = \dfrac{1}{C}[(1-u)I^* - \dfrac{1}{R}v_{Cd} + r_2\tilde{v}_C] \\ u = \dfrac{v_{Cd} - V_{in} - r_1\tilde{i}_{ms}}{kV_{in} + v_{Cd}} \end{cases} \tag{5-39}$$

Now examine the stability of this algorithm. At steady state, the state reaches the desired point shown in (5-38). Then the zero dynamics is as follows.

$$\dot{u} = \frac{1}{C}[(1-u)^2 I^* - \frac{1}{R}(1+ku)V_{in}] \tag{5-40}$$

The static duty ratio under steady state can be obtained by letting $\dot{u} = 0$.

$$u^* = 1 - \frac{-kV_{in} + \sqrt{(kV_{in})^2 + 4I^*R(1+k)V_{in}}}{2I^*R} \tag{5-41}$$

Under this duty ratio,

$$\left.\frac{d\dot{u}}{du}\right|_{u=u_{static}} = -\frac{1}{RC}\sqrt{(kV_{in})^2 + 4I^*R(1+k)V_{in}} < 0 \tag{5-42}$$

This inequality proves the controller is stable at the static point. So it is a

feasible controller.

If the purpose of the controller is to stabilize the output voltage to a desired value v_{Cd}, then the magnetizing current reference should be set according to (5-43).

$$I^* = \frac{V^*(V^* + kV_{in})}{(1+k)V_{in}R} \tag{5-43}$$

The control structure is shown in Fig. 5-2.

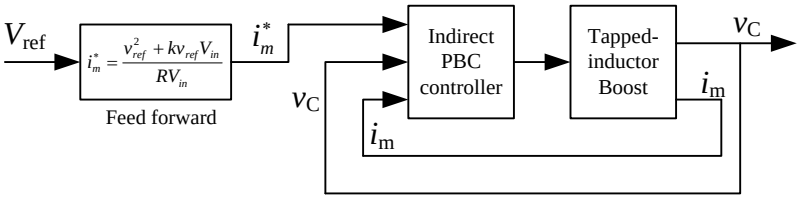

Fig. 5-2 The structure of indirect PBC for Tapped-inductor Boost converter

5.2.3 Simulation results

Simulation results are presented below based on the above indirect PBC algorithm. The simulation parameters for the Tapped-inductor converter are: k=12/11, V_{in}=24V, L_{on}=33μH, R=20Ω, C=220μF. The desired output voltage is 74V. The adjustable damping is selected as $r_1 = 3$.

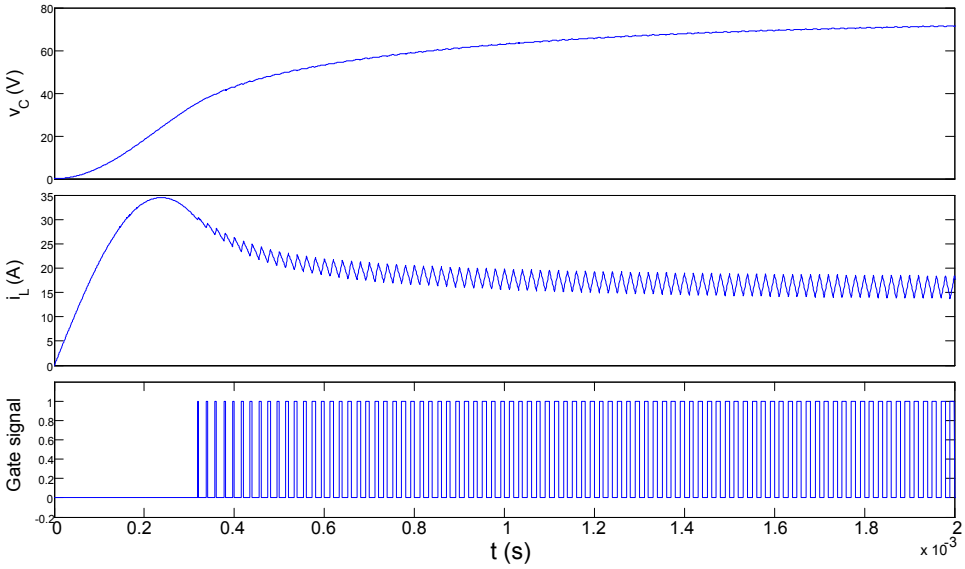

Fig. 5-3 Enlarged transient response of Tapped-inductor Boost converter under indirect PBC

Fig. 5-3 shows the simulation waveforms for the course from start-up to steady

state of Tapped-inductor Boost converter under indirect PBC.

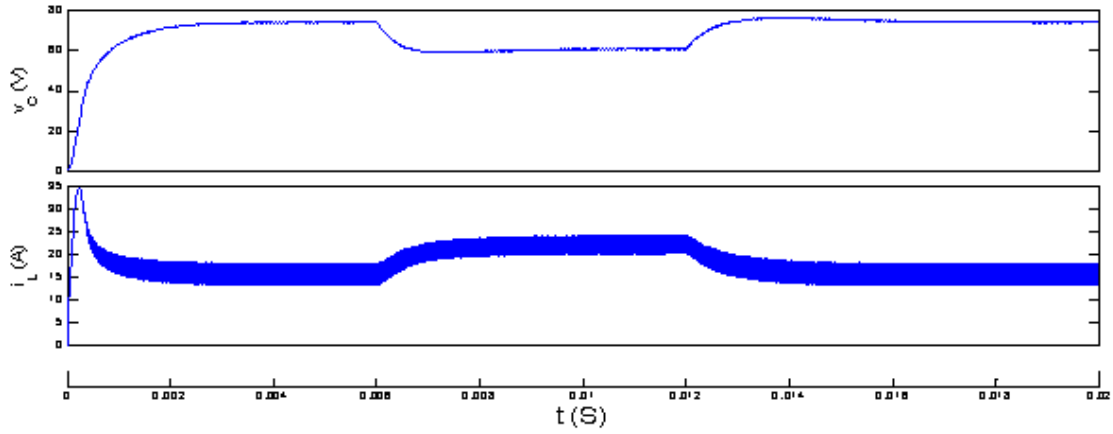

Fig. 5-4 Response of Tapped-inductor Boost converter controller by indirect PBC under load variation

Fig. 5-4 shows the simulation results under varying load. From this figure, it can be found that there is static error of output voltage when the load resistor deviates from nominal value. This is drawback of indirect control. Extra measures, e.g. adaptive strategy or robust strategy, are necessary to enhance robustness of the indirect PBC controller.

5.3 Peak-current-mode control for Tapped-inductor Boost converter

5.3.1 The small-signal model of Tapped-inductor Boost converter

The nonlinear state-space averaged model of Tapped-inductor Boost converter which is shown in (5-11) can be linearized around static operating point.

Assume the desired static value of output voltage, magnetizing current and duty ratio are V_c, I_m and D, respectively. By applying the standard methods of linearization [114] to the state-space averaged model shown in (5-11), the small-signal model of Tapped-inductor Boost converter can be obtained as (5-44).

$$\begin{bmatrix} \dot{\hat{i}}_m \\ \dot{\hat{v}}_C \end{bmatrix} = \begin{bmatrix} 0 & -\frac{1-D}{L_{on}(1+k)} \\ \frac{1-D}{C(1+k)} & -\frac{1}{RC} \end{bmatrix} \cdot \begin{bmatrix} \hat{i}_m \\ \hat{v}_C \end{bmatrix} + \begin{bmatrix} \frac{V_{in}}{L_{on}(1-D)} \\ \frac{(1+kD)V_{in}}{RC(1-D)^2} \end{bmatrix} \cdot \hat{d} \tag{5-44}$$

Based on this model we can obtain the transfer function from $\hat{v}_C$ to $\hat{d}$.

$$\frac{\hat{v}_C}{\hat{d}} = \frac{a_1 s + a_0}{b_2 s^2 + b_1 s + b_0} \tag{5-45}$$

where

$$\begin{aligned} a_0 &= (1+k)(1-D)^2 RV_{in} \\ a_1 &= -(1+k)^2(1+kD)L_{on}V_{in} \\ b_0 &= (1-D)^4 R \\ b_1 &= (1+k)^2(1-D)^2 L_{on} \\ b_2 &= (1+k)^2(1-D)^2 RCL_{on} \end{aligned} \tag{5-46}$$

It can be found that, like conventional Boost converter, the small-signal transfer function of duty ratio to voltage of Tapped-inductor Boost converter also comprises right half plane (RHP) zero. It inherits the property of non-minimum phase from classical Boost converter, which makes the compensation with only voltage feedback be difficult. So current-mode control is adopted to fix this problem.

Based on the small-signal state-space equation (5-44), the transfer function from $\hat{v}_C$ to $\hat{i}_m$ can be obtained as equation (5-47).

$$\frac{\hat{v}_C}{\hat{i}_m} = -\frac{(1+k)(1+kD)L_{on}s - R(1-D)^2}{(1+k)(1-D)RCs + (1-D)(2+k+kD)} \tag{5-47}$$

For the converter with the parameters: k=12/11, V_{in}=24V, D=0.5, L_{on}=33μH, R=20ohm, C=220μF and expected output voltage V_c=74V, the transfer function is derived as (5-48)

$$\frac{\hat{v}_C}{\hat{i}_m} = \frac{-0.0001066s + 5}{0.0046s + 1.818} \tag{5-48}$$

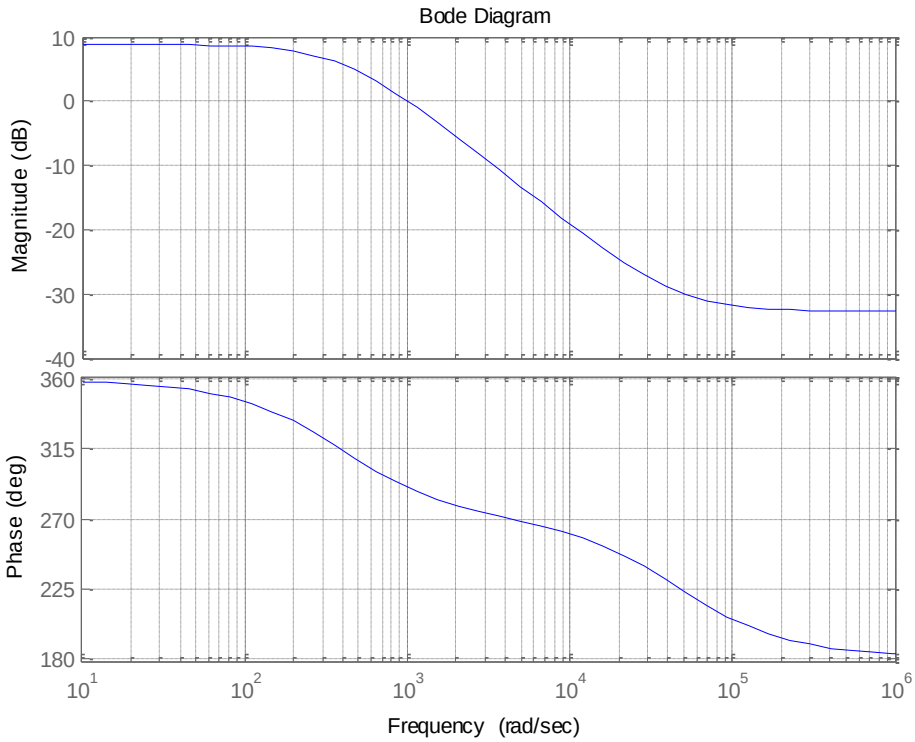

Fig. 5-5 The Bode diagram of small-signal model of Tapped-inductor Boost converter

It can be found that the maximum phase shift of the open loop system is 180^o. It is easy to be compensated. Even just an integrator is sufficient. Here use a type 2 compensator is used.

5.3.2 The design of peak-current-mode controller for Tapped-inductor Boost converter

Now choose the crossover frequency equal to 1/5 switching frequency, i.e. 20kHz. Using a type 2 compensator, the transfer function of compensator is:

$$G_C = 2106.9\frac{0.0068s+1}{s(0.00002s+1)(0.0000056s+1)} \tag{5-49}$$

Then the total transfer function is $G_C * \frac{\hat{v}_C}{\hat{i}_m}$. The open-loop Bode diagram of compensated system is as follows:

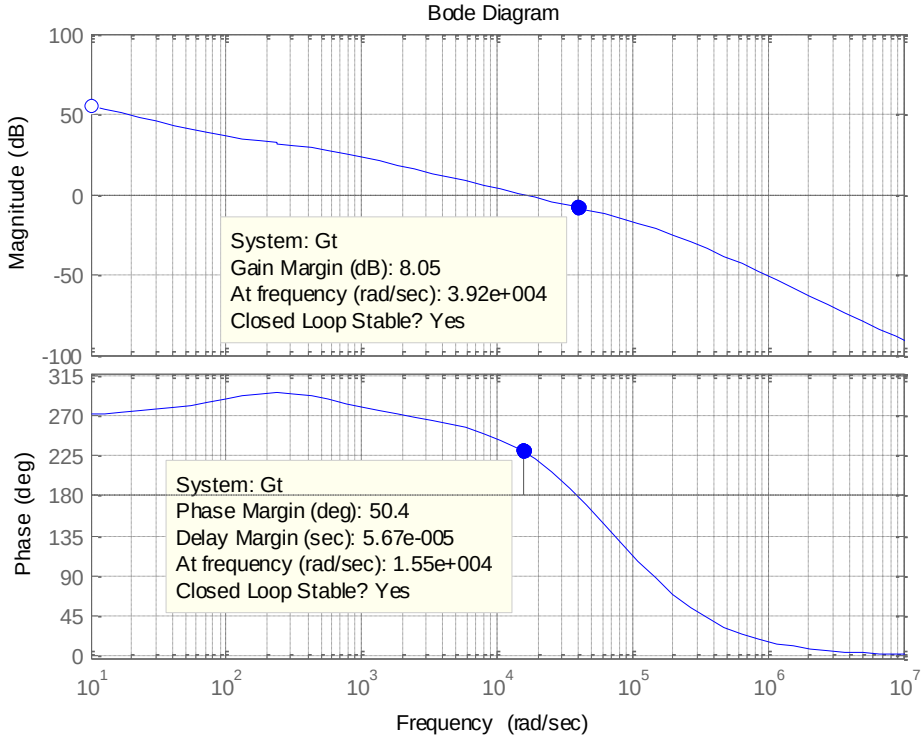

Fig. 5-6 The Bode diagram of compensated small-signal model

The structure of closed loop system is shown in Fig. 5-7 below.

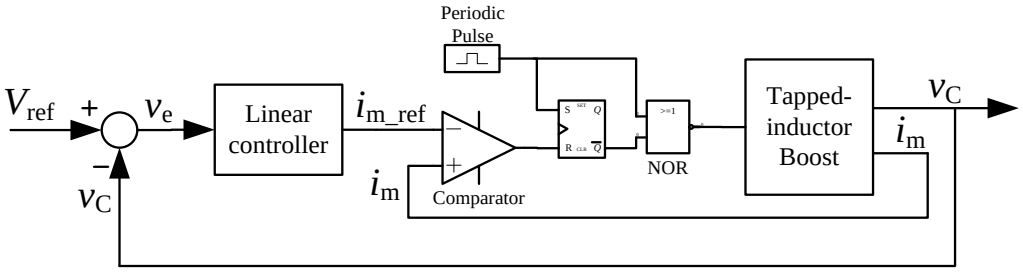

Fig. 5-7 The block diagram of peak-current-mode controller

5.3.3 The simulation results

Fig. 5-8 shows the simulation results of Tapped-inductor Boost converter with peak-current-mode control. The controller is shown in Fig. 5-7. The parameters of linear compensator in Fig. 5-7 are shown in (5-49). From Fig. 5-8, it can be found that the current overshoot is much larger than that in PBC control. But the response time is shorter than that in PBC control.

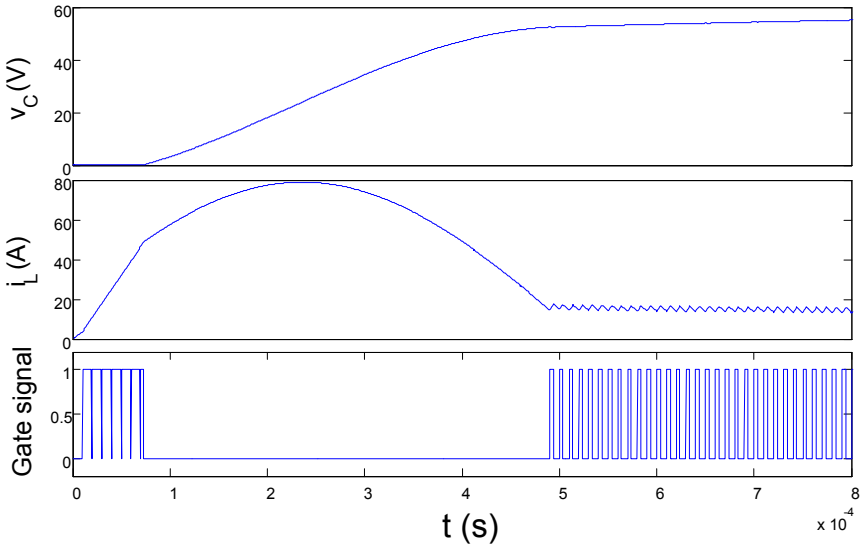

Fig. 5-8 Start-up of Tapped-inductor Boost converter under peak-current mode control

5.4 Experimental results and comparison between PBC and peak-current-mode control

5.4.1 The results of PBC control

Fig. 5-9 shows the response of output voltage under the step of resistance of load. The conditions of experiment are as follows. E=24V, V_{o_ref}=60V, f_s=50 kHz. The PBC controller in Fig. 5-2 involves adaptive estimation of load resistance in this experiment. The parameters of controller are set as R_1=0.19, R_2=0. The nominal resistance of load is changed by 68Ω→45.33Ω→68Ω. From Fig. 5-9 it can be found that under the disturbance the recovery time of output voltage is about 10ms. The maximum voltage dip is about 5V (8.3% of nominal output voltage).

Fig. 5-10 shows the response of output voltage under the step of reference. The conditions of experiment and parameters of controller are the same as above experiment. The reference of output voltage is changed by 60V→40V→60V. From Fig. 5-10 it can be found that under negative step the response time of output voltage is about 40ms, while under positive step the response time is about 20ms. No overshoot occurs.

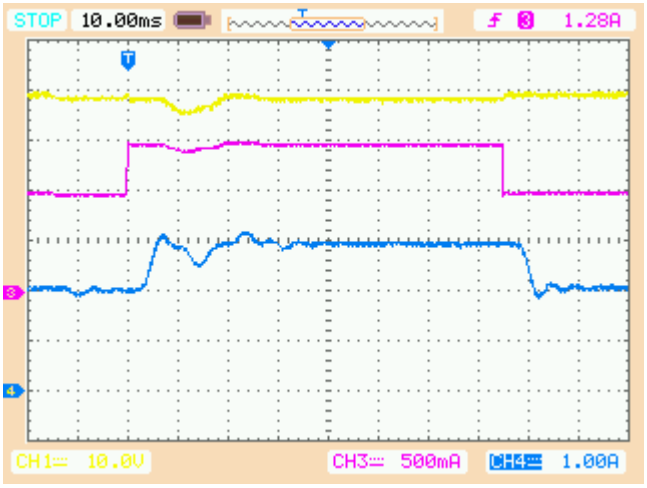

Fig. 5-9 The response of output voltage under load step.

CH1: output voltage (10V/div), CH3: output current (0.5A/div), CH4: i_{ms} (1A/div)

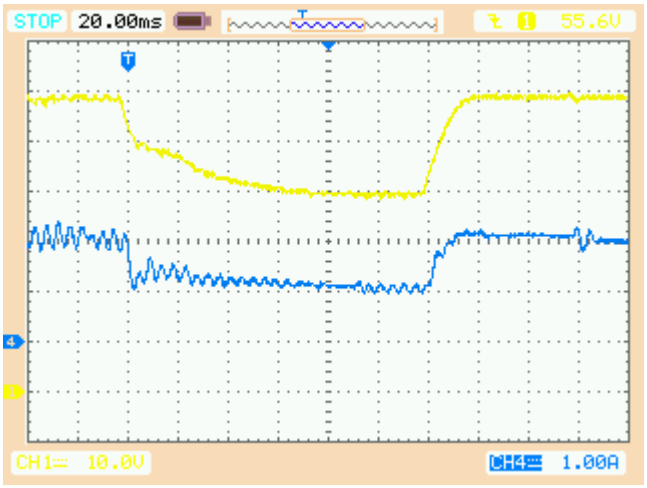

Fig. 5-10 The response of output voltage under reference step.

CH1: output voltage (10V/div), CH4: i_{ms} (1A/div)

5.4.2 The results of peak-current-mode control

Fig. 5-11 shows the transient response of Tapped-inductor Boost converter under load step. The conditions of experiment are as follows. E=24V, V_{o_ref}=60V, f_s=50 kHz. The linear controller in Fig. 5-7 is chosen as PI controller in this experiment. The controller parameters are set as k_p=4, k_i=1. The resistance of load is changed by 30Ω→60Ω→30Ω.

Through the experimental result shown in Fig. 5-11, it can be found that the response time for negative step of load is about 50ms, while the response time for positive step of load is about 20ms. In general, the response time is long.

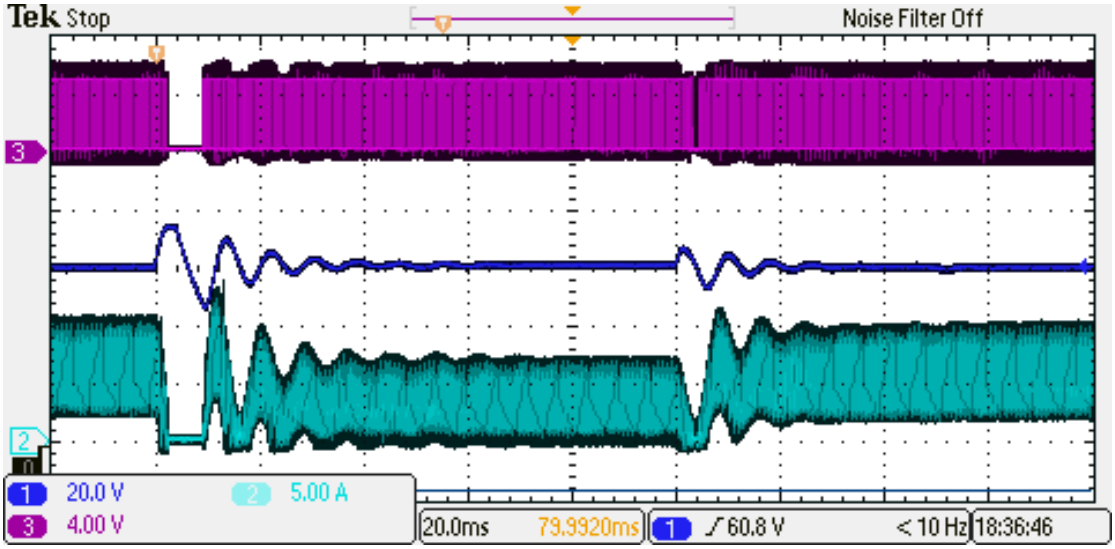

Fig. 5-11 the transient response of Tapped-inductor Boost converter under load step. CH1: output voltage, CH2: current of tapped inductor, CH3: gate signal

5.5 Conclusions

Two controllers have been developed for Tapped-inductor Boost converter. One is peak-current-mode control, another one is passivity-based control.

Peak-current-mode control has the advantage that the control law is simple and it can be implemented by analogy circuit. The controller circuit is the same as that for conventional Boost converter. But in the compensator design the magnetizing inductance should be used to replace the inductance in conventional Boost converter.

The passivity-based control (PBC) is more robust under large signal disturbance. The transient performance of system controlled by PBC is better than that controlled by peak-current-mode control. But the control law of PBC is more complicated than that of peak-current-mode control. Moreover the PBC can only be implemented by digital control which may increase the cost of controller.

Experimental results reveal that the recovery time under PBC control is shorter than that under peak-current-mode control. The voltage vibration under PBC control is smaller than that under peak-current-mode control.

Chapter 6 Conclusions and suggestions for further research

6.1 The works carried out in thesis

Based on the research results of previous scholars, this thesis has carried out the research on energy handling in power conversion. The concepts of energy storage and variation of energy storage have been distinguished. The latter is named as buffer energy. The characteristics of energy storage and buffer energy are explored for basic topologies of DC-DC converters based on the index of energy factor and buffer energy factor. The relation and difference between buffer energy factor and AC power factor has been examined and clarified. The relation between efficiency and buffer energy factor has also been uncovered and proved by experiment. As the enormous potential in the application of DC distribution system, Tapped-inductor converters have been chosen as the object to apply the above methods on energy research. The comparison between Tapped-inductor Boost converter and conventional Boost converter has been carried out. The comparison includes buffer energy factor, efficiency, voltage gain and stress of components. The particularity of dynamic model of Tapped-inductor converter which is different from conventional DC-DC converters has been clarified. One important energy-based control methods: Passivity-based control (PBC) has been used to control the Tapped-inductor Boost converter. The comparison between PBC and peak current mode control has been carried out by both theoretical analysis and experimental results.

6.2 Conclusions

Through the work in this thesis, the following conclusions are obtained.

(1) This thesis presents the concepts and corresponding definitions of ***Energy Storage*** ($\boldsymbol{E_S}$), ***Energy Factor*** ($\boldsymbol{F_E}$), ***Buffer Energy*** ($\boldsymbol{E_B}$)and ***Buffer Energy Factor*** ($\boldsymbol{F_{EB}}$). $\boldsymbol{E_S}$ and $\boldsymbol{F_E}$ are used to indicate the amount of energy stored in DC-DC converters during operation. $\boldsymbol{E_B}$ and $\boldsymbol{F_{EB}}$ are used to indicate the magnitude of variation of energy storage in DC-DC converter.

These novel concepts can be applied to evaluate different topologies of DC-DC converters. Through the comparison of Buck, Boost and Buck-Boost converter, the following conclusions can be obtained. To deliver the same power, Buck-Boost

converter has to store the most energy, while the Buck converter needs to store the least energy. It can be also found that the ratio of stored energy of inductor to capacitor depends on the circuit parameters including inductance, capacitance and load. In Boost and Buck-Boost converters, this ratio is also related to the voltage conversion ratio M. When M increases, the ratio also increases.

Buffer energy factor F_{EB} can reflect the magnitude of variation of energy stored in converter. For Buck, Boost and Buck-Boost converters, F_{EB} increases as inductor L and frequency f_s decreases, resistor of load R increases. That means the magnitude of variation of energy storage increases as L and f_s decreases, R increases. The analysis based on buffer energy factor is also carried out for higher order DC-DC converters which include Cuk, Sepic and Zeta converter. For all the three converters, in general, F_{EB} increases as inductor L and frequency f_s decreases, resistor of load R increases. This is the universal property shared by the three basic first order converters (Buck, Boost and Buck-Boost converters). Small F_{EB} indicates that the power loss will be relatively low and efficiency is expected to be high. Experimental results for Cuk and Zeta converter confirm the relationship between buffer energy factor and efficiency.

(2) The definitions of the novel concepts referred as buffer energy and buffer energy factor has been further extended based on the theory of decomposition of power. The more general definitions make the buffer energy and buffer energy factor can be used to analyze both DC and AC systems. The correlation and difference among buffer energy and reactive energy, buffer energy factor and power factor have been clarified. The advantage of buffer energy and buffer energy factor is that they can indicate the amount of non-active energy (or power) in DC-DC converters whereas conventional reactive power and power factor cannot.

Based on the extended definitions, buffer energy factor can be calculated for a whole circuit of DC-DC converters. Theoretical results explain Boost converter has much lower energy factor than Buck and Buck-Boost converters, which indicate that much less non-active power is absorbed by Boost converter from the front-end power supply. For the same reason SEPIC and Cuk converters have lower energy factor than Zeta converter. But among these three converters, Zeta converter has the least amount of non-active circulating energy inside the converter.

Experimental results show that buffer energy factor can be measured. The measured results are consistent with theoretical analysis.

(3) This thesis investigates the performance of Tapped-inductor converters under steady state. The possible topologies of Tapped-inductor are collected based on previous research. Tapped-inductor Boost converter and conventional Boost converter have been chosen as examples to carry out the comparison. The comparison is carried out under the same input voltage, output voltage and load.

Theoretical analysis illustrates that, with the existence of parasitic parameters of components in circuit, the voltage gain of Tapped-inductor Boost converter is higher than the conventional Boost converter under the same duty ratio; the efficiency of Tapped-inductor Boost converter is higher than the conventional Boost converter under the same voltage conversion ratio.

The comparison of stress of components is also carried out between Tapped-inductor Boost converter and conventional Boost converter. The maximum voltage of transistor of the former is smaller than that of the latter. But the RMS current of transistor of the former is higher than that of the latter. In terms of Diode, the maximum voltage of the former is higher than that of the latter. But the current stress has no definite results. In terms of inductor, the RMS current of the former is higher than the latter.

The buffer energy factors of the two converters have been also carried out. The results of buffer energy factors of inductor and capacitor are the same for the two converters.

Theoretical analyses reveal the superiority of Tapped-inductor converter over their conventional counterpart on the occasion of large voltage conversion ratio.

Experimental results proved the theoretical results on voltage conversion ratio and efficiency of the two converters. The Tapped-inductor converter suffers spike and power loss caused by non-ideal coupling of tapped inductor.

(4) Two controllers have been developed for Tapped-inductor Boost converter. One is peak-current-mode control, another one is passivity-based control.

Peak-current-mode control posses the advantage that the control law is simple and it can be implemented by analogy circuit. The controller circuit is the same as

that for conventional Boost converter. But in the compensator design the magnetizing inductance should be used to replace the inductance in conventional Boost converter.

The passivity-based control (PBC) is more robust under large signal disturbance. The transient performance of system controlled by PBC is better than that controlled by peak-current-mode control. But the control law of PBC is more complicated than that of peak-current-mode control. Moreover the PBC can only be implemented by digital control which may increases the cost of controller.

6.3 Limitations and future work

Buffer energy, buffer energy factor and their related concepts proposed in this thesis have promising application in both static and dynamic analysis and design of DC-DC converters. But not all works in this area can be finished in this thesis. The following works deserve further research.

(1) The influence of buffer energy and buffer energy factor on EMI of DC-DC converter.

Buffer energy is an oscillating energy. It will induce radiated EMI. Research of the influence of buffer energy factor on EMI will be useful for the design of DC-DC converter with high switching frequency.

(2) The development of high-performance control method directly based on the buffer energy factor or buffer energy.

The energy-based control method PBC indeed provides a straight design which can obtain large-signal stability. But the future DC-DC converter needs fast response, because the trend of DC-DC converter is high efficiency and high power density. How to dissipate the energy of disturbance may depend on the research of buffer energy.

References

[1] "ENERGY STAR® Program Requirements for Single Voltage External Ac-Dc and Ac-Ac Power Supplies, Eligibility Criteria (Version 2.0), Revised Final Draft", http://www.energystar.gov/ia/partners/prod_development/revisions/downloads/Spec.pdf

[2] "80 PLUS Certified Power Supplies and Manufacturers": http://www.plugloadsolutions.com/80PlusPowerSupplies.aspx.

[3] "High Frequency Switch-mode Rectifier for Telecommunications", *Standard for communication industry*, Ministry of Industry and information Technology of the People's Republic of China, vol. Volume, pp. 3, 2008.

[4] G. Hua and F. C. Lee, "Soft-switching techniques in PWM converters", *IEEE Transactions on Industrial Electronics,*, vol. 42, pp. 595-603, 1995.

[5] T. Wu, Y. Chang, and C. Chang, "Soft Switching Boost Converter with a Flyback Snubber for High Power Applications", *IEEE Transactions on Power Electronics*, vol. PP, pp. 1-1, 2012.

[6] K.-H. Liu, R. Oruganti, and F. C. Y. Lee, "Quasi-Resonant Converters-Topologies and Characteristics", *IEEE Transactions on Power Electronics*, vol. PE-2, pp. 62-71, 1987.

[7] Z. L. Lou and Z. S. Wang, "An Improved Three-Level Soft-Switching DC/DC Converter", presented at IEEE 5th International Power Electronics and Motion Control Conference (IPEMC), 2006.

[8] K. K. Law, K. W. E. Cheng, and Y. P. B. Yeung, "Design and analysis of switched-capacitor-based step-up resonant converters", *IEEE Transactions on Circuits and Systems I: Regular Papers*, vol. 52, pp. 943-948, 2005.

[9] Y. P. B. Yeung, K. W. E. Cheng, and D. Sutanto, "Investigation of multiple output operation for switched-capacitor resonant converters", *International*

Journal of Circuit Theory and Applications, vol. 30, pp. 411-423, 2002.

[10] Y. P. B. Yeung, K. W. E. Cheng, and D. Sutanto, "Multiple and fractional voltage conversion ratios for switched-capacitor resonant converters", presented at IEEE 32nd Annual Power Electronics Specialists Conference, 2001.

[11] Y. P. B. Yeung, K. W. E. Cheng, S. L. Ho, K. K. Law, and D. Sutanto, "Unified analysis of switched-capacitor resonant converters", *IEEE Transactions on Industrial Electronics*, vol. 51, pp. 864-873, 2004.

[12] Y. P. B. Yeung, K. W. E. Cheng, D. Sutanto, and S. L. Ho, "Zero-current switching switched-capacitor quasiresonant step-down converter", *IEE Proceedings -Electric Power Applications*, vol. 149, pp. 111-121, 2002.

[13] F. Dianbo, L. Bing, and F. C. Lee, "1MHz High Efficiency LLC Resonant Converters with Synchronous Rectifier", presented at IEEE Power Electronics Specialists Conference, 2007.

[14] Y. Bo, F. C. Lee, A. J. Zhang, and H. Guisong, "LLC resonant converter for front end DC/DC conversion", presented at Seventeenth Annual IEEE Applied Power Electronics Conference and Exposition, 2002.

[15] Y. Bo, C. Rengang, and F. C. Lee, "Integrated magnetic for LLC resonant converter", presented at Seventeenth Annual IEEE Applied Power Electronics Conference and Exposition, 2002.

[16] H. Daocheng, D. Gilham, F. Weiyi, K. Pengju, F. Dianbo, and F. C. Lee, "High power density high efficiency dc/dc converter", presented at IEEE Energy Conversion Congress and Exposition (ECCE), 2011.

[17] H. Daocheng, F. C. Lee, and F. Dianbo, "Classification and selection methodology for multi-element resonant converters", presented at Twenty-Sixth Annual IEEE Applied Power Electronics Conference and Exposition (APEC), 2011.

[18] R. Mallwitz, R. Tschirbs, M. Pfaffenlehner, A. Mauder, and C. Schaeffer, "1700V Trench IGBT Modules": Infineon Technology, http://www.infineon.com/search/en?q=trench+technology&sd=PRODUCTS.

[19] K. Shenai, "Optimized trench MOSFET technologies for power devices", *IEEE Transactions on Electron Devices*, vol. 39, pp. 1435-1443, 1992.

[20] R. J. E. Hueting, E. A. Hijzen, A. Heringa, A. W. Ludikhuize, and M. A. A. Zandt, "Gate-drain charge analysis for switching in power trench MOSFETs", *IEEE Transactions on Electron Devices*, vol. 51, pp. 1323-1330, 2004.

[21] L. Lorenz, I. Zverev, A. Mittal, and J. Hancock, "CoolMOS-a new approach towards system miniaturization and energy saving", presented at IEEE Industry Applications Conference, 2000.

[22] B. J. Daniel, C. D. Parikh, and M. B. Patil, "Modeling of the CoolMOS^{TM} transistor - Part I: Device physics", *IEEE Transactions on Electron Devices*, vol. 49, pp. 916-922, 2002.

[23] B. J. Daniel, C. D. Parikh, and M. B. Patil, "Modeling of the CoolMOS^{TM} transistor. II. DC model and parameter extraction", *IEEE Transactions on Electron Devices*, vol. 49, pp. 923-929, 2002.

[24] L. Zhenxian, L. Bing, J. D. van Wyk, and F. C. Lee, "Integrated CoolMOS FET/SiC-diode module for high performance power switching", *IEEE Transactions on Power Electronics*, vol. 20, pp. 679-686, 2005.

[25] L. Lorenz, "High frequency power electronic systems are given by the newest generation of CoolMOS C3 together with SiC-Schottky diode", presented at Proceedings of the Power Conversion Conference, Osaka, 2002.

[26] L. Lorenz, G. Deboy, A. Knapp, and M. Marz, "COOLMOS-a new milestone in high voltage power MOS", presented at The 11th International Symposium on Power Semiconductor Devices and ICs Proceedings, 1999.

[27] Chen, US, Patent 5,216,275

[28] M. E. Baran and N. R. Mahajan, "DC distribution for industrial systems: opportunities and challenges", *IEEE Transactions on Industry Applications*, vol. 39, pp. 1596-1601, 2003.

[29] Z. He, F. Mollet, C. Saudemont, and B. Robyns, "Experimental Validation of Energy Storage System Management Strategies for a Local DC Distribution System of More Electric Aircraft", *IEEE Transactions on Industrial Electronics*, vol. 57, pp. 3905-3916, 2010.

[30] D. Salomonsson and A. Sannino, "Low-Voltage DC Distribution System for Commercial Power Systems With Sensitive Electronic Loads", *IEEE Transactions on Power Delivery*, vol. 22, pp. 1620-1627, 2007.

[31] K. Engelen, E. Leung Shun, P. Vermeyen, I. Pardon, R. D'Hulst, J. Driesen, and R. Belmans, "The Feasibility of Small-Scale Residential DC Distribution Systems", presented at 32nd Annual Conference on IEEE Industrial Electronics, 2006.

[32] D. J. Hammerstrom, "AC Versus DC Distribution SystemsDid We Get it Right?" presented at IEEE Power Engineering Society General Meeting, 2007.

[33] F. Wang, P. Yunqing, D. Boroyevich, R. Burgos, and N. Khai, "Ac vs. dc distribution for off-shore power delivery", presented at 34th Annual Conference of IEEE Industrial Electronics, 2008.

[34] D. Nilsson and A. Sannino, "Efficiency analysis of low- and medium- voltage DC distribution systems", presented at IEEE Power Engineering Society General Meeting, 2004.

[35] F. C. Lee, X. Ming, W. Shuo, and L. Bing, "Design Challenges For Distributed Power Systems", presented at IEEE 5th International Power Electronics and Motion Control Conference, 2006.

[36] Y. Darroman and A. Ferre, "42-V/3-V Watkins-Johnson converter for automotive use", *IEEE Transactions on Power Electronics*, vol. 21, pp.

592-602, 2006.

[37] P. Jong-Hu and C. Bo-Hyung, "The zero Voltage switching (ZVS) critical conduction mode (CRM) buck Converter With tapped-inductor", *IEEE Transactions on Power Electronics*, vol. 20, pp. 762-774, 2005.

[38] K. Nishijima, K. Abe, D. Ishida, T. Nakano, T. Nabeshima, T. Sato, and K. Harada, "A Novel Tapped-Inductor Buck Converter for Divided Power Distribution System", presented at 37th IEEE Power Electronics Specialists Conference, 2006.

[39] D. A. Grant, Y. Darroman, and J. Suter, "Synthesis of Tapped-Inductor Switched-Mode Converters", *IEEE Transactions on Power Electronics*, vol. 22, pp. 1964-1969, 2007.

[40] P. Joung-Hu and C. Bo-Hyung, "Nonisolation Soft-Switching Buck Converter With Tapped-Inductor for Wide-Input Extreme Step-Down Applications", *IEEE Transactions on Circuits and Systems I: Regular Papers*, vol. 54, pp. 1809-1818, 2007.

[41] J. H. Park and B. H. Cho, "Non-isolation Soft-switching Buck Converter with Tapped-Inductor for Wide-input Extreme Step-down applications", presented at 36th IEEE Power Electronics Specialists Conference, 2005.

[42] A. Abramovitz and K. M. Smedley, "Analysis and Design of a Tapped-Inductor Buck-Boost PFC Rectifier With Low Bus Voltage", *IEEE Transactions on Power Electronics*, vol. 26, pp. 2637-2649, 2011.

[43] J. H. Park, B. H. Cho, and T. H. Kim, "PWM-switch Model of Tapped Inductor Converters under Hysteretic Current-mode Control", presented at 32nd Annual Conference on IEEE Industrial Electronics, 2006.

[44] L. Jye-June and B. H. Cho, "A novel high step-up zero-current-switching tapped-inductor boost converter", presented at IEEE 8th International Conference on Power Electronics and ECCE Asia (ICPE & ECCE), 2011.

[45] D. A. Grant and Y. Darroman, "Inverse Watkins-Johnson converter - analysis reveals its merits", *Electronics Letters*, vol. 39, pp. 1342-1343, 2003.

[46] T. H. Kim, J. H. Park, and B. H. Cho, "Small-signal modeling of the tapped-inductor converter under variable frequency control", presented at IEEE 35th Annual Power Electronics Specialists Conference, 2004.

[47] D. A. Grant and Y. Darroman, "Watkins-Johnson converter completes tapped inductor converter matrix", *Electronics Letters*, vol. 39, pp. 271-272, 2003.

[48] K. W. E. Cheng, "Tapped inductor for switched-mode power converters", presented at 2nd International Conference on Power Electronics Systems and Applications, 2006.

[49] P. Joung-Hu and C. Bo-Hyung, "Nonisolation Soft-Switching Buck Converter With Tapped-Inductor for Wide-Input Extreme Step-Down Applications", *Circuits and Systems I: Regular Papers, IEEE Transactions on*, vol. 54, pp. 1809-1818, 2007.

[50] S. Moisseev, S. Hamada, and M. Nakaoka, "Full-bridge soft-switching phase-shifted PWM DC-DC power converter using tapped inductor filter", *Electronics Letters*, vol. 39, pp. 924-925, 2003.

[51] Y. Kaiwei, Y. Mao, X. Ming, and F. C. Lee, "Tapped-inductor buck converter for high-step-down DC-DC conversion", *IEEE Transactions on Power Electronics*, vol. 20, pp. 775-780, 2005.

[52] D. A. Grant and Y. Darroman, "Extending the tapped-inductor DC-to-DC converter family", *Electronics Letters*, vol. 37, pp. 145-146, 2001.

[53] D. Ghodke, K. Chatterjee, and B. Fernandes, "Modified Soft switched Three-Phase Three Level, Dc-Dc Converter for High Power Applications having Extended Duty Cycle Range", *IEEE Transactions on Industrial Electronics*, vol. PP, pp. 1-1, 2012.

[54] A. Abramovitz and K. M. Smedley, "Analysis and Design of a

Tapped-Inductor Buck-Boost PFC Rectifier With Low Bus Voltage", *Power Electronics, IEEE Transactions on*, vol. 26, pp. 2637-2649.

[55] G. Liping, J. Y. Hung, and R. M. Nelms, "Evaluation of DSP-Based PID and Fuzzy Controllers for DC-DC Converters", *IEEE Transactions on Industrial Electronics*, vol. 56, pp. 2237-2248, 2009.

[56] S. Chander, P. Agarwal, and I. Gupta, "Auto-tuned, discrete PID controller for DC-DC converter for fast transient response", presented at India International Conference on Power Electronics, 2010.

[57] S. Kapat and P. Krein, "Formulation of PID Control for DC-DC Converters Based on Capacitor Current: A Geometric Context", *IEEE Transactions on Power Electronics*, vol. PP, pp. 1-1, 2010.

[58] A. Prodic and D. Maksimovic, "Design of a digital PID regulator based on look-up tables for control of high-frequency DC-DC converters", presented at IEEE Workshop on Computers in Power Electronics Proceedings, 2002.

[59] P. Gupta and A. Patra, "Super-stable energy based switching control scheme for DC-DC buck converter circuits", presented at Circuits and Systems, 2005. ISCAS 2005. IEEE International Symposium on, 2005.

[60] P. Gupta and A. Patra, "Energy Based Switching Control Scheme for DC-DC Buck-Boost Converter Circuits", presented at International Conference on Power Electronics and Drives Systems, 2005.

[61] P. Gupta and A. Patra, "A stable energy-based control strategy for DC-DC boost converter circuits", presented at IEEE 35th Annual Power Electronics Specialists Conference, 2004.

[62] C. Dariusz and K. Marian, "Energy-conservation approach to modeling PWM DC-DC converters", *IEEE Transactions on Aerospace and Electronic systems*, vol. 29, pp. 1059-1063, 1993.

[63] F. L. Luo and H. Ye, "Energy factor and mathematical modelling for power

DC/DC converters", *IEE Proceedings: Electric Power Applications*, vol. 152, pp. 191-198, 2005.

[64] P. Gupta and A. Patra, "Super-stable energy based switching control scheme for DC-DC buck converter circuits", presented at IEEE International Symposium on Circuits and Systems, 2005.

[65] M. Zhu and F. L. Luo, "Transient analysis of multi-state dc–dc converters using system energy characteristics", *International Journal of Circuit Theory and Applications*, vol. 36, pp. 327-344, 2008.

[66] K. Marn-Go and Y. Myung-Joong, "An energy feedback control of series resonant converter", presented at 21st Annual IEEE Power Electronics Specialists Conference, 1990.

[67] R. Ortega, A. J. Van Der Schaft, I. Mareels, and B. Maschke, "Putting energy back in control", *IEEE Control Systems*, vol. 21, pp. 18-33, 2001.

[68] R. Ortega, A. van der Schaft, F. Castanos, and A. Astolfi, "Control by Interconnection and Standard Passivity-Based Control of Port-Hamiltonian Systems", *IEEE Transactions on Automatic Control*, vol. 53, pp. 2527-2542, 2008.

[69] L. Tzann-Shin, "Lagrangian modeling and passivity-based control of three-phase AC/DC voltage-source converters", *IEEE Transactions on Industrial Electronics*, vol. 51, pp. 892-902, 2004.

[70] R. Leyva, A. Cid-Pastor, C. Alonso, I. Queinnec, S. Tarbouriech, and L. Martinez-Salamero, "Passivity-based integral control of a boost converter for large-signal stability", *IEE Proceedings -Control Theory and Applications*, vol. 153, pp. 139-146, 2006.

[71] S. Xiaofen and C. Chok-You, "Analysis and passivity-based control of zero-voltage-transition PWM converters", *IEEE Transactions on Power Electronics*, vol. 17, pp. 633-640, 2002.

[72] Y. Lu, K. W. E. Cheng, S. L. Ho, and J. F. Pan, "Passivity-based control of a phase-shifted resonant converter", *IEE Proceedings -Electric Power Applications*, vol. 152, pp. 1509-1515, 2005.

[73] Z. Haihua, A. M. Khambadkone, and K. Xin, "Passivity-Based Control for an Interleaved Current-Fed Full-Bridge Converter With a Wide Operating Range Using the Brayton–Moser Form", *IEEE Transactions on Power Electronics*, vol. 24, pp. 2047-2056, 2009.

[74] M. Perez, R. Ortega, and J. R. Espinoza, "Passivity-based PI control of switched power converters", *IEEE Transactions on Control Systems Technology*, vol. 12, pp. 881-890, 2004.

[75] C. Y. Chan, "Parallel damped passivity-based control of quasi-resonant converters", *IEE Proceedings -Electric Power Applications*, vol. 152, pp. 1093-1100, 2005.

[76] D. Jeltsema and J. M. A. Scherpen, "Tuning of passivity-preserving controllers for switched-mode power converters", *IEEE Transactions on Automatic Control*, vol. 49, pp. 1333-1344, 2004.

[77] D. Jeltsema and J. M. A. Scherpen, "A power-based perspective in modeling and control of switched power converters [Past and Present]", *IEEE Industrial Electronics Magazine*, vol. 1, pp. 7-54, 2007.

[78] "Energy Factor": http://en.wikipedia.org/wiki/Energy_factor.

[79] K. W. E. Cheng, "Storage energy for classical switched mode power converters", *IEE Proceedings: Electric Power Applications*, vol. 150, pp. 439-446, 2003.

[80] P. J. Lawrenson, S. J.M., B. P.T., C. J., and N. N. Fulton, "VARIABLE-SPEED SWITCHED RELUCTANCE MOTORS", *IEE Proceedings, Part B: Electric Power Applications*, vol. 127, pp. 253- 265 1980.

[81] X. D. Xue, K. W. E. Cheng, and S. L. Ho, "Influences of output and Control Parameters on Power Factor of Switched Reluctance Motor Drive Systems", *Electric Power Components and Systems*, vol. 32, pp. 1207-1223, 2004.

[82] X. D. Xue, K. W. E. Cheng, and S. L. Ho, "Improvement of power factor in switched reluctance motor drives through optimizing in switching angles", *Electric Power Components and Systems*, vol. 32, pp. 1225-1238, 2004.

[83] X. D. Xue, K. W. E. Cheng, and S. L. Ho, "Correlation of modeling techniques and power factor for switched-reluctance machines drives", *IEE Proceedings - Electric Power Applications*, vol. 152, pp. 710-722, 2005.

[84] K. W. E. Cheng and Y. Lu, "Formulation of the energy-storage factor for isolated power convertors using integrated magnetics", *IEE Proceedings: Electric Power Applications*, vol. 152, pp. 837-844, 2005.

[85] F. L. Luo and H. Ye, "Small signal analysis of energy factor and mathematical modeling for power dc-dc converters", *IEEE Transactions on Power Electronics*, vol. 22, pp. 69-79, 2007.

[86] C. H. Page, "Reactive Power in Nonsinusoidal Situations", *IEEE Transactions on Instrumentation and Measurement*, vol. 29, pp. 420-423, 1980.

[87] Chester and H. Page., "Reactive Power in non sinusoidal situations", *IEEE Transactions on Instrumentation and measurement*, vol. IM-29, pp. 420-423, 1980.

[88] L. S. Czarnecki, "Considerations on the Reactive Power in Nonsinusoidal Situations", *IEEE Transactions on Instrumentation and Measurement*, vol. 34, pp. 399-404, 1985.

[89] L. S. CZARNECKI, "What is Wrong with the Budeanu Concept of Reactive and Distortion Power and Why It Should be Abandoned", *IEEE Transactions on Instrumentation and Measurement* vol. IM-36, pp. 834-837, 1987.

[90] M. Depenbrock, "The FBD-method, a generally applicable tool for analyzing power relations", *IEEE Transactions on Power Systems*, vol. 8, pp. 381-387, 1993.

[91] J. Itoh and K. Fujita, "Novel unity power factor circuits using zero-vector control for single-phase input systems", *IEEE Transactions on Power Electronics*, vol. 15, pp. 36 - 43, 2000.

[92] N. L. Kusters and W. J. M. Moore, "On the Definition of Reactive Power Under Non-Sinusoidal Conditions", *IEEE Transactions on Power Apparatus and Systems*, vol. PAS-99, pp. 1845-1854, 1980.

[93] M. Saitou and T. Shimizu, "Generalized theory of instantaneous active and reactive powers in single-phase circuits based on Hilbert transform", presented at 33rd Annual IEEE Power Electronics Specialists Conference, 2002.

[94] D. SHARON, "Reactive-power definition and power-factor improvement in nonlinear systems", *IEE Proceedings*, vol. 120, pp. 704-706, 1973.

[95] K. W. E. Cheng, "Tapped inductor for switched-mode power converters", presented at Power Electronics Systems and Applications, 2006. ICPESA '06. 2nd International Conference on, 2006.

[96] J. H. Park and B. H. Cho, "Non-isolation Soft-switching Buck Converter with Tapped-Inductor for Wide-input Extreme Step-down applications", presented at Power Electronics Specialists Conference, 2005. PESC '05. IEEE 36th, 2005.

[97] J. Kingston, R. Morrison, M. G. Egan, and G. Hallissey, "Application of a passive lossless snubber to a tapped inductor buck DC/DC converter", presented at International Conference on Power Electronics, Machines and Drives, 2002.

[98] S. Pattnaik, A. K. Panda, and K. K. Mahapatra, "Analysis of Non-isolated Soft Switching DC-DC Buck Converter", presented at IEEE Region 10 and

the Third international Conference on Industrial and Information Systems, 2008.

[99] P. Jong-Hu and B. H. Cho, "The zero voltage switching (ZVS) critical conduction mode (CRM) buck converter with tapped-inductor", presented at Eighteenth Annual IEEE Applied Power Electronics Conference and Exposition, 2003.

[100] S. Cuk and R. D. Middlebrook, "Advances in Switched-Mode Power Conversion Part I", *IEEE Transactions on Industrial Electronics*, vol. IE-30, pp. 10-19, 1983.

[101] S. Cuk and R. D. Middlebrook, "Advances in Switched-Mode Power Conversion Part II", *IEEE Transactions on Industrial Electronics*, vol. IE-30, pp. 19-29, 1983.

[102] T. G. Habetler and R. G. Harley, "Power electronic converter and system control", *Proceedings of the IEEE*, vol. 89, pp. 913-925, 2001.

[103] T. Siew-Chong, Y. M. Lai, C. K. Tse, and M. K. H. Cheung, "Adaptive feedforward and feedback control schemes for sliding mode controlled power converters", *IEEE Transactions on Power Electronics*, vol. 21, pp. 182-192, 2006.

[104] T. Siew-Chong, Y. M. Lai, and C. K. Tse, "Indirect Sliding Mode Control of Power Converters Via Double Integral Sliding Surface", *IEEE Transactions on Power Electronics*, vol. 23, pp. 600-611, 2008.

[105] T. Siew-Chong, Y. M. Lai, and C. K. Tse, "General Design Issues of Sliding-Mode Controllers in DC-DC Converters", *IEEE Transactions on Industrial Electronics*, vol. 55, pp. 1160-1174, 2008.

[106] M. Castilla, L. C. de Vicuna, M. Lopez, O. Lopez, and J. Matas, "On the design of sliding mode control schemes for quantum resonant converters", *IEEE Transactions on Power Electronics*, vol. 15, pp. 960-973, 2000.

[107] S. Ting-Ting and H. S. h. Chung, "Boundary Control of Boost Converters Using State-Energy Plane", *IEEE Transactions on Power Electronics*, vol. 23, pp. 551-563, 2008.

[108] Y. Wai-To, K. T. K. Au, C. N. M. Ho, and H. S. H. Chung, "Fixed-Frequency Boundary Control of Buck Converter With Second-Order Switching Surface", *IEEE Transactions on Power Electronics*, vol. 24, pp. 2193-2201, 2009.

[109] V. S. Cheung, H. S. Chung, and W. Huai, "Predictive control of buck converter using nonlinear output capacitor current programming", presented at Twenty-Fifth Annual IEEE Applied Power Electronics Conference and Exposition (APEC), 2010.

[110] L. Kelvin Ka-Sing and C. Henry Shu-hung, "A Comparative Study of Boundary Control With First- and Second-Order Switching Surfaces for Buck Converters Operating in DCM", *IEEE Transactions on Power Electronics*, vol. 22, pp. 1196-1209, 2007.

[111] K. K. S. Leung and H. S. H. Chung, "Derivation of a second-order switching surface in the boundary control of buck converters", *IEEE Power Electronics Letters*, vol. 2, pp. 63-67, 2004.

[112] A. I. Maswood and F. Liu, "A novel unity power factor input stage for AC drive application", *IEEE Transactions on Power Electronics*, vol. 20, pp. 857 - 863, 2005.

[113] H. F. Bilgin, K. N. Kose, G. Zenginobuz, M. Ermis, E. N. I. Cadirci, and H. Kose, "A unity-power-factor buck-type PWM rectifier for medium/high-power DC motor drive applications", *IEEE Transactions on Industry Applications*, vol. 38, pp. 1412 - 1425, 2002.

[114] K. W. E. Cheng, *Classical Switched Mode and Resonant Power Converters*. Hong Kong: The Hong Kong Polytechnic University, 2002.

[115] C. Batlle, A. Dòria-Cerezo, and E. Fossas, "Bidirectional power flow control of a power converter using passive Hamiltonian techniques", *International*

Journal of Circuit Theory and Applications, vol. 36, pp. 769-788, 2008.

[116] J. W. Gannett and L. O. Chua, "Energy-related concepts for non-linear time-varying n-ports: Passivity and losslessness", *International Journal of Circuit Theory and Applications*, vol. 9, pp. 401-429, 1981.

[117] S. Jian, "Characterization and performance comparison of ripple-based control for voltage regulator modules", *IEEE Transactions on Power Electronics*, vol. 21, pp. 346-353, 2006.

[118] R. Redl and S. Jian, "Ripple-Based Control of Switching Regulators-An Overview", *IEEE Transactions on Power Electronics*, vol. 24, pp. 2669-2680, 2009.

[119] D. del Puerto-Flores, R. Ortega, and J. M. A. Scherpen, "A cyclodissipativity characterization of power factor compensation of nonlinear loads under nonsinusoidal conditions", *International Journal of Circuit Theory and Applications*, 2011.

[120] S.-J. Jeon and J. L. Willems, "Reactive power compensation in a multi-line system under sinusoidal unbalanced conditions", *International Journal of Circuit Theory and Applications*, vol. 39, pp. 211-224, 2011.

[121] F. L. Luo and H. Ye, *Advanced DC/DC Converters*. Boca Raton, Florida 07030, USA: CRC Press LLC, 2004.

[122] S. Zhanghai, K. W. E. Cheng, S. L. Ho, and L. Jiongkang, "Energy factor and its associated boundary condition analysis for higher order converters", presented at Australasian Universities Power Engineering Conference (AUPEC) 2008.

[123] P. Gupta and A. Patra, "Energy Based Switching Control Scheme for DC-DC Buck-Boost Converter Circuits", presented at Power Electronics and Drives Systems, 2005. PEDS 2005. International Conference on, 2005.

[124] G. Espinosa-Perez, P. Maya-Ortiz, M. Velasco-Villa, and H. Sira-Ramirez,

"Passivity-based control of switched reluctance motors with nonlinear magnetic circuits", *IEEE Transactions on Control Systems Technology*, vol. 12, pp. 439-448, 2004.

[125] H. Komurcugil, "Steady-State Analysis and Passivity-Based Control of Single-Phase PWM Current-Source Inverters", *IEEE Transactions on Industrial Electronics*, vol. 57, pp. 1026-1030, 2010.

[126] J. Linares Flores, J. L. B. Avalos, and C. A. B. Espinosa, "Passivity-Based Controller and Online Algebraic Estimation of the Load Parameter of the DC-to-DC power converter Cuk Type", *IEEE Latin America Transactions, IEEE (Revista IEEE America Latina)*, vol. 9, pp. 784-791, 2011.

[127] G. Escobar, D. Chevreau, R. Ortega, and E. Mendes, "An adaptive passivity-based controller for a unity power factor rectifier", *IEEE Transactions on Control Systems Technology*, vol. 9, pp. 637-644, 2001.

[128] X. F. Shi and C. Y. Chan, "Passivity-based adaptive controllers for quasi-resonant buck convertor", *IEE Proceedings -Electric Power Applications*, vol. 148, pp. 398-402, 2001.

[129] H. Sira-Ramirez and R. Ortega, "Passivity-based controllers for the stabilization of DC-to-DC power converters", presented at Proceedings of the 34th IEEE Conference on Decision and Control, 1995.

[130] R. Ortega, *Passivity-based control of Euler-Lagrange Systems*, 1998.